nagra.

Arbeitsbericht NAB 20-13

SGT-E3 deep drilling campaign (TBO):

Experiment Procedures and Analytical Methods at RWI, University of Bern (Version 1.0, April 2020)

May 2020

National Cooperative
for the Disposal of
Radioactive Waste

Hardstrasse 73
P.O. Box 280
5430 Wettingen
Switzerland
Tel. +41 56 437 11 11

www.nagra.ch

nagra.

Arbeitsbericht NAB 20-13

SGT-E3 deep drilling campaign (TBO):

Experiment Procedures and Analytical Methods at RWI, University of Bern (Version 1.0, April 2020)

May 2020

Rock-Water Interaction Group – RWI
Compiled and edited by H.N. Waber

RWI, Institute of Geological Sciences
University of Bern, Switzerland

KEYWORDS

Porewater Investigations, Laboratory Workflow, Drillcore Sample Preparation, Laboratory Analyses

National Cooperative
for the Disposal of
Radioactive Waste

Hardstrasse 73
P.O. Box 280
5430 Wettingen
Switzerland
Tel. +41 56 437 11 11

www.nagra.ch

Nagra Arbeitsberichte ("Working Reports") present the results of work in progress that have not necessarily been subject to a comprehensive review. They are intended to provide rapid dissemination of current information.
This report was prepared on behalf of Nagra. The viewpoints presented and conclusions reached are those of the author(s) and do not necessarily represent those of Nagra.

List of Contents

List of Tables

List of Figures

1 Introduction

H.N. Waber

Within phase 3 of the sectoral plan for deep geological repositories (SGT-E3), a deep drilling project (TBO) is carried out by Nagra. A major focus will be the characterisation of porewater in the rock formations of low-permeability and the distribution of natural tracers across these formations and extending into the bounding aquifer horizons.

Porewater residing in low-permeability rock cannot be sampled by conventional groundwater sampling techniques and has to be characterised by indirect methods based on originally saturated rock material obtained from boreholes. Collection of drillcores from below the surface will inevitably change intrinsic porewater parameters such as temperature, pressure and O_2- and CO_2-fugacity from those existing under in situ conditions. The drilling process, the on-site sample conditioning and the various preparation steps of the core material after reception in the lab will induce additional modification of specific parameters of the in situ porewater. Induced modifications of the in situ porewater of sedimentary environments are specific to the rock type under investigation and differ based on the reactivity of the rock mineralogy in terms of the carbonate and sulphur systems, ion-exchange and redox conditions.

A consequence of indirect methods for porewater characterisation is the fact that such methods can only deliver partial information about the complete chemical composition, pH and redox state of the in situ porewater. Therefore, the methods have to be applied complementary if aimed at the chemical composition of the porewater. Depending on the degree of detail required about the porewater composition available indirect methods are of largely different complexity with respect to sample conditioning, experimental set-up and analytical efforts. Natural tracer profiles, for instance, focus on chemically conservative compounds in the porewater and the extraction of such compounds is rather straightforward. Nevertheless, substantial differences in conditioning and extraction exist in case of dissolved tracer (e.g. Cl, Br), dissolved gases (e.g. He) or the stable isotope composition of the porewater molecule itself ($\delta^{18}O$, $\delta^{2}H$). Aiming at the chemical composition, pH and redox state of the in situ porewater by indirect extraction techniques based on drillcore material is ambitious and has inevitably to be accompanied by geochemical model calculations.

Depending on the focus of the porewater investigations such characterisation requires specific treatments and designs for the on-site sampling of drillcore material, the preparation of the rock material for individual extraction techniques and the adaption of analytical techniques.

This document describes the workflow, the preparation of the rock material for individual extraction techniques and the analytical techniques after reception of the on-site conditioned drillcore samples in the RWI-Laboratories of the Institute of Geological Sciences, University of Bern. It adopts the sample labelling given by Rufer (2019) who also gives a detailed description of sample collection and sample conditioning in the field.

Chapter 2 of the present document gives a short description of the different types of porewater samples, their designation and analytical work to be carried out as already documented in Waber (2018). Chapter 3 describes the workflow for each porewater sample type. Chapters 4 to 12 give detailed descriptions of sample preparation and analytical methods applied to solid material and extract solutions obtained from the various techniques, respectively. Chapter 13, finally, gives a description of the analytical techniques applied to experiment solution of the various experiments.

The standard workflow and details about extraction techniques given here are those for routine porewater investigations on a large number of samples within a restricted time frame. In some aspects it thus represents a compromise between efficient sample handling, infrastructure and personnel, and the technical/scientific ambition for a highest possible characterisation of the porewater and concentration profiles of natural tracers.

This document describes the status of April 2020. According to gained experience and – most importantly – to the specific rock type under investigations, the standard workflow, detailed procedure of extractions and subsequent analytical programme are subject to change. Furthermore, to resolve specific questions (e.g. redox, pH, ion-accessible porosity, diffusion parameters) that require more time and infrastructure-intensive investigations, the standard workflow and extraction techniques will be modified and adapted for specific samples.

2 Sample Types

H.N. Waber

The characterisation of porewater and transport parameters in the low-permeability rock sequences requires a series of samples that undergo specific on-site conditioning. Rufer (2019) gives a detailed description about the on-site handling and conditioning of each sample type. The sample types that will undergo complete or partial preparation and/or extraction in the RWI-Laboratories and their main analytical programme include:

- **PW samples:** Porewater Chemistry
  - Destructive techniques
  - Aqueous extraction, CEC extraction (selection of samples), water content, bulk and grain density, porosity, mineralogy, and additional optional analyses (e.g. rock and mineral chemistry and isotopes, maturity organic material etc.)
  - Preparation and analytics mainly performed at RWI, except for $\delta^{37}Cl$ on aqueous extracts solutions at Hydroisotop GmbH (Schweitenkirchen, Germany) and complementary CEC extraction at PSI
- **NG samples:** Noble Gas Out-Diffusion
  - Non-destructive technique
  - Characterisation of noble gases dissolved in porewater, water content, porosity, rock chemistry (radionuclides, noble gases)
  - Sample preparation on-site, further preparation and analytics performed at RWI, except for $^{3}He/^{4}He$ at University of Bremen and rock chemistry at Kola Scientific Center (Russia)
- **AD samples:** Advective Displacement
  - Non-destructive technique
  - Complete chemical characterisation of porewater including pH and possibly redox, water content, porosity, transport properties (hydraulic conductivity, diffusion coefficients of non-reactive components), optional post-mortem aqueous and CEC extractions, mineralogy
  - All preparation and analytics performed at RWI
- **SQ samples:** High-Pressure Squeezing
  - Destructive technique
  - Characterisation of porewater compounds, water content, porosity, mineralogy, optional post-mortem aqueous extraction
  - Sample preparation and analytics performed at RWI, squeezing tests performed at CRIEPI (Japan)

- **OD samples:** Out-Diffusion Experiments
  - Non-destructive technique
  - Characterisation of porewater conservative compounds, diffusion coefficients, water content, porosity, mineralogy, C-isotopes on dissolved and solid carbonate
  - All preparation and analytics performed at RWI
- **DI samples:** Through-Diffusion, Sorption
  - Non-destructive technique
  - Characterisation of diffusion coefficients and sorption properties
  - Parts of sample preparation at RWI including water content, mineralogy; diffusion experiments at PSI (Switzerland)
- **RP samples:** Various Rock Properties
  - Non-destructive and destructive techniques
  - Various porewater and petrophysical aspects according to requirement
  - Full or partial preparation and analytical at RWI

3 Porewater Extraction Techniques: Workflow

H.N. Waber

Drillcore samples that are conditioned on the drill-site according to the specific requirements (*cf.* Rufer 2019) will be received in the RWI Laboratories in batches. At the Institute of Geological Sciences, samples will be stored in a cooling room at 4°C until further preparation.

3.1 PW samples: porewater chemistry and rock properties

Drillcore samples of about 25 cm in length are received from the field in their original saturated state and conditioned in vacuum-sealed aluminium bags. The entire sample processing is optimised to a) use non-contaminated, originally saturated rock material from the central part of the core b) minimise air-exposure of rock aliquots used for different purposes, and c) allow enough time for extraction, phase separation and precise analyses. All techniques applied to PW samples are destructive with respect to the rock texture.

PW samples are generally used for

- Natural tracer profiles: aqueous extraction, isotope exchange technique
- Rock geochemical properties: cation exchange (CEC) extraction
- Rock petrophysical properties: water content, bulk wet density, grain density, porosity, BET
- Rock mineralogy: whole rock, clay fraction
- Rock chemistry and isotopes: major and trace elements, isotopes of C, Sr and possibly others

The detailed description of sample processing, experimental procedure and parameters analysed on PW samples is given in Chapters 4 – 7.

The workflow for the standard lab preparation of PW samples is given in Fig. 3-1. The standard preparation of PW samples involves three persons: one geologist and two lab technicians. The geologist inspects the rock sample for its mineralogical and textural homogeneity, separates the central, originally saturated part of the core and disintegrated this material according to the specification for each extraction/analytical procedure. The two lab technicians perform the petrophysical measurements and prepare the liquid extractions and isotope exchange technique utilising originally saturated rock material. Finally, aliquots of saturated rock will be collected, immediately vacuum-sealed and sent to PSI for additional CEC extraction test utilising a different technique. Following the aqueous extraction test, aliquots of the aqueous extract solutions will be sent to Hydroisotop GmbH for the analysis of $\delta^{37}Cl$.

3.2 NG samples: Dissolved noble gases in porewater

Drillcore samples of about 15 cm in length are on-site trimmed by dry cutting to obtain a cuboid shaped cylinder from the central part of the originally saturated core. This sample cuboid is immediately sealed into an evacuated, helium-tight stainless steel cylinder in which the porewater gases can outgas over several months. A detailed description of the on-site sample preparation is given in Rufer (2019).

The general workflow for the preparation, conduction and analytical programme of NG samples is given in Fig. 3-2 and the detailed description of NG sample processing is given in Chapter 8.

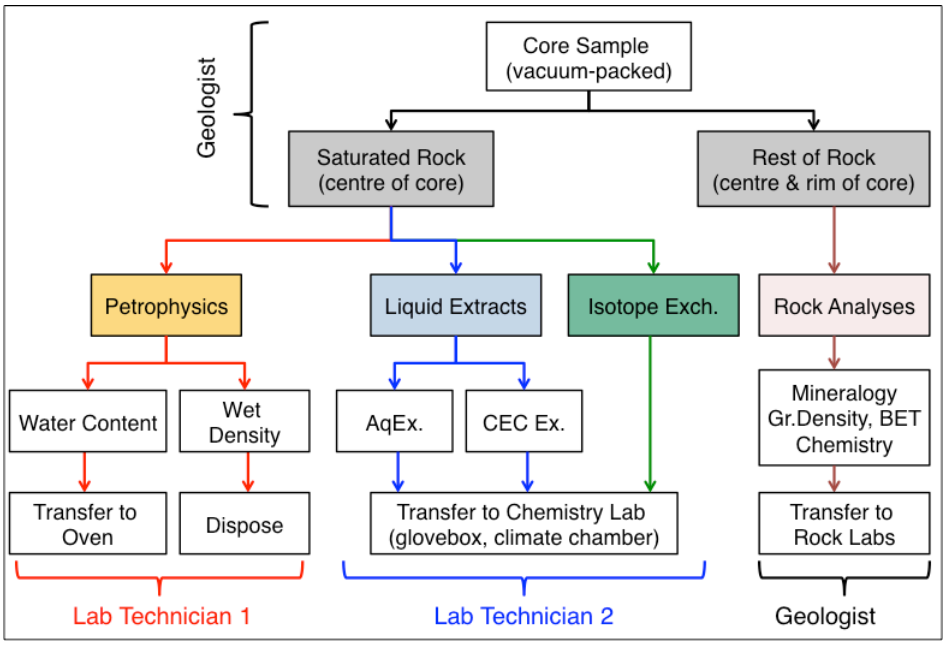

Fig. 3-1: PW samples (Porewater Chemistry): Workflow and assignment of individual tasks to personnel involved in the sample preparation.

Preparation and analyses conducted at RWI and other labs at the Institute of Geological Sciences, University of Bern.

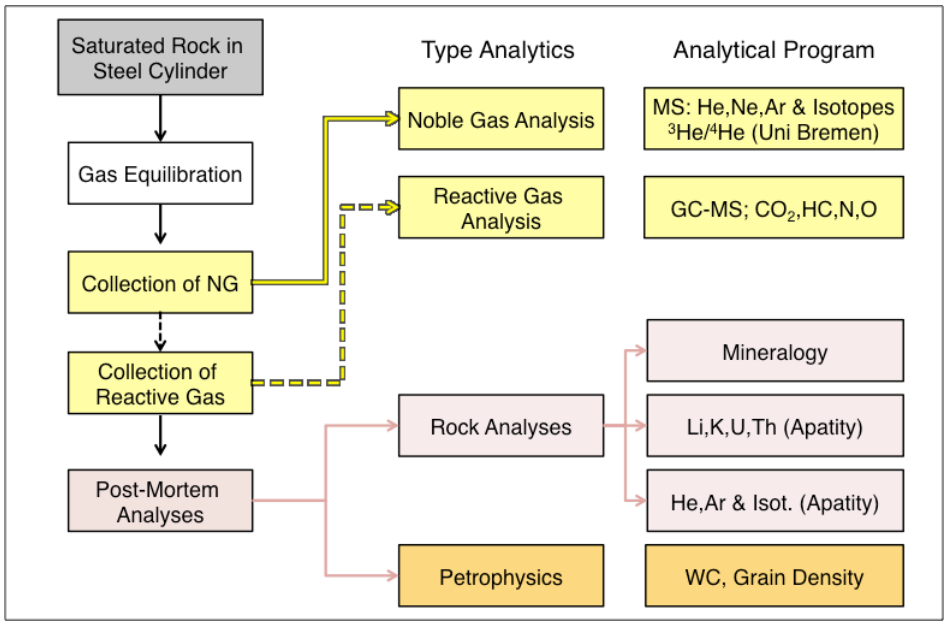

Fig. 3-2: NG Samples (Noble & Reactive Gas): Workflow of individual sample preparation steps and analytical investigations.

All preparation and analyses conducted at RWI labs at the Institute of Geological Sciences, University of Bern except for $^{3}He/^{4}He$ (University of Bremen, Germany), and chemical and noble gas analyses on rock material (Geological Institute, Kola Scientific Centre, RAS, Apatity, Russia); dashed line indicates optional investigations.

The primary goal of NG samples is the determination of porewater ^{4}He concentrations and $^{3}He/^{4}He$ and $^{40}Ar/^{36}Ar$ isotope ratios. The noble gas equilibration technique works with moderately large-volume rock samples (ca. 160 cm^3) and is non-destructive with respect to the rock texture.

NG samples are used for:

- Analysis of ^{4}He in porewater as a conservative natural tracer
- Analysis of $^{3}He/^{4}He$ isotope ratios for the characterisation of He origin(s) and fluxes
- Analysis of $^{40}Ar/^{36}Ar$ in porewater as a possible conservative natural tracer
- Optional analyses of reactive gases (CO_2, hydrocarbon gases, N_2)
- Post-mortem analyses of rock material for mineralogy, water content, grain density and rock chemistry and noble gas contents for He and Ar in situ production calculations

In contrast to other natural tracers ^{4}He, $^{3}He/^{4}He$ and $^{40}Ar/^{36}Ar$ in porewater contain certain time information due to the in situ production of these isotopes by the natural decay of radioisotopes in the rock. In combination with other natural tracers (Cl, Br, $\delta^{18}O$, $\delta^{2}H$) this allows identifying and timing changes in the boundary conditions of solute transport in an aquitard – aquifer system.

3.3 AD samples: Advective displacement experiments

Drillcore samples of about 20 cm in length are received from the field in their original saturated state and conditioned in vacuum-sealed aluminium bags.

The primary goal of AD samples is the advective displacement of the in situ porewater by an artificial porewater spiked with tracer(s) and by applying a hydraulic gradient. The advective displacement technique works with large-volume rock samples (ca. 400 – 600 cm^3) and is non-dstructive with respect to the rock texture.

Specifically, advective displacement samples processed for Nagra's deep drilling program are used for:

- In-line measurements of the displaced porewater electric conductivity and pH.
- Complete chemical analysis of a time series of displaced water aliquots.
- Water stable isotope analysis ($\delta^{18}O$, $\delta^{2}H$) of aliquots.
- Derivation of Cl-accessible porosity and where feasible also Br-accessible porosity.
- Monitoring of hydraulic conductivity evaluated after each sampling interval.
- Sample pre-characterisation (water content, bulk wet density, mineralogy, CEC and cation exchanger population).
- Post-mortem analyses of rock material for water content, bulk wet density and optionally grain density and aqueous extractions, as required for the interpretation of the chemical and isotopic data of the displaced water.
- If observed over sufficient time: monitoring break-through of artificial and natural tracers and derivation of transport properties by modelling (hydraulic conductivity, diffusion coefficients of non-reactive components).

The detailed description of sample processing, experimental procedure and parameters analysed on AD samples is given in Chapter 9.

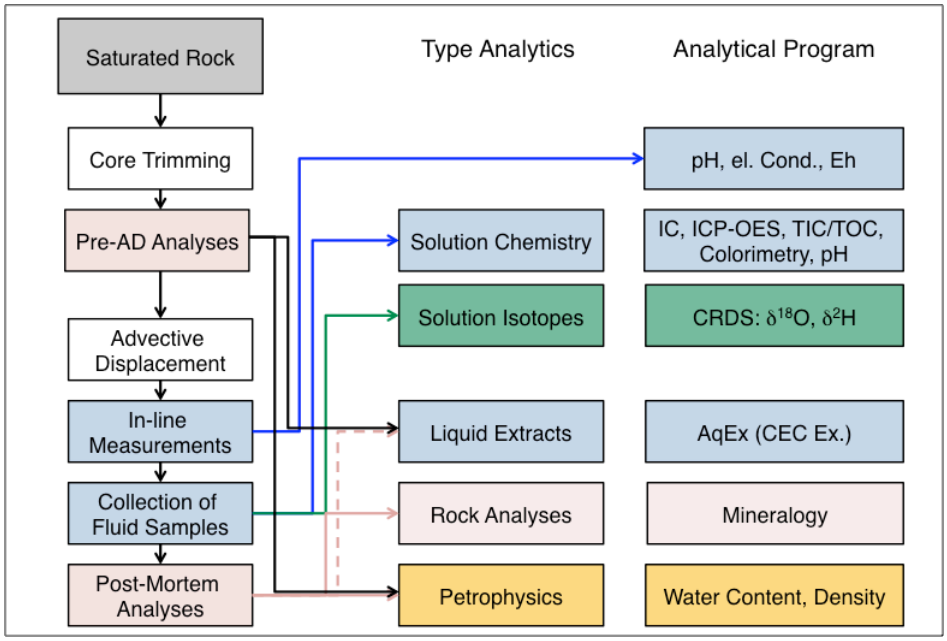

Fig. 3-3: Advective Displacement (AD): Workflow of sample preparation steps and analytical investigations.

All preparation and analyses are conducted at RWI and other labs at the Institute of Geological Sciences, University of Bern; dashed line indicate optional investigations.

3.4 SQ samples: High-pressure squeezing

Drillcore samples of about 20 cm in length are received from the field in their original saturated state and conditioned in vacuum-sealed aluminium bags.

The primary goal of SQ samples is the extraction of porewater by squeezing the low-permeability rock sample under variably high pressure. The squeezing technique works with large-volume rock samples (ca. 500 – 700 cm^3) and is destructive with respect to the rock texture.

SQ samples are used for:

- Production of squeezed water from low-permeability rock
- Monitoring behaviour of squeezed water as function of pressure
- Complete chemical analysis of squeezed water
- Water stable isotope analysis ($\delta^{18}O$, $\delta^{2}H$) of squeezed water
- Post-mortem analyses of the squeezed rock material for mineralogy, water content, grain density, and aqueous extraction tests required for the interpretation of the chemical and isotopic data of the squeezed water

High-pressure squeezing of rock samples is conducted in collaboration with and at the facilities of CRIEPI (Central Research Institute of Electric Power Industry, Chiba, Japan).

The general workflow for the preparation, conduction and analytical programme of SQ samples is given in Fig. 3-4. A standard protocol of preparation steps, experiment execution and technical details are given Chapter 10.

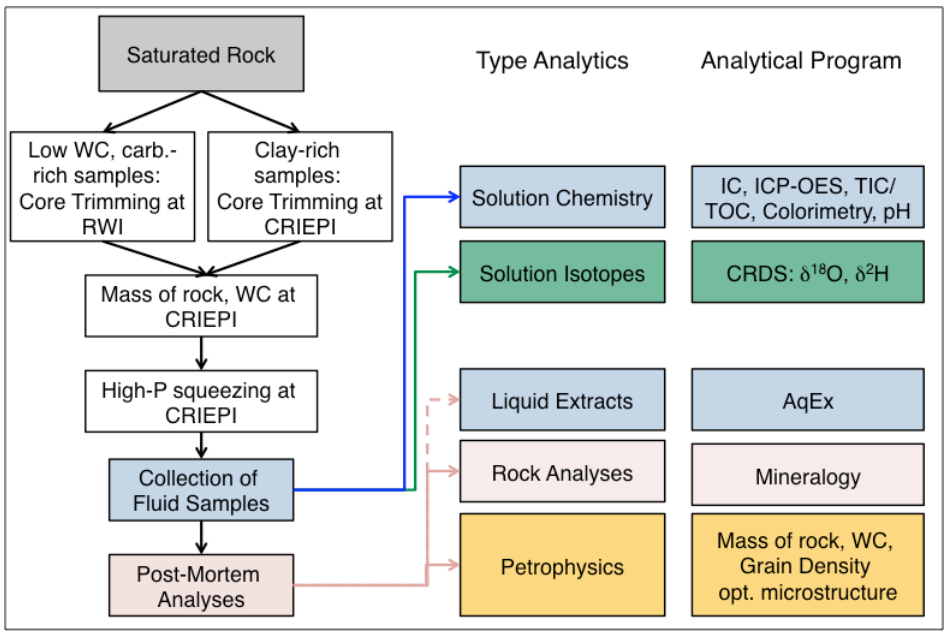

Fig. 3-4: SQ samples (High-Pressure Squeezing): Workflow of individual sample preparation steps and analytical investigations.

Sample preparation for squeezing and high-pressure squeezing and one water content measurement at CRIEPI. All solution and post-mortem analyses conducted at RWI at the Institute of Geological Sciences, University of Bern; dashed line indicate optional investigations.

3.5 OD samples: Chemical out-diffusion experiments

Drillcore samples of about 20 cm in length are received from the field in their original saturated state and conditioned in vacuum-sealed aluminium bags.

The primary goal of OD samples is the determination of porewater concentrations and derivation of pore diffusion coefficients of chemically conservative compounds (Cl, Br). The out-diffusion technique works with large-volume rock samples (ca. 200 – 400 cm^3) and is non-destructive with respect to the rock texture.

OD samples are used for:

- Complete chemical analysis final solutions
- Chemical analysis of time-series subsamples (no TIC so far)
- Carbon stable isotope analysis on dissolved carbon ($\delta^{13}C_{TIC}$)
- Monitoring elution of porewater solutes (incl. reactions)
- Post-mortem analyses of rock material for mineralogy, water content, bulk and grain density and $\delta^{13}C$ on carbonate minerals

For sedimentary rocks, the out-diffusion technique is still limited to non-swelling rocks. It will be applied to carbonate/sand-rich lithologies and lithologies of low water content (< 2 wt.%) where the squeezing and advective displacement techniques are no longer applicable.

Out-diffusion experiments deliver porewater compositions of chemically the conservative compounds Cl and Br. In addition, pore diffusion coefficients of Cl^- and Br^- are derived by fitting the observed concentration elution curves of Cl and Br using transport models. The general work-flow for the preparation, conduction and analytical programme of OD samples is given in Fig. 3-5. The detailed description of sample processing, experimental procedure and parameters analysed on OD samples is given in Chapter 11.

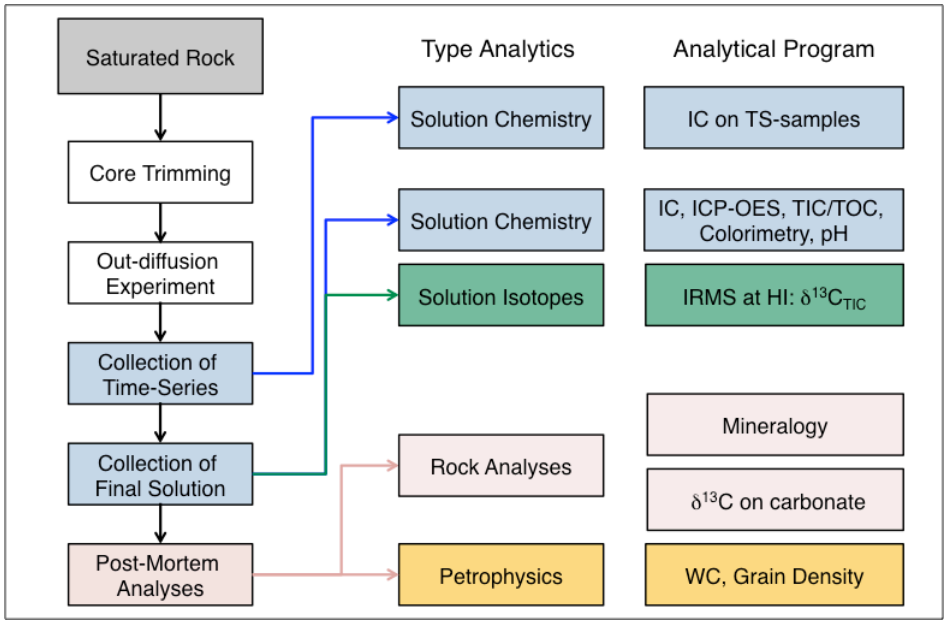

Fig. 3-5: OD samples (Out-Diffusion): Workflow of individual sample preparation steps and analytical investigations.

All preparation and analyses conducted at RWI and other labs at the Institute of Geological Sciences, University of Bern.

3.6 DI samples: through diffusion, sorption

Drillcore samples of about 20 cm in length are received from the field in their original saturated state and conditioned in vacuum-sealed aluminium bags.

The primary goal of DI samples is the derivation of diffusion coefficients by through-diffusion experiments and the sorption characteristics and cation exchange capacity (CEC) of various lithologies. These experiments are conducted at PSI. At RWI, Uni Bern, the initial sample preparation and complementary analysis are conducted. The through-diffusion technique works with small-volume rock samples (ca. 40 cm^3) and is non-destructive with respect to the rock texture.

DI samples are used for:

- Diffusion coefficients of Cl and HTO and possibly others
- Sorption and cation exchange experiments at PSI
- Complementary cation exchange experiments at RWI
- Rock petrophysical and mineralogical characterisation rock material used for through diffusion and sorption/CEC experiments

The general workflow for the preparation of DI samples is given in Fig. 3-6.

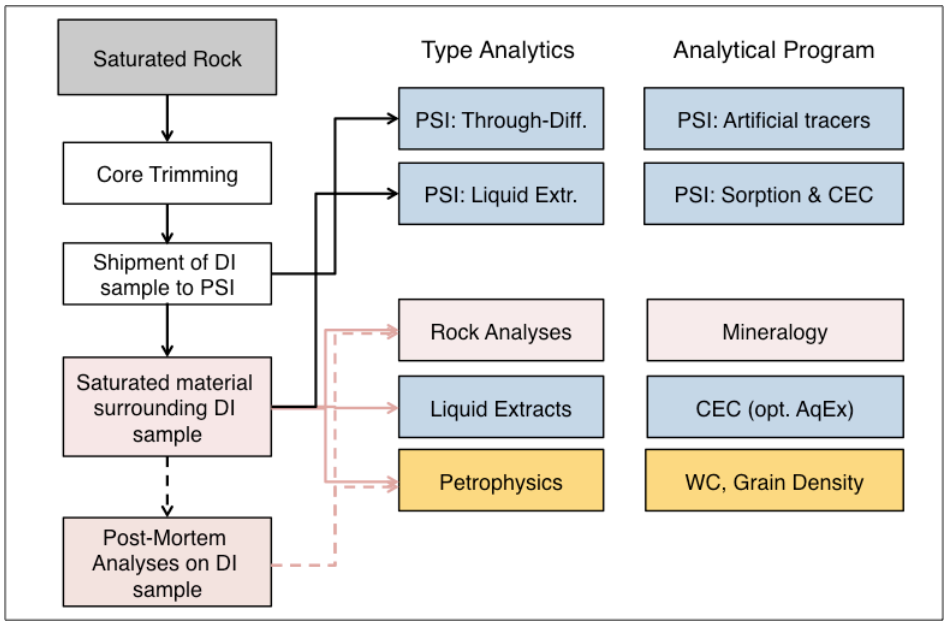

Fig. 3-6: DI samples (Through-Diffusion, Sorption): Workflow of individual sample preparation steps and analytical investigations.

Initial preparation with separation into aliquots for through-diffusion, sorption and water content/mineralogy/CEC at RWI labs at the Institute of Geological Sciences, University of Bern. Final preparation and analyses of through-diffusion and soprtion sub-samples conducted at PSI. Analyses of water content, mineralogy and CEC at RWI labs; dashed lines indicate optional investigations.

3.7 RP samples: Various rock properties

Drillcore samples of about 20 cm in length are received from the field in their original saturated state and conditioned in vacuum-sealed aluminium bags.

The RP samples serve as:

- Back-up samples for PW samples
- For various investigations of rock and petrophysical properties based on request.

The first purpose of these samples to increase the data density of key properties such porosity or of porewater stable isotope composition requires conditioning as the PW samples to prevent oxidation and desiccation of the drillcore material. The second purpose of the sample is less prone to such a modification.

The general workflow for the possible preparation, conduction and analytical programme of RP samples is given in Fig. 3-7. The precise analytical programme of these samples is planned on request and on a day-by-day bases and will follow the descriptions given in the previous sections.

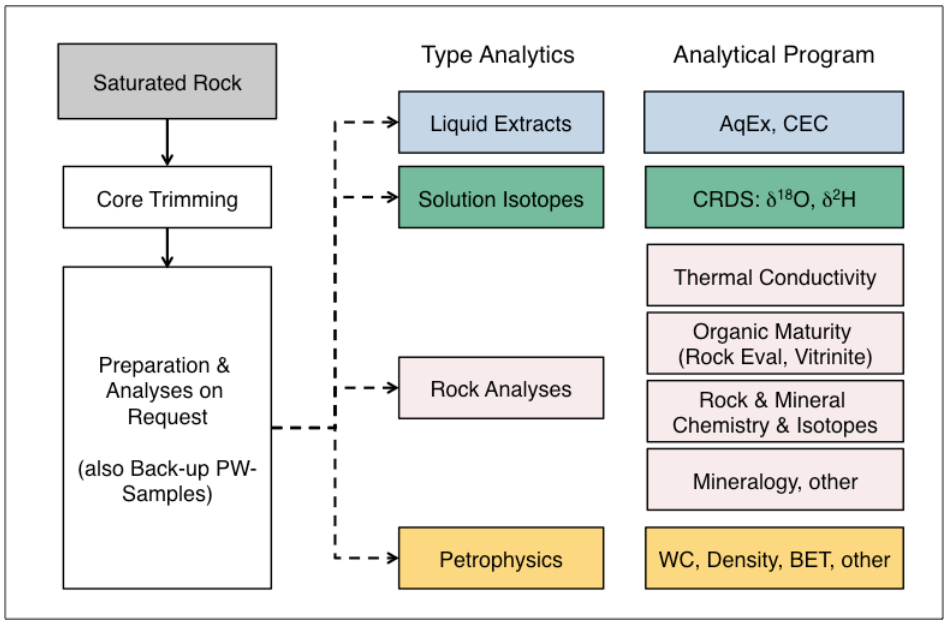

Fig. 3-7: RP samples (Various Rock Properties): Workflow of sample preparation steps and possible analytical investigations.

Analytical program to be decided on a day-by-day basis. RP samples also serve as back-up for PW samples.

4 Rock Analyses

M. Mazurek, U. Eggenberger, W. Zucha, L. Aschwanden, D. Rufer, M. Kiczka

4.1 Bulk-rock mineralogy

The identification of mineral phases and the quantification of their relative proportions is based on powder X-ray diffraction. The quantitative evaluation of the diffraction patterns applies the Rietveld method (Rietveld 1969), or a combined Rietveld-Pawley (Pawley 1981) approach if clay minerals are present in the sample. A step-by-step workflow was developed, in order to improve robustness and traceability of data treatment, and to render the process mostly independent of the person performing the analysis.

4.1.1 Sample preparation and conditioning

According to the lab-internal Standard Operation Procedure, rock material is first crushed with a conventional disc mill for max. 30 s. After splitting, 4 g of rock material ae mixed with 1 g of corundum (internal standard). The mixture is subsequently ground for 6 mins at 50 % speed (1200 rpm) using a Retsch McCrone XRD-mill (www.retsch.com), after adding 10 mL ethanol as grinding aid. This leads to a unimodal grain-size distribution with a median < 5 µm, which is a suitable sample state for powder X-ray diffraction analysis. Moreover, the McCrone mill is known not to destroy the crystal structure even of soft minerals, such as calcite (O'Connor & Chang 1986, Locock et al. 2012). After milling, the powder is dried at 38 °C and subsequently front-loaded into an XRD sample holder using a prism stamp.

4.1.2 Acquisition of XRD patterns

In a first step, a qualitative phase analysis is performed using PANalytical HighScore Plus v. 4.x and a lab-internal database. Once the crystalline phases were determined, the data are quantitatively evaluated, based on structural data and using the Rietveld method, or, if clay minerals are present, using a combined Rietveld and Pawley approach. This is done with PANalytical HighScore Plus v. 4.x, and optionally cross-checked with Coelho Software TOPAS-Academic v. 6.

The lab-internal data base contains structural data for about 200 crystalline phases, which have been manually validated for data quality and correctness. Moreover, all refined parameters have appropriate minimum and maximum limits in order to avoid physically incorrect results. During the refinement procedure, crystal-structure parameters are varied within given limits by the software, in order to best fit the measured XRD pattern. The final result is verified for plausibility by the operator and modified in case of need.

Given the high degree of chemical variability and structural disorder, clay minerals presently cannot be quantified by the Rietveld method. While clay peaks are also calculated and used for the deconvolution of the XRD pattern (Pawley 1981), no attempt of quantification is performed. This means that the sum of all quantified phases is 100 % minus the undetermined phases, i.e. mostly clays. The internal standard (corundum) is used to obtain the absolute contents of the quantified minerals and of the undetermined rest.

Corundum is chosen because of its wide acceptance as internal standard, mainly due to the following characteristics:

- high crystallinity
- strain-free microstructure, which results in sharp reflections
- large number of reflections over the whole 2θ range
- chemical inertness
- no preferred orientation
- non-hygroscopic nature.

For more information on corundum as internal standard, see Madsen et al. (2011).

The chosen evaluation approach is rigorously tested by analysing a substantial number of artificial mixtures in the space quartz-albite-orthoclase-microcline-calcite-dolomite-celestite-clay. For the clay end member, a sample of Opalinus Clay was decarbonated by acid washing, and the contents of quartz and feldspars were minimised by repeated grain-size separation of the < 2 µm fraction by sedimentation in a water column. The mineralogical space covered by the mixtures corresponds to that of the Füchtbauer triangle (Füchtbauer 1988), i.e. mixtures of clay minerals, carbonates and quartz/feldspars.

In addition, the elemental contents of S, inorganic and organic C obtained on a CNS analyser are integrated with the XRD data. The contents of carbonate minerals are adjusted in order to fit with the content of inorganic C. The adjustment is minor in most cases, indicating a good consistency between the methods. In case of rocks in which S occurs mainly in reduced form, pyrite content is obtained from the concentration of S. For pyrite contents > 1 wt.%, a good agreement is found with pyrite content determined from XRD. For rocks in which S occurs mainly as SO_4, S is recalculated in terms of anhydrite or gypsum contents.

4.2 Inorganic carbon, organic carbon, and total sulphur of whole rock by CNS analyser

About 1 – 10 mg sample powder are weighed, transferred into a Sn vessel, combusted at 1000 °C and oxidised by addition of O_2. The evolved CO_2, SO_2 and N_2 gas is then transferred into a gas chromatograph by He carrier gas. Total C, N and S are quantified using a thermal conductivity detector (Carlo Erba EA 1108). For the analysis of organic C, carbonate is removed by recurrent addition (about 7 – 10 times over 1.5 – 2 days) of 20 µL 1 M HCl at 70 °C prior to analysis. Inorganic C is calculated by difference. Standardisation for all elements is performed using cystine ($C_6H_{12}N_2O_4S_2$). Detection limits are 0.02 wt.% (C), 0.01 wt.% (N) and 0.05 wt.% (S), and accuracy is < 5 %.

4.3 Clay mineralogy

The structure of clays is characterised by two-dimensional sheets and the order of the tetrahedral and octahedral sheets are layered. Due to the chemical variability and structural disorder clays cannot be quantified by a routine Rietveld method as applied for primary minerals. The identification of clay mineral phases and the quantification is based on the determination of their relative proportions by powder X-ray diffraction. To distinguish the complex layered structure of sheet-silicates, oriented sample specimen are used. For the quantification of clays, a full pattern fit method based on the ARQUANT approach was developed to determine the relative amount of

clay types present. The quantification is calculated by the difference to bulk-rock mineral content, determined by internal standard method, combined with a Rietveld-Pawley (Pawley 1981) approach for clay minerals present in the sample (see Section 4.1 'Bulk-rock mineralogy').

A step-by-step workflow was developed in order to improve robustness. The data treatment is based on a defined set of reference structures, the automated fitting process is mostly user independent, including background-correction during runtime. A detailed description of the procedure and the quantification method used can be found in the SOP *"FSXRD_GM_Nagra_V02; Arbeitsanweisung XRD Gesamtmineralogie Nagra"*.

4.3.1 Sample preparation and conditioning

According to the lab-internal SOP, rock material is first crushed with a conventional disc mill for 30 s. After splitting, approximately 15 g of rock material is immersed in an alkaline solution. Ultrasonic is used for 5 mins to disperse the particles and the material is transferred to an Atterberg cylinder and filled with 0.01 molar NH_4OH. After 16 hrs the clay fraction is released into centrifuge vessels. A multiple step procedure of Ca-saturation ($CaCl_2$), coagulation, dissolution of possibly present carbonates and cleaning by using a centrifuge is performed.

The final decanted material is transferred into a smaller container and a slurry is produced. After ultrasonic treatment, the slurry is transferred to a duplicate of labeled round glass plates. The samples are left to dry at room conditions overnight. Once a sample is measured (as *"air"* sample), the same glass plate is saturated with ethylene glycol overnight and re-measured (as *"eg"* sample). Finally, the sample is heated up to 550 °C and measured (as *"heat"* sample).

4.3.2 Acquisition of XRD patterns

X-ray patterns are measured with a CubiX3 or a PANalytical XPertPRO diffractometer, both using a Cu source and almost identical beam conditions and measuring parameter: data are recorded from 3 to 40° 2θ, with a step size of 0.02° and an acquisition time of 1.5 s per step while using a fixed divergence slit, a 15 mm beam mask and 0.04 radian soller slits. Three consecutive measurements are performed for each sample: at air dried conditions, after Ethylenglycol saturation overnight and finally after heating.

4.3.3 Evaluation of XRD patterns

In a first step, the three measurements of the same sample are checked and compared for consistency (names, intensity), presence/absence of clay minerals and sample height correction (peak shift) is applied:

- Names and labelling
- Count rates to verify sample preparation and thickness
- Presence (illite-smectite ML) or absence (smectite, chlorite) of clay types
- Pattern shift for sample height correction is performed (usually based on traces of quartz)

The quantitative determination of the clays is done in two steps. First, the relative amount of clay types is determined by a Full-Pattern-Fit (FPF) method. Then the sum of all clays, determined by the difference of the sum of all primary mineral phases to 100 %, is used to calculate the amount of the individual clay types and groups. This method assumes, that all phases present in a sample are crystalline.

The FPF Method is a mathematical approach where the measured pattern is fitted to a set of predefined patterns by a least square procedure until a minimum in difference is achieved. The predefined patterns are modelled with NewMod2 (Mertens et al. 2016). This approach is used in most FPF programmes such as PyXRD (Dumon & Van Ranst 2016), Sybilla (Zeelmaekers et al. 2010) or ARQUANT (Blanc et al. 2007) and are described in detail by these authors. Since there is no support anymore for some of these programmes (PyXRD, ARQUANT) or the code is too time-consuming and complex for routine analysis (NewMod2, Sybilla – several hours per sample) and sometimes very instable, a proprietary code (ClayFit) has been developed with Python at the Institute of Geological Sciences.

A set of 35 clay structures relevant for clays described in sedimentary rocks in Switzerland has been calculated with NewMod (Reynolds 1985) and NewMod2, including different types of illite, chlorite, kaolinite, smectite, illite – smectite-ML and chlorite – smectite-ML. The used structure parameters are identical as defined in the ARQUANT database. The modelled structures have been corrected for 2-Theta dependent orientation effect of reflections of crystallites by the Lorentz-Factor and then stored in the database file. Additional parameters for the reference structures were added to the database (e.g. fraction of ML, mineral group) for final calculation. Details of modelling and structural parameters are listed in the database file *"clayfit_db.xlsx"*.

Background correction of type: $y = m_1 + m_2*\exp(-m^3*x)$ are applied for measured as well as for reference phases during calculation. This allows also acceptable fitting at low 2-Theta angles, important for clay types with large lattice space like smectites.

The evaluation approach is tested by analysing a set of pure standard clays, mixtures of illite:chlorite:illite – smectite-ML and samples from previous studies (OPA, MX80 etc.). Additionally, the method is compared against the manual method of existing investigations (Frickberg, Bülach-1) and found to be suitable achieving backwards compatible results. The ClayFit method allows a more detailed reporting of several mixed layer clays, whereas the previous method describes only one type of illite – smectite-ML. The sum of illite + illite – smectite-ML of the previous method is comparable with the sum of illite + illite – smectite-ML types from ClayFit. Therefore, also the sum of smectite and of illite originating from the different mixed layer clays are reported.

4.4 Thin section investigations

Rock chips are cut with a diamond saw using little water. Thin sections with a thickness of 30 µm are then prepared. For clay-rich lithologies, paraffin oil instead of water is used, in order to minimise disaggregation of the rock due to swelling. The sections are studied with a conventional optical polarising microscope under transmitted and reflected light.

4.5 Scanning electron microscopy

Samples are embedded in resin and the surface of interest is processed using grinding paper, oil-based diamond suspensions and petroleum, and cleaned in an ultrasonic hexane bath. The uncoated sample surface is examined in a ZeissEVO-50 XVP scanning electron microscope (SEM) equipped with an EDAX Sapphire light element detector in the low vacuum mode (10 Pa) with a beam acceleration of 20 kV and a working distance of 9 mm. Backscatter electron (BE) images are acquired on the polished sample surface. Resulting BE images depict the average proton number at beam location. The beam current is adjusted to yield a dead time of 10 – 20 % for EDX analysis (energy dispersive spectroscopy). EDX measurements are acquired for 60 s life time on points or small homogenous areas, and are semi-quantitatively analysed without standardisation using the EDAX Genesis software (ZAF matrix correction). Carbon and oxygen are excluded from the quantification, and the remaining elements are scaled to yield 100 mol%.

4.6 Isotope data on rocks and minerals

4.6.1 Carbon and oxygen isotopes of carbonates

Carbon and oxygen isotope ratios of whole rock carbonate are measured on 1 g powder aliquots. Vein calcite is micro-drilled with a 2 mm diamond drill. Measurements are performed in duplicate on 150 – 250 µg of homogenised powder under conversion of all carbon to CO_2-gas by digestion in phosphoric acid under helium atmosphere at 70 °C.

Measured $\delta^{13}C$ and $\delta^{18}O$ values are reported relative to the Vienna Pee Dee Belemnite (VPDB) standard, with $\delta^{18}O$ (VSMOW) values being calculated according to the conversion:

$$\delta^{18}O_{VSMOW} = 1.03092 * \delta^{18}O_{VPDB} + 30.92\ ‰$$

given in Kim et al. (2015). Standardisation is accomplished using international standards IAEA-603 (IAEA 2016), NBS 19 and NBS 18 (both Friedman et al. 1982). Analytical absolute errors (2 σ s.d.) are ≤ 0.16 ‰ for $\delta^{13}C$ and ≤ 0.20 ‰ for $\delta^{18}O$, with analytical blank levels equivalent to ≤ 0.5 µg carbonate.

The stable C- and O-isotope compositions of the resulting CO_2-gas are measured on a Finnigan Delta V Advantage gas chromatography isotope ratio mass spectrometer (GC IRMS) equipped with an on-line gas preparation and introduction system (Gas Bench-II) and a CTC Combi-Pal autosampler.

For pure calcite, the analysis requires approximately 150 – 200 µg of powdered mineral sample to obtain adequately high measurement signals. For impure samples, the total mass being weighed in is increased according to the sample's fractional carbonate content. Sample material is weighed in on a microscale (Mettler Toledo, XPE 26) and transferred to the bottom of 10 ml borosilicate exetainer vials (Labco). 4 – 6 drops of 99.0 % pure (crystalline, water-free) phosphoric acid (H_3PO_4, melting point 42.35 °C) are manually added just beyond the rim of the vial, while holding it horizontally. Thus, contact of phosphoric acid and mineral sample is avoided in this stage of preparation, as long as the vial is not tilted. The vials are subsequently sealed with butyl rubber septa and attached horizontally to a flushing manifold, which allows parallel flushing of up to 28 sample flasks with pure helium (He 5.0). A flushing time of ≥ 5 mins and a gas flow of > 100 Nl/h is chosen to guarantee a complete expulsion of residual air in the vials. After flushing, samples are placed vertically in the autosampler, where they are heated to 70.0 ± 0.1 °C. After 30 mins of heating, complete contact of sample material with phosphoric acid is checked for. Samples are left to digest for a total digestion time of at least 60 mins before being analysed. The produced CO_2 gas is transferred into the GasBench using a sampling needle with He as a carrier gas. Water vapour, a potential by-product of the calcite – phosphoric acid reaction, is removed using Nafion traps. The CO_2 is separated from other possible contaminant gases using a gas chromatographic column (Poraplot Q with fused-silica column) heated to 70.0 °C. The CO_2 is then passed into the mass spectrometer, where the measured $^{18}O/^{16}O$ and $^{13}C/^{12}C$ isotope ratios are normalised against the isotope ratios of a CO_2 reference gas from a tank. Each sample analysis consists of four reference gas and six sample gas measurements.

A measurement session generally includes a zero enrichment test (10 successive measurements of the CO_2 reference gas to determine measurement reproducibility), background checks on the analyte isotopologue masses, at least two blank measurements (flushed exetainer vials, one empty and one with phosphoric acid) and measurements of two reference standard materials (NBS 18 and NBS 19, IAEA) in triplicate at the beginning and end of the sample run. In addition, an internal standard (Carrara marble, IVA) is measured at regular intervals in-between samples,

accounting for around ten percent of analyses, and used as drift standard. The measured $\delta^{13}C$ and $\delta^{18}O$ values (normalised against the reference gas) are ultimately calibrated against the measurements of the NBS 18/NBS 19 standard materials and reported as $\delta^{13}C_{VPDB}$ and $\delta^{18}O_{VPDB}$, respectively. Samples and intermediate drift standards are generally measured in duplicate. Typical precisions of measurements are summarised in Tab. 4-1 below.

Tab. 4-1: Accuracy and precision of internal IVA standard material and IAEA reference materials (since 2018).

For the IAEA reference materials (NBS 18 and NBS 19) only the pre-measurement reproducibility is given, as they are used as calibration standards during analysis.

	$\delta^{13}C_{VPDB}$	**$\delta^{18}O_{VPDB}$**
IVA		
Reference value ± 2 SD	2.073 ± 0.048	-2.025 ± 0.082
Measured average ± 2 SD (N = 126)	2.060 ± 0.022	-2.024 ± 0.042
Max. recorded 2 SD of a single measurement *(non-discarded analyses only)*		
IVA	0.147	0.290
NBS 18	0.137	0.271
NBS 19	0.132	0.276
Upper acceptance limit for 2 SD	0.160	0.300

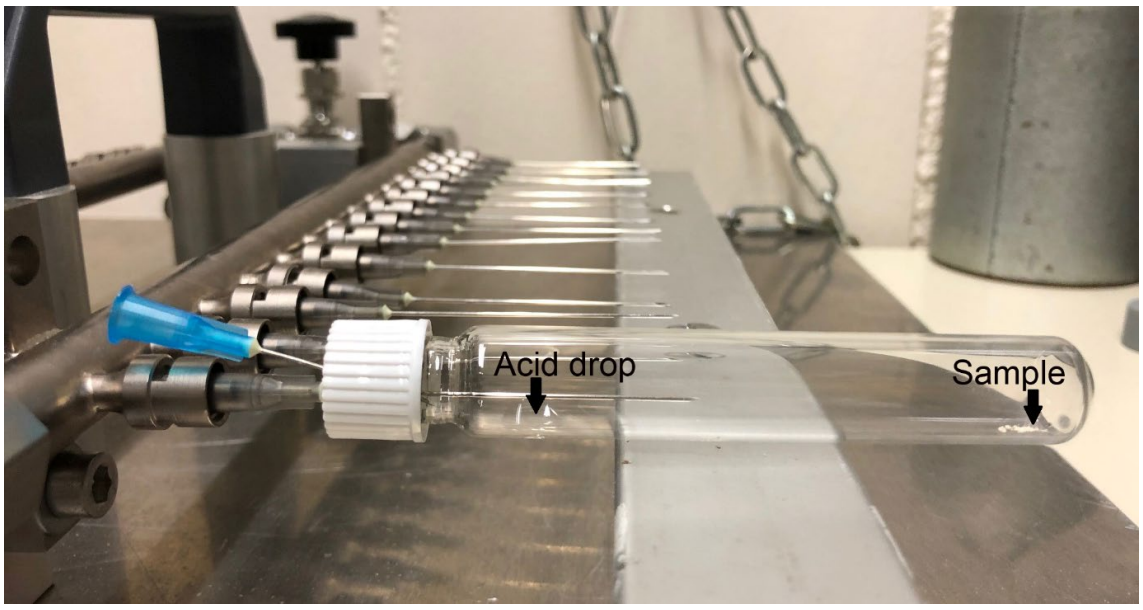

Fig. 4-1: Flushing manifold with a horizontally mounted exetainer vial. The spatial separation of the phosphoric acid and the carbonate sample are indicated by the arrows.

4.6.2 Strontium isotopes

Sr analyses of the whole rock carbonate fraction are performed on 0.02 to 0.05 g of dried rock powder, leached for at least one hour with 0.7 – 1 mL of 0.5 M acetic acid. After the leaching, the samples are centrifuged for 10 mins and the solid fraction is removed. After drying of the solution, the sample is spiked with ^{84}Sr, dried again and at least 100 µL of concentrated HNO_3 is added and evaporated. The residue is dissolved with 300 µL of 1 M HNO_3 and passed through a chromatographic column.

Sr isotopic analysis of vein samples is done with around 2 mg of powder drilled from the vein and leached with around 1 mL 6 M HCl. After leaching, the sample is dried and spiked with ^{84}Sr. The subsequent steps are the same as for the whole-rock carbonate procedure.

The Sr isotope measurements are made on an ICP mass spectrometer at Uni Bern. Every 5 – 6 samples, the international NBS 987 standard (certified $^{87}Sr/^{86}Sr$ ratio of 0.710245) is measured to correct for analytical deviation. The strontium concentration (ppm) in the sample is calculated from the sample spike weights and the measured $^{84}Sr/^{86}Sr$ ratio. Absolute analytical error (2 σ) on the $^{84}Sr/^{86}Sr$ ratio is generally around 0.000020.

4.7 Fluid-inclusion studies

Fluid inclusion studies performed at the University of Bern follow the general principles and practice of fluid inclusion studies outlined by Roedder (1984), Goldstein & Reynolds (1994) and Samson et al. (2003). Moreover, a detailed description of the method is provided by Diamond et al. (2015) and summarised as follows.

4.7.1 Petrographic investigations

Petrographic examination of the samples is performed at high magnification (objectives between 4× and 100×) using an Olympus BX51 polarising microscope. To facilitate this, a ~ 150 µm thick section is cut from each sample and polished on both sides to provide good transparency. Observations are made in normal transmitted light and in UV epi-illumination (to identify fluorescent, i.e. aromatic, hydrocarbons). Petrography is performed in three steps, which are described in the following.

4.7.1.1 Identification of assemblages of primary and secondary inclusions

First, groups of cogenetic inclusions (hereafter termed "fluid inclusion assemblages") are identified based on their geometric relationships with respect to their host mineral. These petrographic criteria allow the ages of the assemblages to be recognised with respect to events of mineral growth and brittle fracturing. Thus, assemblages of inclusions arrayed on crystal growth horizons are obviously trapped during growth of the host mineral and therefore termed primary. Inclusions trapped in healed fractures are obviously trapped at some time after crystal growth and therefore termed secondary. The relative ages of different secondary assemblages can be recognised from cross-cutting relationships.

4.7.1.2 Identification of entrapment mode

In a second step, still under the microscope at room temperature, the fluid phases within individual inclusions are identified and their volumetric proportions are estimated by eye (e.g. "80 vol.% liquid + 20 vol.% vapour"). In particular, the variation of the volume fractions within each assemblage is determined (e.g. "uniformly 20 vol.% vapour", or "variable between 10 and

90 vol.% vapour"). These variations, or lack thereof, can be interpreted within the theoretical framework of modern fluid inclusion studies (e.g. Diamond 2003a) to identify the original phase-state of the free paleofluids in the rocks. Thus, assemblages with uniform phase-volume fractions indicate that just one, homogeneous, paleofluid was present in the rock at the time of inclusion entrapment (e.g. "saline water" or "methane gas"). The volume fraction of vapour is uniform in this case, because all the inclusions, regardless of their shape or size, exsolve the same relative amount of vapour upon post-entrapment cooling to room temperature.

If the inclusions are small or flat (i.e. with relatively high surface free energy) and if the contained water is dense (from entrapment at low, diagenetic temperature) then bubble nucleation is inhibited and the result is a metastable liquid state. This phenomenon is well known and understood in the literature (e.g. Diamond 2003a). Empirically it has been found that liquid-only inclusions form at temperatures below about 70 °C (e.g. Goldstein & Reynolds 1994) and they also have been trapped from a homogeneous (i.e. single-phase) fluid. Thus, such assemblages are described during petrographic studies as having "uniformly 0 vol.% vapour", and they have the same significance as other assemblages of liquid + vapour inclusions with uniform phase proportions.

In contrast, assemblages with variable phase-volume fractions indicate that two or more paleofluids were present in the rock at the time of inclusion entrapment (e.g. "saline water + immiscible, coexisting methane gas"). In this case, the variable volume fractions arise from trapping of the coexisting phases (e.g. liquid and gas) in random proportions from the heterogeneous mixture.

4.7.1.3 Identification of paleofluid generations

Finally, the various inclusion assemblages are compared and, based on their relative ages, grouped into paleofluid generations. Organising these generations along a timeline reveals a paragenetic sequence, in which the history of fluid evolution in the samples with respect to mineral growth and fracturing can be visualised.

Once the above petrographic study using transmitted-light microscopy is completed, selected inclusions from each paleofluid generation are analysed by microthermometry and Raman spectroscopy. These techniques are described in the following.

4.7.2 Microthermometry

Heating and cooling experiments are performed to determine temperatures of equilibrium phase transitions within individual fluid inclusions, from which bulk salinity can be estimated and constraints placed on fluid trapping temperatures. Measurements are made with a Linkam MSD-600 heating – cooling stage mounted on an Olympus BX51 microscope. The inclusions are viewed during measurements through an Olympus 100×/0.80 LM PlanFI objective lens. The stage is calibrated using phase transitions in $CO_2 – H_2O$ and pure H_2O synthetic fluid inclusions, such measurements below 0 °C are accurate to ± 0.1 °C whereas those above room temperature are accurate to ± 0.5 °C.

4.7.2.1 Determination of homogenisation temperatures

The homogenisation temperature (T_h) is the equilibrium temperature at which a fluid inclusion transforms from a heterogeneous (multiphase) state (e.g. liquid + vapour) to a homogeneous state (e.g. liquid) upon gradual heating. In inclusions with liquid-like bulk densities the homogenisation transition is preceded by gradual shrinkage of the vapour bubble and the transition itself is defined at the moment when the bubble disappears completely. Reproducible equilibrium measurements are performed at a heating rate of ~ 0.5 °C/min.

4.7.2.2 Deduction of trapping temperatures from true homogenisation temperatures

In general, values of T_h are used to estimate fluid trapping temperatures in two ways (Diamond 2003a):

1. For inclusion assemblages trapped homogeneously (i.e. from one paleofluid phase), T_h provides a minimum constraint on the temperature at which the fluid was trapped by the host mineral. Most assemblages of homogeneously trapped fluid inclusions display a range of T_h values of ~10 – 15 °C, presumably owing to fluctuations in density, P or T during trapping. Thus, the highest value of the range can be used as the tightest constraint on the trapping temperature, i.e. $T_{trap} > T_{h,max}$. In cases where aqueous fluids are trapped at shallow depths (e.g. less than ~ 2 km) the difference between T_{trap} and T_h is only a few degrees. The trapping temperatures can be determined by following the descriptions and guidelines provided in Diamond et al. (2015).
2. Fluid inclusions that are trapped heterogeneously contain essentially random mechanical mixtures of the two or more fluids present in the rock pores. For reasons not explained here in detail (see Diamond 2003a, 2003b), the T_h value of the inclusion with the smallest fraction of vapour is assumed to be equal to T_{trap}. In general, this T_h value corresponds to the lowest in the assemblage, i.e. $T_{trap} = T_{h,min}$. Likewise, all the inclusions with higher fractions of vapour will homogenise at temperatures above $T_{trap.}$ The maximum T_h that can be observed is equal to the critical temperature of the fluid mixture. It is important to appreciate that, although T_h values up to several hundred degrees can be measured readily, none of the values higher than the lowest in the assemblage have any relevance for real temperatures attained in nature. They are simply artefacts of the random mixture of liquid and vapour initially enclosed in the inclusions at T_{trap} (Diamond 2003a, 2003b).
3. The inclusions that consist only of metastable liquid water, without vapour, cannot yield T_h values, and therefore the above principles of interpretation do not apply. The only constraint on trapping temperature that these inclusions provide is the empirical rule that they were trapped below about 70 °C (Goldstein & Reynolds 1994).

4.7.2.3 Determination of melting temperatures

Microthermometry at sub-zero temperatures is performed after the homogenisation temperatures of the fluid inclusions have been measured – i.e. to avoid any artefacts from potential stretching. For determining equilibrium phase transitions at sub-zero temperatures, the fluid inclusions are first cooled to -190 °C to promote nucleation of solid salt-hydrates and/or ice. The normal procedure of microthermometry at sub-zero temperatures is to heat slowly and determine the sequence of equilibrium transitions that defines the major components and bulk salinity of the inclusion uniquely, e.g. first the eutectic temperature followed by any peritectics and then the final melting temperature of the most stable solid phase from which the bulk salinity of the inclusions can be calculated in terms of equivalent wt.% NaCl or $CaCl_2$ + NaCl mixtures (denoted $NaCl_{eq}$ and $CaCl_2$+$NaCl_{eq}$; Hall et al. 1988, Oakes et al. 1990). This value can be taken as a proxy for the mass of total dissolved solids (TDS).

4.7.3 Laser Raman spectroscopy

This method is used to identify gases and certain minerals and hydrates within the fluid inclusions. Only compounds with dominantly covalent bonding yield Raman signals (e.g. methane, calcite, ice, solid CO_2), and so strong electrolytes such as NaCl cannot be detected when present in dissolved or anhydrous solid form. However, the various halide salts can be at least qualitatively

identified when present in hydrated form at very low temperatures (e.g. hydrohalite, $NaCl \cdot 2H_2O$; antarcticite, $CaCl_2 \cdot 6H_2O$). The samples need to be cooled well below room temperature to nucleate such hydrates.

This method is normally non-destructive but occasionally metastable components such as certain hydrocarbons may break down under the laser beam. Details of the method are given in Burke (2001). In practice, fluid inclusions hosted by calcite cannot always be analysed by Raman spectroscopy. This is due to the strong birefringence of calcite, which makes it difficult to aim the laser into small inclusions.

A Horiba Jobin-Yvon LabRam HR-800 confocal instrument at the Institute of Geological Sciences, University of Bern is used for the measurements. Red (632.8 nm) He-Ne and green (532.12 nm) Nd-YAG lasers are used for signal excitation, focussed through an Olympus BX41 microscope with an Olympus 100/0.95 UM PlanFI objective lens.

4.8 Organic geochemistry

Many investigations related to the organic geochemistry of rock materials do not follow standardised procedures, with different laboratories using different analytical methods, protocols and evaluation tools. Therefore, the methodologies will be documented in the respective reports together with the data.

5 Petrophysical Methods

M. Mazurek, T. Gimmi, L. Aschwanden

5.1 Gravimetric wet water content and water-loss porosity

The gravimetric wet water content (defined below) of the preserved core samples is obtained by gravimetric determination of water loss. Gravimetric water-loss is measured by drying sample aliquots of several hundred grams at 105° C to constant weight. Two or more subsamples are taken for all samples and measured separately. The gravimetric wet water content (w_w) is then calculated according to:

$$w_w = \frac{m_w - m_r}{m_w} = \frac{m_{pw}}{m_w} \tag{5-1}$$

where m_w is the mass of the wet rock, m_r is the mass of the dry rock, and m_{pw} is the mass of porewater.

Two types of uncertainties can be distinguished for measured parameters: (1) the analytical error and (2) the error derived from the standard deviation of measurements of multiple subsamples, which also includes errors related to spatial heterogeneity of properties. The error for a function, such as that defined in eq. (5-1), can be determined from errors of the measured parameters according to the first order error propagation approximation assuming uncorrelated parameters:

$$\sigma_f^2 = \sum_{i=1}^{n} \left(\frac{\partial f}{\partial x_i} \sigma_{x_i} \right)^2 \tag{5-2}$$

where $\sigma_{x_i}^2$ is the variance (square of standard deviation or, more generally, of error) of the variable x_i, and f is the function of the variables x_i. For the gravimetric wet water content, w_w, the relative error derived from the last term of eq. (5-1) according to eq. (5-2) is:

$$\left(\frac{\sigma_{w_w}}{w_w} \right)^2 = \left(\frac{\sigma_{m_w}}{m_w} \right)^2 + \left(\frac{\sigma_{m_{pw}}}{m_{pw}} \right)^2 \tag{5-3}$$

where $\sigma_{m_{pw}}$ should account for the error of the difference calculation according to eq. (5-2), e.g.:

$$\sigma_{m_{pw}}^2 = \sigma_{m_{rw}}^2 + \sigma_{m_r}^2 \approx 2\sigma_{m_r}^2 \text{ or } \sigma_{m_{pw}} \approx \sqrt{2}\sigma_{m_r} \tag{5-4}$$

Very similar errors are then derived when using the middle term instead of the last term in eq. (5-1). The analytical error of the weight determinations of the samples, i.e. σ_{m_r}, is 0.002 g, which allows for determination of the propagated analytical error σ_{w_w} for each subsample with the aid of eqs. (5-3) and (5-4). The standard deviation of w_w from measurements of different subsamples, which also includes the effect of small-scale variability of w_w, is generally larger than the analytical error. Therefore, this standard deviation is reported.

It is often convenient to use also the water content relative to the dry mass (w_d) of the rock (in the following termed "dry water content"). It is defined as:

$$w_d = \frac{m_w - m_r}{m_r} = \frac{m_{pw}}{m_r} \tag{5-5}$$

and its propagated error (using the last term) is calculated as:

$$\left(\frac{\sigma_{w_d}}{w_d}\right)^2 = \left(\frac{\sigma_{m_r}}{m_r}\right)^2 + \left(\frac{\sigma_{m_{pw}}}{m_{pw}}\right)^2, \tag{5-6}$$

where again eq. (5-4) has to be used for $\sigma_{m_{pw}}$.

The water-loss porosity or volumetric moisture content of a rock sample (ϕ_{WL}) is the ratio of its connected water-filled pore volume to its total volume (V_w/V_t). It can be obtained according to:

$$\phi_{WL} = \frac{w_w \cdot \rho_g}{w_w \cdot \rho_g + (1 - w_w) \cdot \rho_{pw}} \tag{5-7}$$

where ρ_{pw} = density of the porewater, ρ_g = grain density of the rock, and w_w = wet water content of the rock relative to its wet weight (eq. 5-1). For the porewater, a density of 1.00 g/cm^3 is assumed throughout. This is justified for samples with relatively low salinity (below that of seawater). It is also justified when considering that the gravimetric water content relates to the mass of the evaporated water and not to the mass of solution. For high salinity samples, a correction of the dry sample mass for precipitated salts would be required. The propagated error for the above formula for water-loss porosity is:

$$\sigma^2_{\phi_{WL}} = \frac{(1-w_w)^2}{[w_w\rho_g + (1-w_w)\rho_{pw}]^4}\left[\left(w_w\rho_{pw}\,\sigma_{\rho_g}\right)^2 + \left(w_w\rho_g\,\sigma_{\rho_{pw}}\right)^2 + \left(\frac{\rho_g\,\rho_{pw}}{(1-w_w)}\sigma_{\rho_g}\right)^2\right] \tag{5-8}$$

If σ_{ρ_g}, $\sigma_{\rho_{pw}}$, and σ_{w_w} inserted in this equation include only the analytical errors, the propagated $\sigma_{\phi_{WL}}$represents also an analytical error. The analytical error for the porewater density, $\sigma_{\rho_{pw}}$, is considered to be negligible in this case.

Please note that for the derivation of eq. (5-5) it is assumed that $V_t = V_w + V_s$ (with V_s the solid volume), i.e. that the sample is saturated. The volumetric water content for possibly unsaturated samples is better calculated from the bulk wet density ρ_{bw} or the bulk dry density ρ_{bd} (see definitions below) and w_w or w_d as:

$$\phi_{WL} = \frac{w_w \rho_{bw}}{\rho_{pw}} = \frac{w_d \rho_{bd}}{\rho_{pw}}. \tag{5-9}$$

The corresponding propagated relative errors are:

$$\left(\frac{\sigma_{\phi_{WL}}}{\theta_{WL}}\right)^2 = \left(\frac{\sigma_{w_w}}{w_w}\right)^2 + \left(\frac{\sigma_{\rho_{bw}}}{\rho_{bw}}\right)^2 + \left(\frac{\sigma_{\rho_w}}{\rho_w}\right)^2 \text{ or } \left(\frac{\sigma_{\phi_{WL}}}{\theta_{WL}}\right)^2 = \left(\frac{\sigma_{w_d}}{w_d}\right)^2 + \left(\frac{\sigma_{\rho_{bd}}}{\rho_{bd}}\right)^2 + \left(\frac{\sigma_{\rho_w}}{\rho_w}\right)^2 . \quad (5\text{-}10)$$

At full saturation, the volumetric water content should be equal to the porosity, whereas the volumetric water content of partially saturated samples, where some pores are gas-filled, is necessarily smaller than the porosity.

5.2 Grain and bulk densities, pycnometer porosity

Grain density (ρ_g) measurements are performed using milled rock powder (grain size with a mean of ~ 50 µm) which is dried for 24 hrs at 105 °C. Sulphate-rich samples are dried for 48 hrs at 40 °C. After drying, the samples are transferred into a desiccator and let cool down to room temperature. The grain density is then determined from the sample mass and the corresponding volume of the solid phase (V_s) of the sample. Accordingly, approximately 7 – 9 g sample material is weighted into a sample cup using a Mettler Toledo AT261 analytical balance (precision of ± 0.1 mg) and placed into a MicromeriticsTM AccuPyc II 1340 helium gas displacement pycnometer for determining V_s. A total of 10 purge and measuring cycles are performed per sample using gas fill pressures of 19.5 psi and equilibration rates of 0.005 psi/min. The grain density is determined as the average of the 10 measuring cycles if the standard deviation is ≤ 0.01 g/cm^3, otherwise the whole measurement sequence is repeated. The error given for the grain density from He pycnometry represents the standard deviation of the 10 successive volume estimates on a single sample.

The propagated error of the grain density from He pycnometry can be calculated as:

$$\left(\frac{\sigma_{\rho_g}}{\rho_g}\right)^2 = \left(\frac{\sigma_{m_r}}{m_r}\right)^2 + \left(\frac{\sigma_{V_s}}{V_s}\right)^2 \approx \left(\frac{\sigma_{V_s}}{V_s}\right)^2 \quad (5\text{-}11)$$

As stated above, the given error for the grain density from He pycnometry generally represents the standard deviation of 10 successive volume estimates on a single sample.

Bulk wet density, ρ_{bw}, is measured in duplicate or triplicate on the on-site conditioned samples using the paraffin displacement method which is based on Archimedes' principle. The entire procedure has to be conducted on saturated rock material, i.e. immediately after unpacking and removing the rim material from the preserved drillcore sample. Two separate, homogeneous rock samples of a volume of about 1.5 – 2 cm^3 are taken from the centre of the drillcore. The mass and volume of the wet sample is determined by weighing the rock sample in air and during immersion into paraffin using the density accessory kit of Mettler Toledo™. The bulk wet density is calculated according to:

$$\rho_{bw} = \frac{\rho_p \cdot m_w}{m_w - m_{wp}} = \frac{\rho_p \cdot m_w}{\Delta m_{wp}} \quad (5\text{-}12)$$

where m_w is the mass of the wet rock sample in air, m_{wp} is mass of the wet rock sample in paraffin, $\Delta m_{wp} = m_w - m_{wp}$, and ρ_p is the paraffin density.

The relative analytical error on bulk wet density is:

$$\left(\frac{\sigma_{\rho_{bw}}}{\rho_{bw}}\right)^2 = \left(\frac{\sigma_{\rho_p}}{\rho_p}\right)^2 + \left(\frac{\sigma_{m_w}}{m_w}\right)^2 + \left(\frac{\sigma_{\Delta m_{wp}}}{\Delta m_{wp}}\right)^2 \approx \left(\frac{\sigma_{\rho_p}}{\rho_p}\right)^2 \quad (5\text{-}13)$$

and is dominated by that in paraffin density. It is estimated to be ± 1.2 %. The error including possible small-scale variability is determined from the standard deviation of the bulk wet density from the 2 – 3 subsamples.

Bulk dry density (ρ_{bd}) is calculated from the water content relative to the dry mass (w_d) of the rock (in the following termed "dry water content") and the bulk wet density according to:

$$\rho_{bd} = \frac{\rho_{bw}}{1 + w_d} \quad (5\text{-}14)$$

The propagated relative error in the calculated bulk dry density is:

$$\left(\frac{\sigma_{\rho_{bd}}}{\rho_{bd}}\right)^2 = \left(\frac{\sigma_{\rho_{bw}}}{\rho_{bw}}\right)^2 + \left(\frac{\sigma_{w_d}}{1 + w_d}\right)^2 \quad (5\text{-}15)$$

The pycnometer porosity, Φ_{pyc}, is calculated from bulk dry and grain density according to:

$$\phi_{pyc} = 1 - \left(\frac{\rho_{bd}}{\rho_g}\right) \quad (5\text{-}16)$$

The propagated relative error in pycnometer porosity is:

$$\left(\frac{\sigma_{\phi pyc}}{\phi_{pyc}}\right)^2 = \left(\frac{\rho_{bd}}{\rho_g - \rho_{bd}} \cdot \frac{\sigma_{\rho_{bd}}}{\rho_{bd}}\right)^2 + \left(\frac{\rho_{bd}}{\rho_g - \rho_{bd}} \cdot \frac{\sigma_{\rho_g}}{\rho_g}\right)^2 \quad (5\text{-}17)$$

5.3 Nitrogen ad/desorption isotherms and external surface area (BET)

Ad-/desorption isotherms and BET surface areas are determined by nitrogen adsorption. Samples are mildly crushed (about 30 s in a disc mill, same programme as for clay mineralogy). Around 0.5 – 1 g of the sample powders are weighed into the standard sample cell (1.8 cm^3 volume) to an accuracy of 0.001 g and thoroughly desorbed of primary gases by heating under vacuum at 150 °C overnight with the BELPREP – vac III pre-treatment device. After the sample has cooled to room temperature, the dry mass is recorded.

Adsorption isotherms are measured in equilibrium with liquid nitrogen (N_2) using a BELSORP-miniX surface analyser. After the determination of the dead volume in the sample cell (with helium), the cell is evacuated again and N_2 is dosed stepwise until the pressure in the cell reaches pressure conditions near saturation (0.994 p/p_0). The desorption of N_2 follows immediately after reaching the equilibrium conditions at 0.994 p/p_0 and is recorded until the pressure decreases to 0.3 p/p_0. Thus, the adsorption isotherm is recorded from 0.01 to 0.994 p/p_0, and the desorption isotherm is recorded from 0.994 to 0.3 p/p_0. The N-surface area is calculated using the Brunauer,

Emmet and Teller method (BET; Brunauer et al. 1938) for a pressure range of p/p_0 from 0.05 to 0.3. The specific surface area (expressed as m^2/g) is obtained from the N-surface area and the sample mass.

The reproducibility of the BET measurements is generally very good (better than 0.1 %), unless the surface areas are very low. Uncertainties including those of the preparation of the samples are probably larger and are estimated to be around ± 5 %.

6 Aqueous & CEC Extraction Techniques

H.N. Waber

6.1 Aqueous extraction technique

6.1.1 Sample preparation and experimental procedure

For aqueous extraction tests, saturated rock material from the central part of the on-site conditioned drill cores is selected to exclude any contamination from the drilling process. Such material is obtained by removing about 2 cm of the outer core rim using a chisel and hammer immediately after unpacking drill cores in the laboratory. Rock chips of about 10 cm^3 of the central part of the core are further disintegrated by hand along grain boundaries to pieces of a few mm^3 to avoid opening of mineral fluid inclusions. About 30 g of the disintegrated, saturated rock is immediately immersed in pre-prepared polypropylene tubes containing 30 mL of degassed oxygen- and CO_2-free ultra-pure water. This degassed water is prepared by N_2-bubbling for at least 30 mins in the O_2-free atmosphere inside the glovebox. Subsequently, the headspace of tubes is flushed with N_2-gas to remove all air. The tubes are then closed under this N_2-gas stream and quickly transferred into a glovebox where they are shaken end-over – end-under in an oxygen-free atmosphere. Such atmosphere is provided in an anaerobic chamber (glovebox, 95:5 N_2:H_2) equipped with two oxygen scrubbers (palladium catalyst). The chamber is regularly vented with a mixture of 8 % H_2 in N_2 to maintain a H_2 concentration between 3 % and 5 %. Such level of H_2 combined with the action of the two O_2 scrubbers ensures a permanent O_2-free atmosphere.

The preparation time from the large chips until immersion of the small pieces into the water and closure of the polypropylene tube is minimised to less than 5 mins to suppress sulphide mineral oxidation and pore-water evaporation as much as possible. All sample handling is conducted using surgical rubber gloves in order to minimise Cl^- contamination from the skin. For each preparation campaign a blank extraction is also performed.

Extraction conditions are chosen to 1) attain equilibrium with calcite by extracting over 24 hours and 2) to suppress sulphide mineral oxidation. Duplicate extraction allows quality control with respect to the homogeneity of the extracted rock material. This is crucial in the case of the possible occurrence of solid sulphate and chloride minerals in the rock, but also in the case of sulphides (e.g. pyrite) where it helps to identify possible oxidation during the rock preparation and extraction process.

The solid:liquid (S:L) ratio relative to the saturated (wet) weight of rock is chosen to be 1:1 for the majority of samples. The mass of rock chips used in the extractions is commonly 30 g. For lithologies of largely different mineralogy aqueous extraction tests are also conducted on 4 different S:L ratios of 0.1, 0.25, 0.5, and 1. For conversion of the solid:liquid ratio relative to the dry weight of rock in the extraction tests, the wet weight of extracted rock is converted to dry weight using the water content measured on each sample.

After extraction, the polypropylene tubes that now contain a dark coloured suspension are removed from the glovebox and phase separation is conducted by centrifugation. The supernatant leach solution is quickly removed using a syringe. From the syringe, the clear extract solution is transferred into PPE bottles under filtration with 0.45 followed by 0.2 μm PES filters and stored for analyses.

6.1.2 Chemical and isotope analyses of aqueous extract solutions

After filtration, the supernatant solution is split into two aliquots. One aliquot is used for immediate analysis of pH and titration for the total alkalinity. The remaining solution of the aliquot is then stored in a refrigerator for later analyses of anions by ion-chromatographic techniques (*cf.* Chapter 13) and Cl-isotope composition in an external laboratory. The second aliquot is acidified to a pH of about 2 – 3 immediately after filtration and stored in a refrigerator for later analyses of cations by ion-chromatographic and spectrometric techniques (*cf.* Chapter 13).

6.1.3 Conversion of aqueous extract data to porewater concentrations

The solutes in an aqueous extract solution may originate from different potential sources that have to be identified before aqueous extract ion concentration can be converted to porewater ion concentrations. These sources are:

1. Original solutes in porewater
2. Solutes in mineral fluid inclusions
3. Induced mineral dissolution, precipitation, and ion exchange and sorption reactions during the extraction test.

In clay-dominated argillaceous rock samples, the volumes of fluid inclusions in the matrix are usually low relative to the volume of porewater, rendering this source of solutes as negligible (e.g. Waber et al. 2003a). In contrast, this source may become important in the more carbonate-rich and quartz-rich rocks of these stratigraphic units. A possible impact of fluid inclusion solutes on the ion concentration in aqueous extract data is circumvented by disintegrating the rock material along its grain boundaries (see above), thus inhibiting (or at least greatly reducing) the opening of fluid inclusions in quartz and carbonate minerals, as will occur when grinding the rock.

Mineral reactions will inevitably take place during aqueous extraction and will modify the porewater solute concentrations. Therefore, conversion of solute concentrations measured in aqueous extract solution to porewater solute concentrations is only applicable for ions that are not involved in any reaction (i.e. behave chemically conservative) and for which the only source is the porewater. In the Jurassic sedimentary rocks at the Mont Terri URL, these conditions are met by the anions Cl^- and Br^-, whereas all cations and other anions are to variable degrees involved in mineral reactions (Waber et al. 2003a).

In addition to the chemical behaviour of an element, the porosity that is accessible to this element in its dissolved state has to be known for conversion of solute concentrations measured in aqueous extract solution to porewater solute concentrations. This accessible porosity is species-specific, depends on the rock mineralogy and texture and has to be derived from comparison of different extraction techniques such as advective displacement (*cf.* Chapter 9) or squeezing (*cf.* Chapter 10), through-diffusion experiments and/or theoretical approaches based on the rocks' petrophysical properties and mineralogy.

Once the chemical conservative behaviour of an element during aqueous extraction is proven and the species-specific accessible porosity is known, the solute concentration measured in the aqueous extract solution can be converted to the porewater solute concentrations according to:

$$C_{pw} = C_{aqex} \cdot \frac{m_{w,aqex}}{m_{pw}} \cdot \frac{S_w}{f_a} = C_{aqex} \cdot \frac{1}{\left(\frac{S^*}{L^*}\right) \cdot w_w} \cdot \frac{S_w}{f_a} \qquad (6\text{-}1)$$

where C_{pw} is the apparent solute concentration in porewater (mg/kg$_{H2O}$), C_{aqex} is the concentration of chemically conservative solutes in the aqueous extract solution (mg/kg$_{H2O}$), $m_{w,\,aqex}$ is the mass of extraction water added, m_{pw} is the mass of porewater in the sample used for aqueous extraction, S_w is the water saturation of the sample relative to in situ conditions, f_a is the fraction of solute accessible pore volume per water-accessible (water-loss) porosity, $S^*{:}L^*$ is the ratio of wet solid added to the mass of extraction water (wet solid:liquid ratio, see below), and w_w is the gravimetric water content of the rock sample relative to dry mass (kg$_{H2O}$/kg$_{rock}$).

Based on previous experiences (e.g. Waber et al. 2003b, Mazurek et al. 2012, Waber et al. 2012, Wersin et al. 2013, Mazurek et al. 2017), the porewater in the Jurassic lithologies of Northern Switzerland is expected to have an ionic strength below that of seawater and the (ab initio unknown) density of porewater can be assumed to be 1 g/cm^3 without introducing significant uncertainty. Similarly, the saturation state, S_{wet}, is taken to be 1.00 based on the applied sampling and sample preparation protocols (see above).

The uncertainty of the so-derived porewater compositions can be assessed by:

$$\sigma_{C_{pw}} = \sqrt{\left(\frac{\sigma_{C_{aqex}}}{C_{aqex}}\right)^2 + \left(\frac{\sigma_{S^*/L^*}}{\frac{S^*}{L^*}}\right)^2 + \left(\frac{\sigma_{w_w}}{w_w}\right)^2 + \left(\frac{\sigma_{f_a}}{f_a}\right)^2} \qquad (6\text{-}2)$$

From eqs. (6-1) and (6-2) it can be seen that the uncertainties of C_{aqex}, of f_a and S_w are the main contributors to the overall uncertainty of C_{pw}. Whereas the relative uncertainties for C_{aqex} is well-defined to be ± 5 %, those of S_w and f_a are more difficult to assess.

For the Opalinus Clay at the Mont Terri URL it could be shown that assuming for S_w a relative error of ± 5 %, based on the applied sampling and sample preparation protocols, and for f_a one of ± 10 % based comparison of aqueous extraction data to borehole water, squeezed water and long-term diffusion data (Pearson et al. 2003, Gimmi et al. 2014, Waber & Rufer 2017), the propagated relative uncertainties for porewater concentrations of the chemically conservative Cl^- and Br^- become about 10 – 15 %. A larger uncertainty has to be considered for the samples of the Passwang Formation where f_a is not known and has to be assumed.

Note that the preparation of the aqueous extract occurs using the saturated rock material, including the mass of porewater as indicated by wet solid:liquid ratio $S^*{:}L^*$. The conversion of the wet solid:liquid ratio to the dry solid liquid ratio $S{:}L$ for extraction of previously dried rock can be formulated as:

$$\frac{Solid_d}{m_{w,add}} = \frac{Solid_w - m_{pw}}{m_{w,add}} = \frac{Solid_w - (w_d \cdot m_{Solid,d})}{m_{w,add}} \qquad (6\text{-}3)$$

6.2 Cation exchange (CEC) extraction technique

The determination of the cation exchange capacity (CEC) and the exchangeable cation populartions is performed using Ni^{+2} as index cation in a Ni-ethylenediamine cationic dye ($Ni(en)_3$, also referred to as Ni-en). The method follows essentially the protocols developed at PSI and described in Baeyens & Bradbury (1994) and Bradbury et al. (1997) with the improvements and modifications described in Hadi et al. (2019).

6.2.1 Sample preparation and experimental procedure

For CEC extraction tests, saturated rock material from the central part of the on-site conditioned drill cores is selected to exclude any contamination from the drilling process. The material is simultaneously obtained with that used for aqueous extraction and prepared in the same way (*cf.* Section 6.1.1) and the preparation criteria and processing of the rock material is essentially the same as for aqueous extraction experiments.

Following preparation of the rock material, the disintegrated, saturated rock material is immediately immersed in pre-prepared polypropylene tubes containing 30 mL of Ni-en solution. Subsequently, the headspace of tubes is flushed with N_2-gas to remove all air. The tubes are then closed under this N_2-gas stream and quickly transferred into a glovebox where they are shaken end-over – end-under in an oxygen-free atmosphere. Such atmosphere is provided an anaerobic chamber (glovebox, 95:5 N_2:H_2) equipped with two oxygen scrubbers (palladium catalyst). The chamber is regularly vented with a mixture of 8 % H_2 in N_2 to maintain a H_2 concentration between 3 % and 5 %. Such level of H_2 combined with the action of the two O_2 scrubbers ensures a permanent O_2-free atmosphere.

The $Ni(en)_3$ stock solution is prepared from hydrated Ni-nitrate ($Ni(NO_3)_2*6H_2O$) and ethylenediamine ($C_2H_8N_2$) in degassed O_2- and CO_2-free ultrapure water. This degassed water is prepared N_2-bubbling for at least 30 mins. The pH of the $Ni(en)_3$ stock solution is adjusted to a pH of 8.2 to 8.3 by adding concentrated nitric acid (HNO_3 65 %). All these preparation steps take place in the O_2-free atmosphere inside the glovebox. The molality of the $Ni(en)_3$ solution is chosen to be about 1.5 – 2 times that of the expected cation exchange capacity. The optimal molality of the $Ni(en)_3$ solution is such that the strongly exchanging Ni^{2+} ion displaces all original cation from the exchange sites and the difference between the Ni^{2+} concentration before and after the experiment, i.e. the Ni-consumption, becomes large enough to minimise the analytical uncertainty in this difference.

As for aqueous extractions the extraction conditions are chosen to 1) attain equilibrium with calcite by extracting over 24 hrs and 2) to suppress sulphide mineral oxidation. Duplicate extraction allows quality control with respect to the homogeneity of the extracted rock material.

The solid:liquid (S:L) ratio relative to the saturated (wet) weight of rock is chosen to be 1:1 for the majority of samples. The mass of rock chips used in the extractions is commonly 30 g. For lithologies of largely different mineralogy aqueous extraction test are also conducted on 4 different S:L ratios of 0.1, 0.25, 0.5, and 1. For conversion of the solid:liquid ratio relative to the dry weight of rock in the extraction tests, the wet weight of extracted rock is converted to dry weight using the water content measured on each sample.

After extraction, the polypropylene tubes that now contain a dark purple suspension, are removed from the glovebox and phase separation is conducted by centrifugation of the polypropylene tubes. The supernatant leach solutions are quickly removed using a syringe. From the syringe, the coloured extract solution is transferred into PPE bottles under filtration with 0.45 followed by 0.2 μm PES filters and stored for analyses.

6.2.2 Chemical analyses of Ni-en extract solutions

After filtration, the supernatant $Ni(en)_3$ extract solution is immediately analysed for pH and diluted by a factor of 10 to 100 before storage to supress changes of the solution and mineral precipitation. This is followed by cation analysis using spectrometric techniques and anion analyses of the $Ni(en)_3$ extract solution using ion-chromatographic techniques as described in Chapter 13.

6.2.3 Derivation of CEC and exchangeable cation populations

The cation exchange capacity, CEC, of a rock sample is derived from the consumption of the index cation during extraction. It is thus represented by the difference in concentration of the index cation in the $Ni(en)_3$ stock solution before and in the $Ni(en)_3$ extract solution after the experiment. The CEC of a rock samples is calculated according to:

$$Ni_c = C_{Ni\,st}\frac{m_{wst}}{m_s} - C_{Ni\,ex}\frac{m_{pw}+m_{wst}}{m_s} \tag{6-4}$$

where Ni_C is the Ni-consumption (or CEC), $C_{Ni\,st}$ is the Ni^{+2} concentration in the stock solution prior to the extraction $C_{Ni\,ex}$ is the Ni^{+2} concentration in the extract solution after the experiment, m_{wst} is the mass of stock solution, m_s is the mass of solid added to the stock solution, and m_{pw} is the mass of porewater in the rock sample.

The uncertainty of the derived CEC is approached by the propagation of all analytical error as conducted by T. Gimmi and can be expressed as:

$$\sigma^2_{Ni_c} = \left(\frac{m_{wst}}{m_s}\sigma_{C_{Ni\,st}}\right)^2 + \left(\frac{m_{pw}+m_{wst}}{m_s}\sigma_{C_{Ni\,ex}}\right)^2 + \left(\frac{C_{Ni\,st}-C_{Ni\,ex}}{m_s}\sigma_{m_{wst}}\right)^2 + \left(\frac{C_{Ni\,ex}}{m_s}\sigma_{m_{pw}}\right)^2 + \left(\frac{C_{Ni\,st}m_{wst}-C_{Ni\,ex}[m_{pw}+m_{wst}]}{m_s^2}\sigma_{m_s}\right)^2 \tag{6-5}$$

It should be noted that in this derivation the error of the spectrometric determination of Ni^{+2} in the stock solution and the $Ni(en)_3$ extract solution should be taken as the precision of the measurements (± 2 %) and not the accuracy (± 6%). This is because both these solutions are analysed in the same sample batch with the same instrument and standard conditions Because it is the difference of these two analytical values that is relevant, the accurate concentration is not relevant for error considerations. Further variations of the derivation of the uncertainty in the derivation of CEC are given in Appendix A.

The major cations analysed in the $Ni(en)_3$ extract solution represent for each cation the sum of its inventory exchanged from the clay surfaces and interlayers and its concentration in the porewater. As a consequence, the sum of analysed cation will exceed that of the Ni-consumption as a function of ionic strength of the porewater.

The derivation of the in situ cation exchange population requires, therefore, correction for the inventory of cations present in the porewater. Several such correction procedures have been proposed in the past (e.g. Baeyens & Bradbury 1994, Bradbury et al. 1997, Waber et al. 2003a and b, Wersin et al. 2013, Hadi et al. 2019). In all these approaches the concentrations obtained of the $Ni(en)_3$ extract solution had to be compared to aqueous extraction data that were conducted in parallel in order to have information about the anion concentrations in the extract solution. Recent developments in the analytical procedure now also allows exact quantification of anion concentrations in the $Ni(en)_3$ extract solution by applying special ion-chromatographic techniques (*cf.* Chapter 13). The implementation of such data into a refined correction procedure is, however, pending and will be further developed during the TBO programme.

7 Isotope Exchange Technique

P. Wanner

7.1 Analyses of stable water isotopes ($\delta^{18}O$, $\delta^{2}H$)

The stable oxygen and hydrogen isotope ratios of water ($\delta^{18}O$ and $\delta^{2}H$) is analysed using a Picarro L2120-i cavity ring down spectrometer (CRDS) with vaporisation module V1102-i. Raw data $\delta^{18}O$ and $\delta^{2}H$ values are obtained by a tenfold measurement of each sample. Afterwards, post run-correction (memory and drift) of measured $\delta^{18}O$ and $\delta^{2}H$ raw values is made following the method described by van Geldern & Barth (2012). To receive $\delta^{18}O$ and $\delta^{2}H$ values on the Vienna Standard Mean Ocean Water (VSMOW) scale, raw values are calibrated against two internal standards, which were referenced to the VSMOW scale using international IAEA standards. The two standards used for calibration differ in their isotope composition and span a calibration interval between -27.41 ‰ and -2.65 ‰ for $\delta^{18}O$ values and between -209.8 ‰ and -13.9 ‰ for the $\delta^{2}H$ values, respectively. The analytical uncertainty of the $\delta^{18}O$ and $\delta^{2}H$ measurements was determined based on multiple internal and IAEA standard analysis and corresponds to 0.1 ‰ and 1.5 ‰, respectively.

7.2 Diffusive isotope exchange technique

To determine the stable oxygen and hydrogen isotope composition ($\delta^{18}O$ and $\delta^{2}H$) of the porewater and its mass in the drill core samples, the diffusive exchange technique is used. The technique is based on the equilibration between a test water with known isotope composition and the porewater of the rock core material, which has an unknown isotope signature using the gas phase as a diaphragm (e.g. Rogge 1997, Rübel 2000, Rübel et al. 2002, Rübel & Bath 2003).

For porewater – test water equilibration, around 200 g of saturated rock pieces from the centre of the drill core samples with a size of 3 – 4 cm^3 are prepared and placed in a vapour-tight glass container along with a small crystallisation dish containing a test water with a known mass and isotopic composition. During rock material preparation, the air exposure time is limited to less than 5 mins to minimise evaporation effects. After placing the test water and the rock pieces into vapour-tight glass container, it is closed and stored in a Styrofoam box for at least 5 weeks at constant temperature (23°C) to ensure isotopic equilibration between the test water and porewater of the saturated rock material.

After equilibration, the test water is removed from the crystallisation dish and stored in two vapour-tight 1.5 mL glass vials and the saturated rock material is weighted. The stable oxygen and hydrogen isotope composition ($\delta^{18}O$ and $\delta^{2}H$) of the stored test water is then analysed by isotope ratio infrared spectroscopy (IRIS) using a Picarro L2120-i cavity ring down spectrometer (CRDS) as described in detail in section 7.1. Additionally, the gravimetric water content of the rock material, which was emplaced in the vapour-tight glass container, is obtained by drying the material in an oven at 105 ºC until the rock material reaches a constant mass.

Based on the $\delta^{18}O$ and $\delta^{2}H$ measurements of the equilibrated test water, the isotope composition ($\delta^{18}O$ and $\delta^{2}H$) and the mass of the porewater can be calculated based on the following mass balance relationship (Rogge 1997, Rübel 2000):

$$m_{PW} \cdot C_{PW(t=0)} + m_{TW} \cdot C_{TW(t=0)} = (m_{PW} + m_{TW}) \cdot C_{TW(t=\infty)} \quad (7\text{-}1)$$

where m_{PW} and m_{TW} are the masses of porewater and test water, respectively, c_{PW} is the original (in situ) isotope composition of porewater ($\delta^{18}O_{PW}$, $\delta^{2}H_{PW}$), and c_{TW} is the isotope composition ($\delta^{18}O_{TW}$, $\delta^{2}H_{TW}$) of the test water. Isotope compositions, on the left side of the equation are prior to equilibration (t = 0), while isotope compositions on the right side refers to the time after equilibration is achieved (t = ∞).

In eq. (7-1), the mass (m_{TW}) and isotope composition ($\delta^{18}O_{TW}$, $\delta^{2}H_{TW}$) of test water before and at the end of the experiment are known, whereas the isotope composition and the mass of the porewater ($\delta^{18}O_{PW}$, $\delta^{2}H_{PW}$, m_{PW}) are unknown. To resolve the three unknowns (m_{PW}, $\delta^{18}O_{PW}$, $\delta^{2}H_{PW}$), two isotope exchange experiments are conducted for each core sample with test waters having different isotope compositions. The two used test waters included laboratory tap water (LAB) and melt water of and ice core drilled in Greenland (NGW). The isotope composition of the LAB test water is $\delta^{18}O$ = -11.43 ‰ and $\delta^{2}H$ = -83.1 ‰, respectively and that of the NGW test water equals $\delta^{18}O$ = -26.66 ‰ and $\delta^{2}H$ = -206.3 ‰, respectively. Based on the two isotope exchange experiments, eq. (7-1) can be formulated for the two experiments and for the $\delta^{2}H$ and $\delta^{18}O$ measurements, respectively yielding four independent equations that include the three unknowns (m_{PW}, $\delta^{18}O_{PW}$, $\delta^{2}H_{PW}$). By combining these four equations the unknown porewater mass (m_{PW}) or water content ($WC = m_{pw}/m_R$) and isotope composition ($C_{PW} = \delta^{18}O_{PW}$, $\delta^{2}H_{PW}$) can be expressed and calculated as a function of the known test water masses (m_{TW}), test water isotopic composition ($\delta^{18}O_{TW}$, $\delta^{2}H_{TW}$) and the mass of the rock material that was used for the isotope exchange experiments (mR_1 mR_2):

$$WC = \frac{m_{PW}}{(m_{R1}+m_{R2})/2} = \frac{m_{TW1}\cdot m_{R1}\cdot(C^{0}_{TW2}-C^{\infty}_{TW2})+m_{TW1}\cdot m_{R2}\cdot(C^{\infty}_{TW1}-C^{0}_{TW1})}{m_{R1}\cdot m_{R2}\cdot(C^{\infty}_{TW2}-C^{\infty}_{TW1})} \tag{7-2}$$

$$C_{PW} = \frac{C^{\infty}_{TW1}\cdot m_{TW2}\cdot m_{R1}\cdot(C^{\infty}_{TW2}-C^{0}_{TW2})-C^{\infty}_{TW2}\cdot m_{TW1}\cdot m_{R2}\cdot(C^{\infty}_{TW1}-C^{0}_{TW1})}{m_{TW2}\cdot m_{R1}\cdot(C^{\infty}_{TW2}-C^{0}_{TW2})-m_{TW1}\cdot m_{R2}\cdot(C^{\infty}_{TW1}-C^{0}_{TW1})} \tag{7-3}$$

where m_{TW1} and m_{TW2} are the masses of test waters 1 and 2, respectively, m_{R1} and m_{R2} correspond to the masses of saturated (wet) rock in experiments 1 and 2, respectively and C_{TW1} and C_{TW2} are the isotope compositions ($\delta^{18}O$ and $\delta^{2}H$) of test waters 1 and 2, respectively, whereby the superscripts 0 and ∞ denote the isotope composition prior to and after test water – porewater equilibration.

A perquisite for the determination of the isotope composition of the porewater (C_{PW}; eq. 7-3) from the two diffusive exchange experiments (LAB and NGW) is the equality of the water contents of the rock samples that are used in the two experiments (Hobbs et al. 2011). Thus, if the water content in the rock samples of the two diffusive exchange experiments differs by more than 10 – 20 %, the diffusive exchange experiment cannot be used.

The uncertainty associated with the water content (WC) (eq. 7-2) and isotope composition (C_{PW}) (eq. 7-3) can be determined based on Gauss's law of error propagation:

$$\sigma(WC) = \sqrt{\begin{matrix}\{dm_{WC}dm_{TW1}\cdot\sigma(m_{TW1})\}^2+\{dm_{WC}dm_{TW2}\cdot\sigma(m_{TW2})\}^2+\\ \{dm_{WC}dC^{0}_{TW1}\cdot\sigma(C^{0}_{TW1})\}^2+\{dm_{WC}dC^{0}_{TW2}\cdot\sigma(C^{0}_{TW2})\}^2+\\ \{dm_{WC}dC^{\infty}_{TW1}\cdot\sigma(C^{\infty}_{TW1})\}^2+\{dm_{WC}dC^{\infty}_{TW2}\cdot\sigma(C^{\infty}_{TW2})\}^2\end{matrix}} \tag{7-4}$$

$$\sigma(C_{PW}) = \sqrt{\begin{array}{c}\{dC_{PW}dm_{TW1} \cdot \sigma(m_{TW1})\}^2 + \{dC_{PW}dm_{TW2} \cdot \sigma(m_{TW2})\}^2 + \\ \{dC_{PW}dm_{R1} \cdot \sigma(m_{R1})\}^2 + \{dC_{PW}dm_{R2} \cdot \sigma(m_{R2})\}^2 + \\ \{dC_{PW}dC^0_{TW1} \cdot \sigma(C^0_{TW1})\}^2 + \{dC_{PW}dC^0_{TW2} \cdot \sigma(C^0_{TW2})\}^2 + \\ \{dC_{PW}dC^\infty_{TW1} \cdot \sigma(C^\infty_{TW1})\}^2 + \{dC_{PW}dC^\infty_{TW2} \cdot \sigma(C^\infty_{TW2})\}^2\end{array}} \quad (7\text{-}5)$$

where σ(m) = 0.002 g and σ(C) = 0.1 ‰ for $\delta^{18}O$ and 1.0 ‰ for δ^2H, and d = sensitivity of parameter a to parameter b. The error for the porewater mass and isotope composition is calculated individually for each sample.

The uncertainty of the water content (WC) and the porewater isotope composition (C_{PW}) depends mainly on the mass ratio of porewater to test water. The uncertainty can be reduced when the ratio between the porewater and the test water is close to one. To obtain a test water porewater ratio close to one, test water volumes of 3 – 5 mL for the individual experiments and rock types are used based on based on previous experiences with the different rock units (Malm, Dogger, Lias, Keuper, Muschelkalk) (Pearson et al. 2003). Moreover, to assess potential uncertainties caused by the evaporation of test water or porewater weight records of the empty and filled vapour-tight glass container and crystallisation dish, the mass of the rock and of the test water were collected. The isotope diffusive exchange technique is also sensitive to possible condensation of test water on the glass container walls and on the rock fragments, as well as to large differences between the salinity of the test water and porewater. Condensation and large differences in salinity may result in uncontrollable desiccation-condensation processes with related isotope fractionation effects during the diffusive exchange experiments. Whereas condensation of test water can be inhibited by lowering the water-vapour pressure above the test-water surface through the addition of NaCl salt, the amount of NaCl added should be optimised with respect to the expected porewater Salinity. Salinity-induced liquid-vapour fractionation is minimal for the oxygen isotopes of the water molecule but may become significant for the hydrogen isotopes. According to Horita et al. (1993), the systematic effect on the δ^2H value at room temperature is about 2.7‰ × ΔM, where ΔM denotes the difference in salinity in mol/kgH2O between solutions. From previous investigations it is known that the porewater Cl content varies between about 0.1 to 0.4 M in the Malm, Dogger, Lias and upper Keuper units (Pearson et al. 2003), whereas in the lower Keuper and Muschelkalk units the Cl contents of up to 0.7 M can be expected. Thus, to suppress condensation and to minimise the difference in salinity between test water and porewater the salinity of the test waters was adjusted to 0.3 M NaCl in the Malm, Dogger, Lias and upper Keuper and to 0.7 M in the lower Keuper and Muschelkalk units. The difference in salinity is therefore < 0.25 mol/kgH_2O and the absolute error due to salinity effects on the δ^2H value of the test waters becomes < 1 ‰ being well within the analytical uncertainty.

8 Dissolved Noble Gases in Porewater

D. Rufer

The determination of porewater noble gas concentrations is based on the quantitative release of (dissolved) gases in the porewater of a rock sample under conditions different from those prevailing in situ (e.g. Osenbrück et al. 1998, Rübel et al. 2002, Rufer et al. 2018). Due to their low solubility in water under ambient conditions (Weiss 1971, 1970), noble gases are quantitatively released from the porewater of the rock sample. The chemical inertness of noble gases inhibits any reaction during outgassing so that the released amounts of noble gases can be calculated into concentrations in porewater using the mass of porewater of the rock sample.

After sealing the drillcore sample piece into the evacuated sample container (for a detailed description of the sampling procedure see Rufer 2019), the dissolved gases are quantitatively released from the porewater by molecular diffusion into the container's void volume. The time required to reach equilibrium conditions depends on the transport properties of the rock material as well as the sample size and geometry. It has been demonstrated that for sedimentary rocks, equilibration times of up to two months suffice to attain steady state with regards to He and, that under these conditions, significantly less than 1 % of the ^{4}He stays dissolved in the porewater (Bigler 2003, Osenbrück et al. 1998).

8.1 Noble gas sample processing and analysis

Noble gas analyses are conducted at the Institute of Geological Sciences, University of Bern, to determine ^{4}He, ^{20}Ne, ^{22}Ne and ^{40}Ar concentrations, and ^{40}Ar/^{36}Ar isotope ratios according to the analytical methods outlined below and illustrated in Fig. 8-1. ^{3}He/^{4}He isotope ratio measurements are performed at the Institute of Environmental Physics, University of Bremen, Germany according to the procedure given in Sültenfuss et al. (2009).

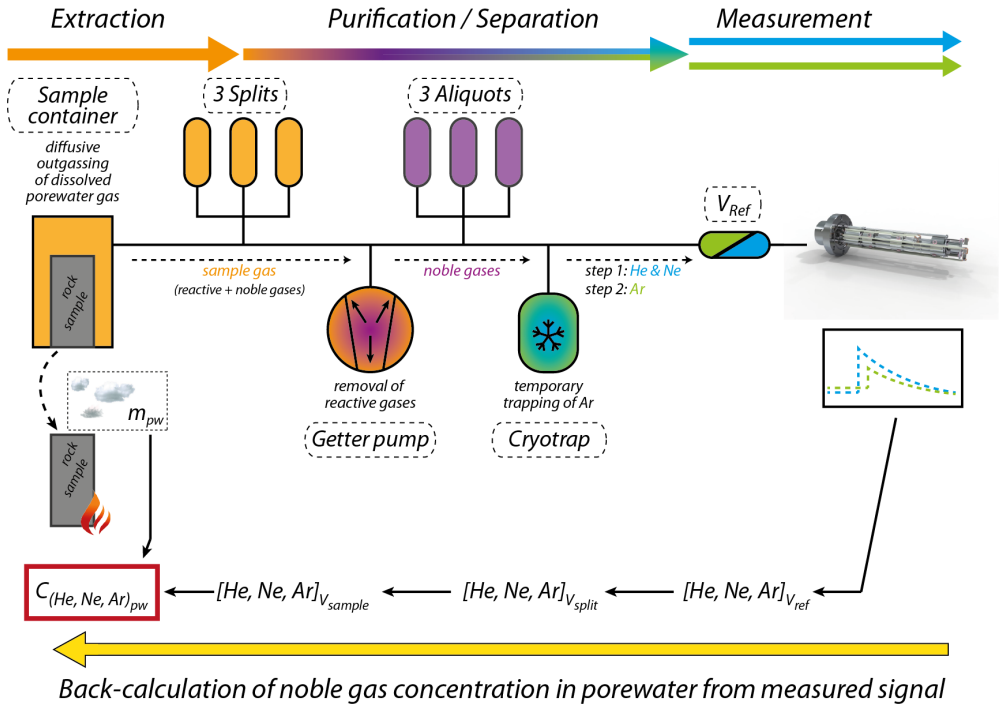

Fig. 8-1: Schematic workflow of the noble gas analytics at the University of Bern.

8.1.1 Extraction of sample gas

The outgassed sample gas is extracted from the sample container by rapid expansion into 1 to 3 identical, evacuated volumes (termed *"splits"*), with the splits and sample container being closed off again within 2 mins. This is ample time to attain pressure equilibrium between sample container and split volumes, while at the same time minimising pressure-change induced alteration of the equilibrated gas composition by renewed out diffusion of gas or evaporation of H_2O from the drillcore sample piece. The equilibrated pressure in the splits is recorded using a gas-type independent manometer (resolution: 0.2 mbar, accuracy: $\pm < 1$ mbar).

Samples are extracted either on the main gas processing line or (in most cases) on a separate extraction line for reasons of workflow efficiency.

Splitting the extracted sample gas into multiple identical fractions provides redundancy in case of analytical problems and allows either for replicate analysis or pooling the gas from multiple splits for a single analysis in case analyte concentrations are expected to be low. In addition to the 3 splits, a separate aliquot can be extracted for e.g. analysis of reactive gas species in another lab. This additional aliquot is extracted after the splits are closed off, so as to have identical extraction conditions with regards to the gas in the splits, regardless of whether a reactive gas aliquot is taken or not.

8.1.2 Purification and separation of the sample gas

Purification and separation of the different noble gas species of interest from the extracted sample gas is achieved by first removing all reactive gas species from the gas of the selected split(s) using a Zr-V-Fe non-evaporable getter (SAES St707, Benvenuti & Chiggiato 1996) operated at 280 °C. The resultant gas, containing primarily noble gases, is again split into 1 – 3 equal volumes (termed *"aliquots"*) to provide failsafe redundancy and to allow managing the gas amount for the next step.

The gas from the selected aliquot(s) is admitted to a LN_2 cooled cold trap using activated charcoal as an adsorber. This causes Ar and more heavy noble gases to be adsorbed on the cryotrap, resulting in a free gas phase containing primarily the light noble gases He and Ne.

The purified free gas phase is then expanded into a calibrated reference volume, from which the gas is subsequently admitted into the mass-spectrometer for measuring. This is first done for the light noble gas fraction (He and Ne), after which the cryotrap is allowed to warm up and release the sorbed Ar and heavy noble gases, which are then similarly expanded into the (again evacuated) reference volume and admitted into the mass spectrometer.

From the light noble gas fraction, an additional aliquot can be extracted for determination of $^3He/^4He$ ratios at the University of Bremen. Similar to the reactive gas aliquot, this aliquot is taken after the gas has been expanded into the reference volume and the volume has been closed off, therefore not affecting the relative gas amount being measured, regardless of whether such an aliquot is removed or not.

8.1.3 Measurement of noble gases

The purified noble gases are measured using a Hiden Analytical HAL/3F triple filter quadrupole mass spectrometer (QMS) operated in static mode (Poole et al. 1997). The QMS is equipped with a faraday cup detector and a single channel electron multiplier (SCEM) with a 300 amu (atomic mass unit) range. Gas ionisation is achieved by oxide coated Iridium filaments with the emission

current and cathode potential tuned down to reduce the isobaric interference of doubly ionised $^{40}Ar^{++}$ on the $^{20}Ne^{+}$ signal to below 1 % of the $^{40}Ar^{+}$ signal, which is necessary if $^{20}Ne/^{22}Ne$ ratios are to be determined. To allow consistent quantification between measurements of different analytes, the sensitivity tuning of the ion source and the SCEM gain is kept constant. To help suppress matrix gas background buildup and to reduce H_2 concentrations (produced by decomposition of H_2O in the hot getter, which then removes H_2 only very inefficiently), a non-evaporable SAES GP-50 getter (also using SAES St707 material) is attached to the mass spectrometer chamber and operated at room temperature (at which the H_2 removal rate is high).

Both the faraday and the SCEM detector operate optimally in a specific analyte gas pressure range, beyond which they either cannot measure at all (SCEM above 5×10^{-6} mbar) or suffer from either increasingly large scatter or long integration times (faraday below ca. 1×10^{-7} mbar).

In order to select the suitable detector for the measurement of a specific purified gas fraction, a small amount of gas is measured immediately after the sample gas has been gettered (removing the reactive gases), but before it is cryotrapped. With this gas containing all noble gases present in the sample, a rough[1] estimation of the different analyte pressures to be expected can be made.

Prior to each measurement of a new analyte gas, a background measurement is performed using the same measurement protocol to be used for the analyte gas. After pumping the mass spectrometer again, the gas in the reference volume is admitted into the mass spectrometer volume via a pipette volume immediately after the mass spectrometer is isolated from the turbomolecular pump. With this, the onset of the rising background coincides temporally with the sharp onset of the decaying analyte signal peak (Fig. 8-2). This allows performing a background correction of the signal of each measured analyte gas species using the corresponding signal of the previously measured background by temporal alignment of the respective peak onsets. This background corrected signal is then regressed to the time of peak onset to determine the intensity of the analyte gas species signal for this gas admission (Fig. 8-3).

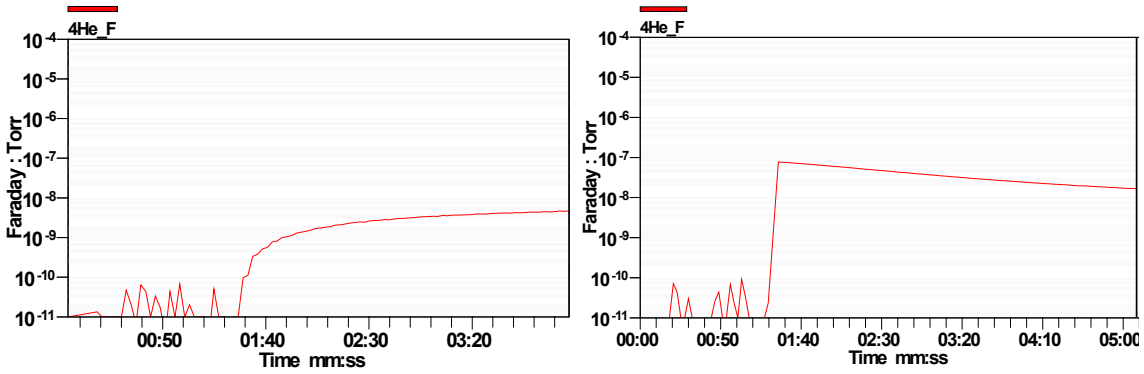

Fig. 8-2: Typical signal intensities as a function of time for a rising background (left) and a gas measurement (right).

The admission and measuring of gas from the reference volume is performed three times, with each subsequent admission containing less gas due to the repeated pipetting. Barring excessive background buildup in the mass spectrometer (e.g. due to insufficient pumping between gas admissions) or contamination of the gas in one of the admissions, the resulting three signal intensities should lie on an exponential decay curve defined by the volume ratio of the pipette volume

[1] This measurement has only a limited accuracy due to the highly variable noble gas composition in the sample gas causing matrix effects that variably influence i.a. the ionisation efficiency of specific gas species.

and the reference volume and can therefore be normalised to the signal intensity of the first admission (Fig. 8-4). The relevant signal intensity for a specific gas species is the average of the normalised signal intensities of all (non-discarded) analyte gas admissions.

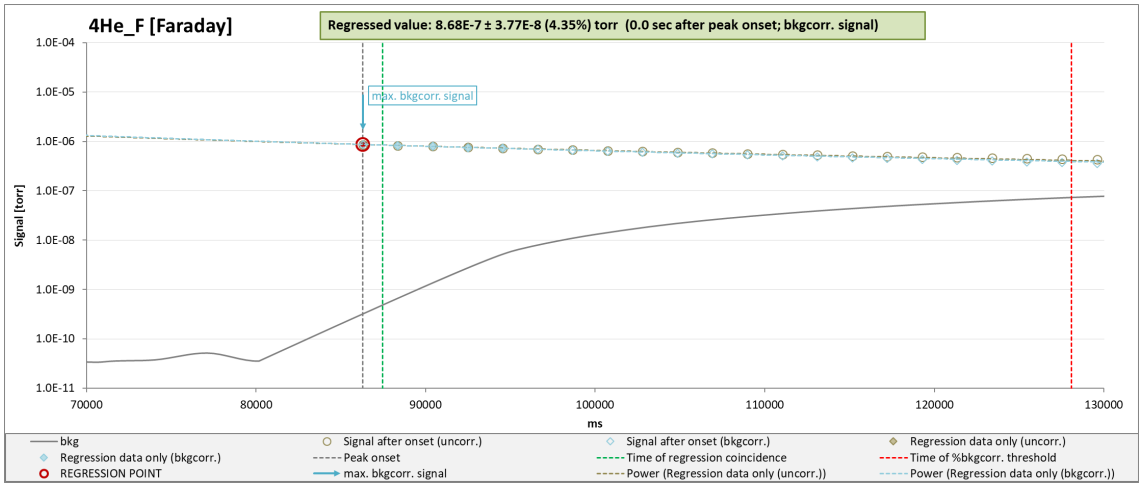

Fig. 8-3: Example of a background corrected gas signal being regressed to the time of peak onset.

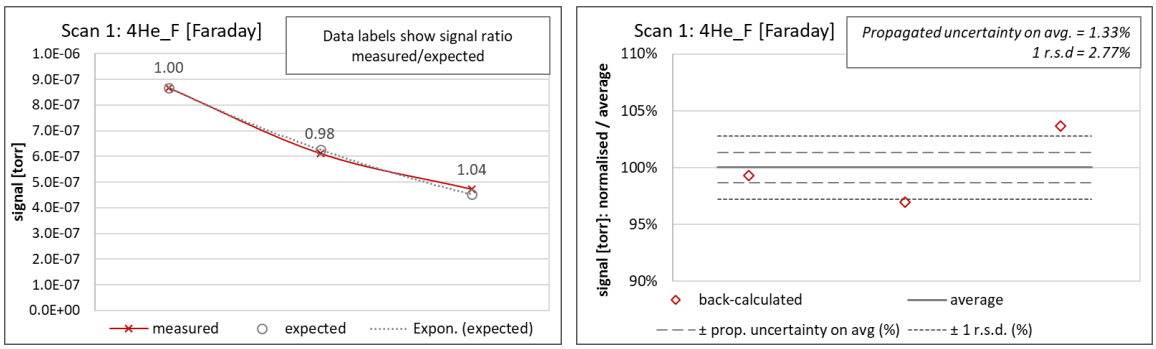

Fig. 8-4: Comparison of measured and expected signal intensities for three subsequent gas admissions (left) and the same data normalised to the intensity of the first admission and given relative to the average of all three normalised values (right).

8.1.4 Calculation of noble gas concentrations in porewater from measured signals

The QMS measurement results in the quantification (in ccSTP[2]) of each measured noble gas species *in the calibrated reference volume* as well as the measured isotope ratio.

The amount of a certain noble gas species in the reference volume is, however, only a fraction of the amount present in one of the extracted splits or initially in the sample container.

2 STP as defined by IUPAC after 1982 (0 °C, 100 kPa) (McNaught &Wilkinson 1997).

The initial amount of a noble gas species (particularly He) in the sample container can vary by over four orders of magnitude between samples from a single borehole while the analysis is optimised for analyte concentrations in the range of two to three orders of magnitude being admitted to the mass spectrometer. This necessitates that different gas fractions from the same sample can be diluted separately and variably by up to three orders of magnitude during purification and separation.

As the gas is extracted and then moves through the processing line, fractions of gas are inevitably lost due to expansion into a new section of the line and closing off of the former section. The amount of gas being processed further can, however, also be voluntarily reduced by splitting or aliquoting into multiple or very small volumes of which e.g. only one is processed further. The corresponding relative gas losses can be calculated based on the volume ratio of "retained" to "lost" gas volume.

During gettering and cryotrapping, the processed gas is also fractionated, and only certain gas species are removed (such as the reactive gases during gettering) or temporarily retained (such as the heavy noble gases during cryotrapping). If such fractioned gases are then not processed further in an identical manner (e.g. because one of purified gas fractions needs to be aliquoted to reduce the gas amount), the amounts of various noble gas species measured in the reference volume correspond to different fractions of these noble gases initially present in the sample container, depending on the processing scheme of the specific noble gas species, which in turn can be different from sample to sample. Therefore, for every single processing step all involved volumes as well as all available pressure readings before and after e.g. an expansion are meticulously recorded. This allows to constantly keep track of the fraction of gas that is being retained throughout the entire purification and separation process.

In generalised form, the amount (in ccSTP) of a specific noble gas species (in the following He is used as an example) in the volume of one split ($[He]_{Vsplit}$, Fig. 8-1) is calculated based on the noble gas amount in the reference volume ($[He]_{Vref}$) as:

$$[He]_{Vsplit} = \frac{[He]_{Vref}}{f_{He_{Vsplit \rightarrow Vref}}} \tag{8-1}$$

with $f_{He_{Vsplit \rightarrow Vref}}$ being the cumulated relative fraction of He from that specific split during its specific purification and separation scheme (see above).

In contrast to the variable relative gas reduction during purification and separation, the relative gas loss during extraction is only dependent on the number of splits being used (n) and the actual gas volume in the sample container. The amount of He in the sample container can therefore be calculated as:

$$[He]_{Vsample} = \frac{\frac{[He]_{Vsplit}}{V_{split}}}{\frac{n \cdot V_{split} + V_{extr.line} + \left(V_{sample\ cont.} - V_{rock}\right)}{}} \tag{8-2}$$

with $V_{extr.line}$ being the volume of the extraction line between the sample container and the splits (which is slightly different for extraction on the main line or the external extraction line), $V_{sample\ cont.}$ being the volume of the empty sample container and V_{rock} being the volume of the drillcore sample piece, which is calculated geometrically using the average length and width measured along the small axes on top and bottom of the cuboid and the central height along the long axis.

After correcting the calculated He amount in the sample container for air-derived excess gas ($[He]_{Vsample,corr}$; see Section 8.3), the He concentration in the porewater (in ccSTP/g_{pw}) is calculated as:

$$C_{He_{pw}} = \frac{[He]_{Vsample,corr}}{m_{PW}} \quad (8\text{-}3)$$

with m_{pw} being the gravimetrically determined mass of porewater in the drillcore sample piece (see Section 5.1).

8.2 Uncertainty on noble gas measurements

The overall uncertainty for the entire analytical procedure (consisting of extraction, purification and measurement of a specific noble gas species of a sample) is in the order of calculation – dependent on:

- The uncertainty on the calculated gas amount of a specific gas species in the reference volume:

  This is calculated by propagating a) the individual regression fit uncertainties, b) the uncertainty on normalising subsequent gas admissions to the first admission and c) the uncertainty on this gas species' calibration curve relating the averaged signal intensity to the gas amount in V_{ref}.

- The uncertainty on the cumulative gas amount reduction factor $f_{He_{Vsplit \rightarrow Vref}}$ during gas purification and separation:

  This is calculated by propagating the uncertainties on all volumes involved in volumetric manipulations of the gas being processed

- The uncertainty on the gas amount reduction factor during extraction:

  This is calculated by propagating the uncertainties on all involved volumes, with the uncertainty on V_{rock} being propagated from the uncertainties on the dimension measurements

- The uncertainty on the excess air correction

  This is primarily defined by the uncertainty on the determination of the amount of Ne in the sample container, which is propagated with the uncertainties associated with the porewater mass (see next point) and the required tabled constants.

- The uncertainty on the porewater mass determination:

  This is calculated according to the uncertainty propagation given in Section 5.1

If replicate analyses are performed (e.g. by measuring multiple aliquots of a purified gas or processing and measuring multiple splits of a sample gas) the average value of all valid results are reported, with an uncertainty propagated from the individual results' uncertainties.

It must be noted that all reported uncertainties pertain only to the analytical methods in the lab, after the sample has been stored for diffusive equilibration. They do not comprise uncertainties that arise prior to the sample being processed in the lab, such as effects due to:

- The drilling of the core section, such as variable degree of degassing of the core due to variations in drilling time or drilling media composition and pressure, as well as leaving the core downhole for extended periods of time because of mechanical problems.

- The retrieval of the core, such as variable influence of pressure relief due to textural differences of the core material, which could lead to some (selective) loss of noble gases.
- The handling of the core after retrieval and during on-site sampling of the noble gas samples, such as variations in exposure time of the sample to air (in particular of the central piece before it is sealed in the sample container) and variations in pumping duration during flushing of the sample container.

While it is almost impossible to assess the influences of such drilling- and sampling-related aspects in a quantitative manner, the comprehensive and detailed sampling metadata recorded for all drillcore samples (see Rufer 2019) and generally reported in a separate report for a specific borehole can help to qualitatively identify or refute potential causes for seemingly aberrant noble gas data.

Nonetheless, the total uncertainty that must be attributed to noble gas data is almost certainly larger than the analytical uncertainty, and this has to be considered during data interpretation.

8.2.1 Monitoring analytical accuracy and precision using reference gases

Together with samples, a reference gas of known composition is repeatedly analysed to verify the analytical accuracy and precision of the measurements. In order to be roughly similar to the expected noble gas compositions of samples that were flushed with Kr during sampling, the reference gas mixtures are produced by doping air with varying amounts of commercially available pressurised He, Ne and Kr to obtain He/Ar ratios of approximately 0.5, as well as He/Ne and He/Kr ratios of approximately 5 - 10. All doping gases have a purity of more than 99.99 % and the pure gases to be admixed are prepared using fixed volumes but differing pressures. In addition, non-doped air is measured to ascertain the accuracy of $^{20}Ne/^{22}Ne$ and $^{40}Ar/^{36}Ar$ ratios.

8.3 Evaluation of air contamination

The equilibrated gas in sample container consists of the gas which has degassed from the porewater and - possibly - variable amounts of contaminant gas, such as air. The degree of air contamination of a measured gas is commonly determined via its Ne content (e.g. Bigler et al. 2005, Rübel et al. 2002, Waber 2012). With negligible in situ geogenic productions ($^{20}Ne = 1.5 \times 10^{-21}$, $^{22}Ne = 5.2 \times 10^{-21}$ ccSTP/(g_{rock} a); Leya & Wieler 1999), any excess Ne in the sample container ($[Ne]_{Vsample,exc.}$) above that of Ne derived from air-saturation of the porewater during sedimentation or infiltration of surface water is interpreted as being derived from air contamination. Using the atmospheric ratio of Ne and a measured noble gas (e.g. He or Ar), the amount of the latter in the sample container can be corrected for air-derived excess:

$$[He,Ar]_{Vsample,exc.} = \frac{[Ne]_{Vsample} - (m_{pw} \cdot C_{Ne_{asw}})}{\frac{C_{Ne_{air}}}{C_{(He,Ar)_{air}}}} \quad (8\text{-}4)$$

$$[He,Ar]_{Vsample,corr} = [He,Ar]_{Vsample} - [He]_{Vsample,exc} \quad (8\text{-}5)$$

with $[He,Ar]_{Vsample}$ and $[Ne]_{Vsample}$ being the measured He or Ar and Ne amount in the sample container, with the additional suffixes $_{exc.}$ and $_{corr}$ signifying air derived excess gas and excess corrected values, respectively; m_{pw} being the mass of porewater of the drillcore sample piece; $C_{Ne_{asw}}$ being the Ne concentration in air-saturated water (approximately 1.9×10^{-7} ccSTP/g; Weiss 1971) and $C_{Ne_{air}}$ and $C_{(He,Ar)_{air}}$ being the atmospheric abundance of Ne (18.18 ppmv) and He (5.24 ppmv) or Ar (0.934 vol.%), respectively (Prinn 2004).

Similarly, corrected $^{3}He/^{4}He$ and $^{40}Ar/^{36}Ar$ ratios can be calculated as (suffixes analogous to eqs. 8-4 and 8-5):

$$\left(\frac{^{3}He}{^{4}He}\right)_{Vsample,corr} = \frac{\left(\frac{^{3}He}{^{4}He}\right)_{Vsample} - \left(\left(\frac{^{3}He}{^{4}He}\right)_{air} \cdot \frac{He_{Vsample,exc.}}{He_{Vsample}}\right)}{1 - \frac{He_{Vsample,exc.}}{He_{Vsample}}} \quad (8\text{-}6)$$

$$\left(\frac{^{40}Ar}{^{36}Ar}\right)_{Vsample,corr} = \frac{\left(\frac{^{40}Ar}{^{36}Ar}\right)_{Vsample} - \left(\left(\frac{^{40}Ar}{^{36}Ar}\right)_{air} \cdot \frac{Ar_{Vsample,exc.}}{Ar_{Vsample}}\right)}{1 - \frac{Ar_{Vsample,exc.}}{Ar_{Vsample}}} \quad (8\text{-}7)$$

with $(^{3}He/^{4}He)_{air} = 1.36 \times 10^{-6}$ (de Laeter et al. 2003) and $(^{40}Ar/^{36}Ar)_{air} = 298.56$ (Lee et al. 2006). It should be noted that the isotope ratios of the gas in the sample container can be considered to be practically identical to the respective ratios in the initial porewater due to the quantitative degassing of the dissolved noble gases.

Air is – relative to the average porewater gas composition – strongly depleted in He and enriched in Ar, both of which also have a less radiogenic isotope signature in air than in the porewater gas. This means that He and Ar in porewater-derived gas are very differently affected if this gas comes into contact with air.

Waber & Rufer (2017) have illustrated this for a noble gas sample from a typical aquitard clayrock (Opalinus Clay from the BDB-1 borehole, Mt. Terri URL, Switzerland), which is assumed to become increasingly more contaminated by air (Figs. 8-5 and 8-6).

The *total amount* of helium in the increasingly contaminated sample gas is hardly affected due to the large difference of more than two orders of magnitude between the He-rich uncontaminated porewater gas and the He-poor air (Fig. 8-5, lower panel). The induced deviation from the initial He content of the sample gas would exceed the analytical uncertainty only at extremely high contamination levels of > 60 % air. In contrast, the amount of argon in the increasingly contaminated sample gas shows a drastic increase even at low degrees of contamination, as the Ar concentration in air is generally significantly higher than in the uncontaminated porewater gas. As a result, the Ar amounts of the contaminated sample gas already deviate for more than the analytical uncertainty from the uncontaminated value at less than 1 % of air contamination (Fig. 8-5, upper panel).

While the isotope ratios of $^{3}He/^{4}He$ and $^{40}Ar/^{36}Ar$ are similarly affected by air contamination, the effect is, however, to some degree counteracted by the far larger difference in $^{3}He/^{4}He$ isotope ratio in air relative to the porewater (up to one order of magnitude) when compared to the difference in $^{40}Ar/^{36}Ar$ (roughly 5 – 20 %). In consequence, $^{3}He/^{4}He$ ratios of the increasingly contaminated sample gas only show no deviation within analytical uncertainty up to a relative air contamination of 15 %, whereas for $^{40}Ar/^{36}Ar$, a significant deviation is reached at a relative air contamination of approximately 5 %.

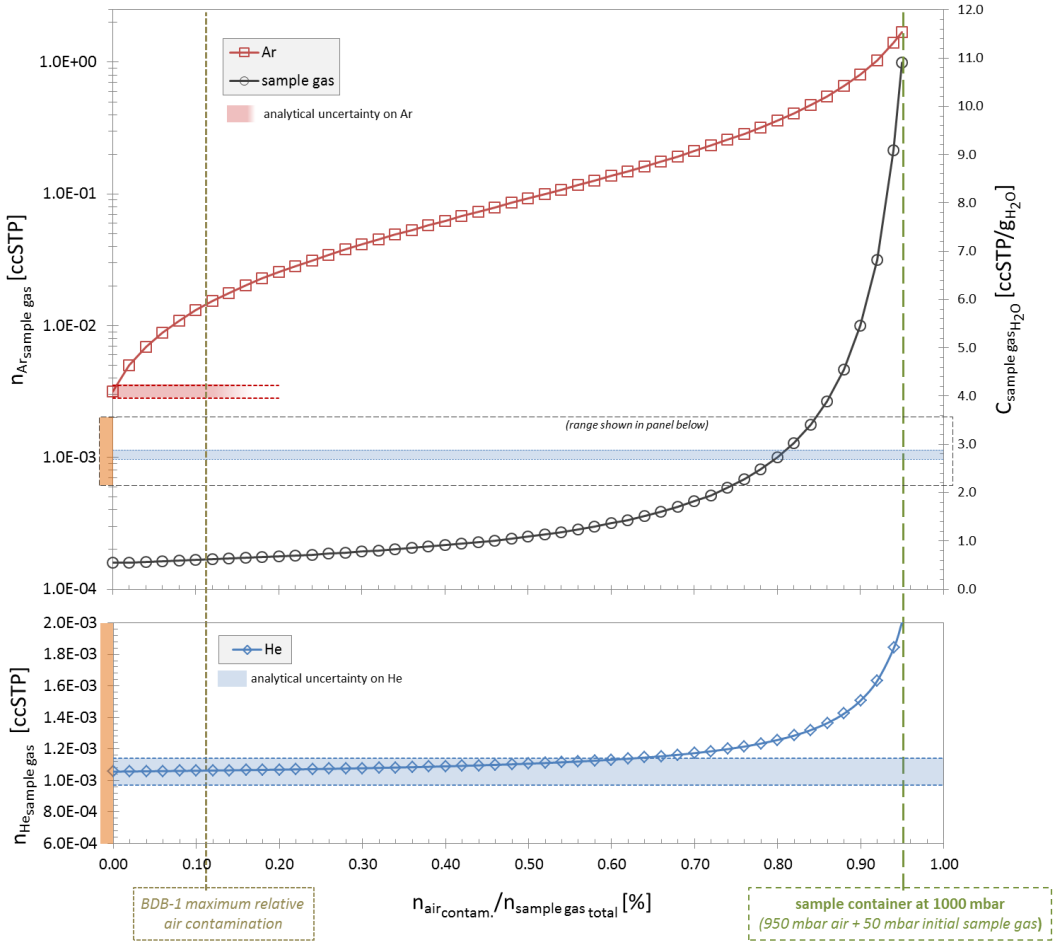

Fig. 8-5: Ar (upper panel) and He (lower panel) amount in an increasingly contaminated sample gas as a function of relative air contamination.

The analytical uncertainty on the He and Ar amounts of the uncontaminated sample gas are given by the shaded horizontal bars. The ordinate range of the lower panel is marked on the ordinate axis of the upper panel by the vertical grey bar. For the uncontaminated sample gas composition and analytical parameters see Waber & Rufer (2017).

8.4 Noble gas and parent radionuclide analyses on rock samples

For the calculation of in situ He production rates in the rock and release coefficients from the rock into the porewater, U, Th, Li and K contents, as well as ^{4}He and ^{3}He/^{4}He ratios are measured in the rock matrix.

Element concentrations are measured by X-ray spectrometry on bulk samples for U and Th, and by flame spectroscopy on completely digested rock material for K and Li. The analyses are performed at the Kola Scientific Centre in Apatity and by Neva Geological Expedition in St. Petersburg, Russia. Isotopic abundances and ratios are determined by fusion of the dried bulk rock samples at 1600 °C, purification and separation of the released gas with Ti – Zr getter and LN_2 cooled cold traps, and measurement by mass spectrometry as described in Tolstikhin et al. (2010). In these samples, ^{4}He originally dissolved in the porewater has been lost by out-gassing prior to the determination of ^{4}He in the rock.

The analytical uncertainties (1 σ) for these measurements are given by the labs as follows: [K] = ± 3 %; [Li] = ± 20 %; [U], [Th] and [^{4}He] = ± 10 %. The ^{4}He blanks were 1 × 10^{-6} ccSTP ^{4}He/g_{rock} (I. Tolstikhin, *pers. comm.* 2016).

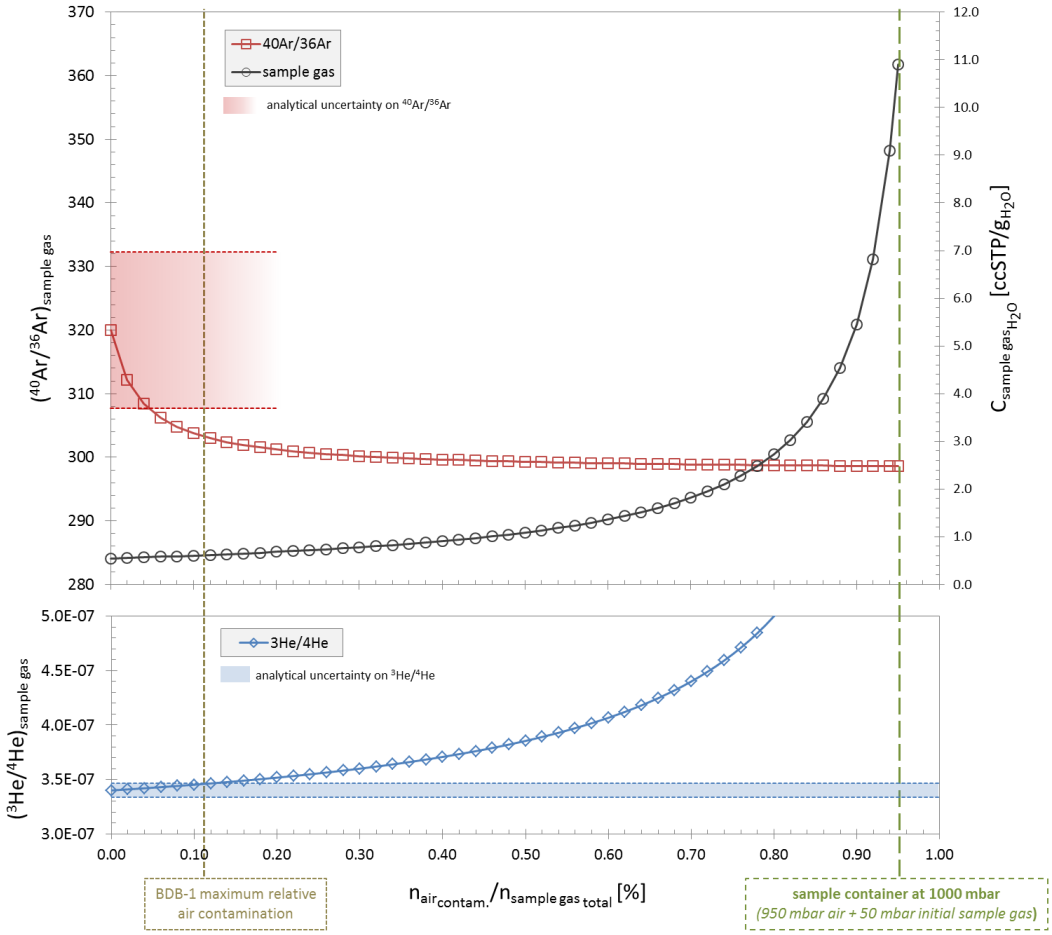

Fig. 8-6: ^{40}Ar/^{36}Ar (upper panel) and ^{3}He/^{4}He (lower panel) isotope ratios in an increasingly contaminated sample gas as a function of relative air contamination.

The ranges of analytical uncertainty on the ^{3}He/^{4}He and ^{40}Ar/^{36}Ar isotope ratios of the uncontaminated sample gas are indicated by the shaded horizontal bars. For the uncontaminated sample gas composition and analytical parameters see Waber & Rufer (2017).

9 Advective Displacement Technique

U. Mäder, A. Jenni, M. Kiczka, H.N. Waber

The method of advective displacement was developed for rocks with a very low hydraulic conductivity as an alternative or additional option to long-term borehole sampling, destructive rock squeezing, or aqueous extraction of granulated material. The advective displacement technique aims at obtaining small aliquots of displaced porewater from well-preserved cylindrical core samples while minimising artefacts from core handling, storage, and changes in physical conditions. In-depth data interpretation requires accompanying analysis of some petrophysical parameters, mineralogy, aqueous extracts, and clay-specific analysis for CEC, cation-occupancy and possibly BET surface area. X-ray CT data is used for selection of suitable samples and planning of the subdivision of samples (cutting). The advective displacement technique is therefore a comprehensive methodology to derive a wide range of physico-chemical properties, including also transport parameters when combined with appropriate tracers (e.g. deuterium, anions) over sufficient time.

Specifically, advective displacement samples processed for Nagra's deep drilling program are used for:

- In-line measurements of the displaced porewater electric conductivity and pH.
- Complete chemical analysis of a time series of displaced water aliquots.
- Water stable isotope analysis ($\delta^{18}O$, $\delta^{2}H$) of aliquots.
- Derivation of Cl-accessible porosity and where feasible also Br-accessible porosity.
- Monitoring of hydraulic conductivity evaluated after each sampling interval.
- Sample pre-characterisation (water content, bulk wet density, mineralogy, CEC and cation exchanger population).
- Post-mortem analyses of rock material for water content, bulk wet density and optionally grain density and aqueous extractions, as required for the interpretation of the chemical and isotopic data of the displaced water.
- If observed over sufficient time: monitoring break-through of artificial and natural tracers and derivation of transport properties by modelling (hydraulic conductivity, diffusion coefficients of non-reactive components).

This section provides the generic details of the set-up, materials, procedures, workflows and sample preparation of the advective displacement technique, and some of the accompanying analytical methods if different from procedures described elsewhere in this report. The workflow requires a dedicated team for the advective displacement experiments, including some pre-treatment for analytical work before samples are fed into the laboratory procedures detailed elsewhere in this report.

Selected literature on the development of the advective displacement method includes Mäder (2004), Mäder et al. (2004), Mäder & Waber (2017a) and Mäder (2018). Applications of the method are documented in Mäder (2006), Mäder et al. (2008), Mazurek et al. (2012), Wersin et al. (2013, 2016), Mäder & Waber (2017b), Mäder (2018).

9.1 Workflows for advective displacement experiments

The general workflow for the preparation, conduction and analytical programme of advective displacement samples (AD samples) follows standard protocols of preparation steps (Fig. 3-3). The preparation involves dry cutting of three sections from the preserved saturated core sample (Tab. 9-1). After removal of the core rim, the top and bottom sections are used for pre-AD analyses that include aqueous leaching, measurements of water content, densities and optionally other parameters. These investigations follow the protocol used for the PW samples (Chapter 3). The central section is further trimmed on a lathe to a diameter of 80 mm for the AD experiments. Sample preparation commonly requires two persons, and one person will be periodically busy with in-line measurements, monitoring the experiment and managing samples and analytical results. Initial (pre-AD) measurements of water content, densities and aqueous extraction (e.g. Cl, Br) at the time of preparation of the AD samples serve as a control parameter and are required for interpreting the chloride-accessible porosity. Post-mortem analyses of water content, density and optional leaching tests serve in combination with geochemical modelling for identifying experimental artefacts and provide support for measured parameters to represent in situ conditions – or not.

Depending on hydraulic conductivity, sample size and aims, the experiment time may vary between about 2 months and 1 – 2 years. Shorter time periods of 2 – 3 months are required to simply characterise the first few mL of displaced water as a proxy of the in situ chemical and isotopic composition of the porewater, and the chloride-accessible porosity. Longer time periods are required to obtain transport parameters by observing the tracer breakthrough and interpreting the behaviour in terms of hydraulic conductivity and diffusion coefficients. Pre-characterisation will be conducted on short- and long-term experiments. Post-mortem analyses – except for water content and sample dimensions - will only be conducted on long-term experiments, or as indicated by results.

Tab. 9-1: Generalised standard protocol of advective displacement (AD samples).

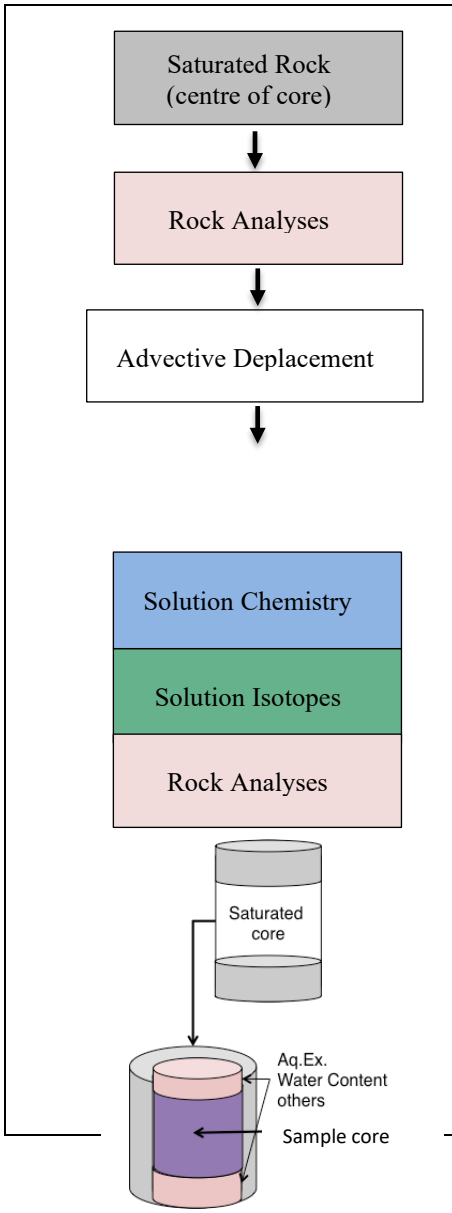

Sequence:

- Preparation of AD-Set-up
- Preparation of artificial porewater (APW)
- Preparation of saturated rock for pre-AD analyses (aqueous leaching, water content, density)
- Trimming of originally saturated core
- Mounting trimmed core, start of APW injection
- Monitoring experiment with in-line measurements and periodical sampling of outflow
- Solution chemical and isotope analyses
- Dismantling of trimmed core after experiment
- Post-mortem investigations of water content, density optional mineralogy, aqueous and CEC extraction tests and others

Technical:

- Time of sample preparation & mounting: 1 – 2 days
- Rock mass: 900 – 1300 g
- Rock volume: 400 – 600 cm^3
- Outflow sample aliquot: 0.5 – 5 mL
- Experiment time: 2 – 3 months for initial porewater, 12 – 24 months for breakthrough behaviour
- In-line measurement of pH, EC
- Solution chemistry: pH, IC, ICP-OES, TIC/TOC, colorimetry
- Solution isotopes: $\delta^{18}O$, $\delta^{2}H$ by CRDS

Deviations from standard procedure:

- For specific rock types and based on expert judgement the experimental and analytical protocol and experiment time may be adjusted
- The exact protocol of solution analyses depends on the sample volume and salinity

9.2 Method and apparatus for advective displacement of porewater

The method of advective displacement subjects a rock core sample to a hydrostatic confining pressure and injects an artificial porewater on one side of the core to displace the in situ porewater that can be sampled as outflow on the other side (Fig. 9-1). The applied hydraulic gradients are large (100 s – 1000 s of m/m_{H2O}) at confining pressures of 3 – 10 MPa, and the induced flow rates are small (0.05 – 1.5 ml/d). Hydraulic conductivities typically range from 10^{-12} to 10^{-14} m/s (consolidated clayey rocks, compacted bentonite, some igneous rocks). Experiments typically take a few weeks to many months. Mäder (2018) provides a detailed description of the method, with some applications. The laboratory the University of Bern, Geological Sciences, comprises 8 advective displacement stations dedicated to Nagra's deep drilling program as of the end of 2019.

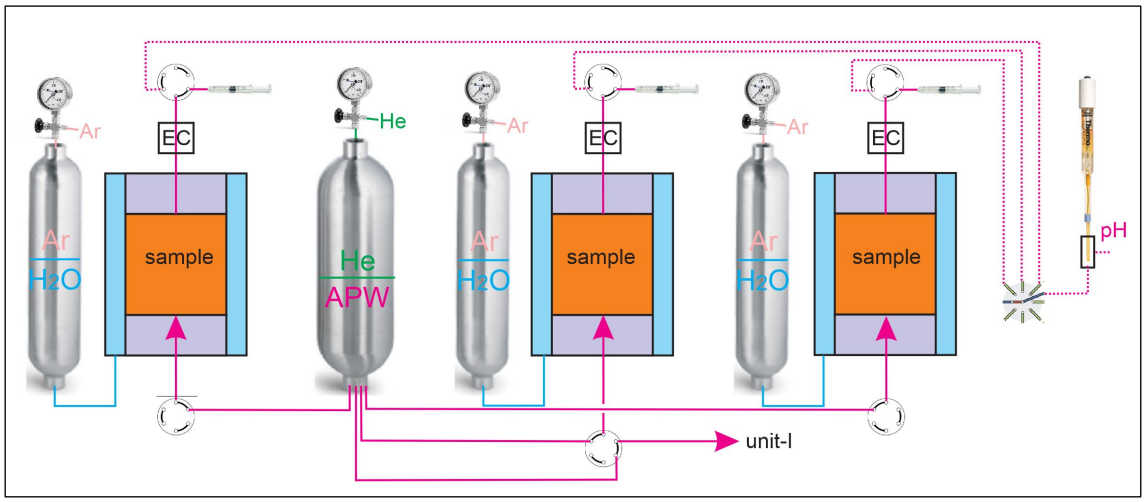

Fig. 9-1: Schematic of 3 advective displacement stations, with individual pressure tanks for the confining water, and a common tank for the artificial porewater feeding to 3 sample cores.

The outflow is directed through an electric conductivity cell to sampling syringes, or intermittently to a miniature pH electrode. Valves at inlet and outlet are 6-port two-position stream switching valves. APW: artificial porewater.

The advective displacement apparatus (Fig. 9-2) consists of a steel pressure vessel, removable end caps, and a spindle that adjusts to the length of a sample core. The core assembly (#6 and #7 in Fig. 9-2) consists of a cylindrical rock sample with filter discs (or screens) at both ends and titanium adapters that sandwich the rock core. Steel inserts couple to the titanium pieces on both sides and slide into the pressure vessel. Sealing between parts is achieved by O-rings (NBR standard products). The core assembly is sealed with Teflon tape and latex rubber against the confining medium as detailed further below.

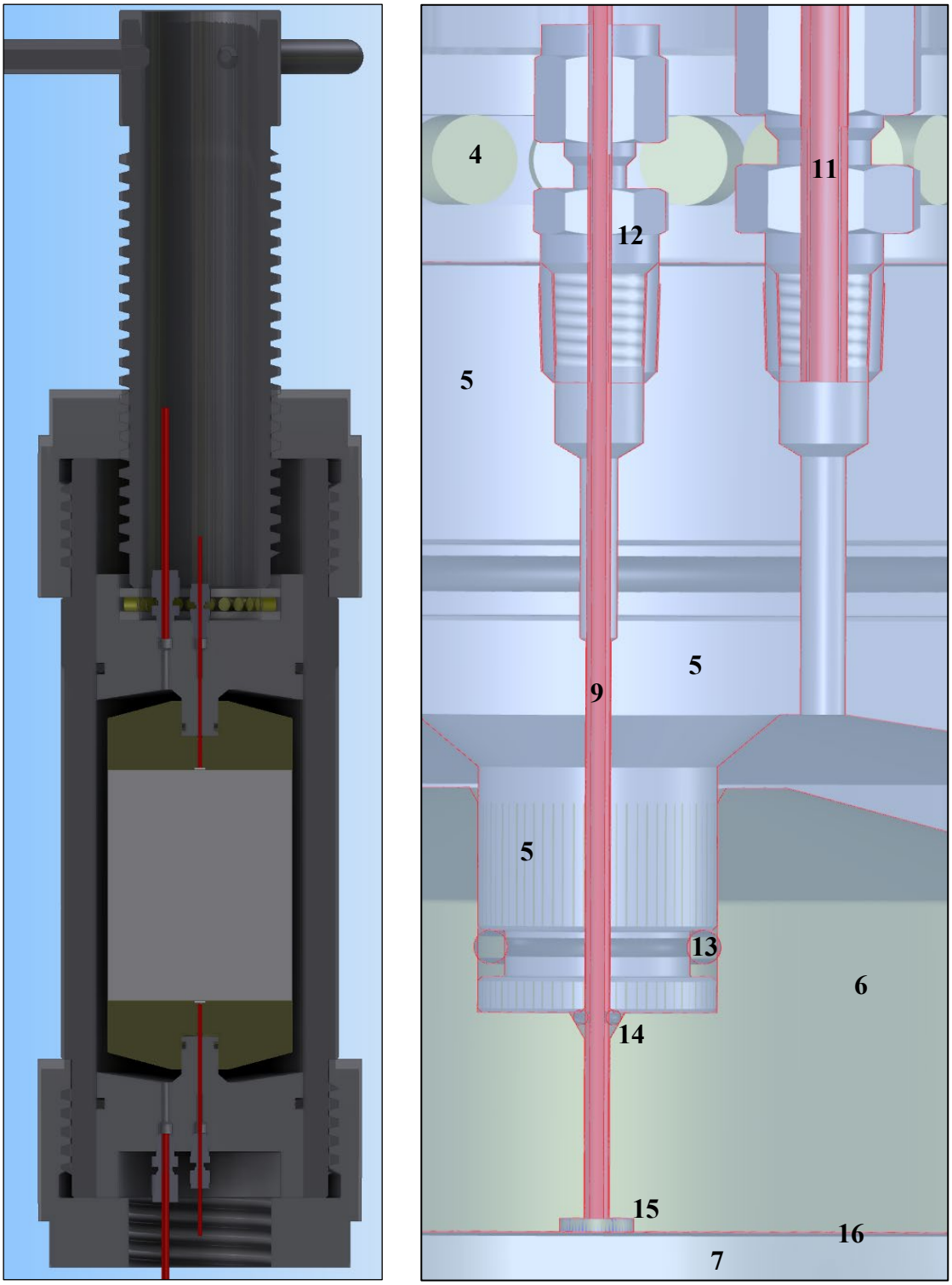

Fig. 9-2: Scale drawing of advective displacement device with inner diameter of 90 mm.

(1) Steel pressure vessel with end caps (2), adjustable spindle (3) and rolling bearings (4). Steel inserts (5) hold sample assembly comprising titanium adapters (6) and sample (7). PEEK injection capillary (8) and outlet (9). Pressure lines to the confining fluid (10) and (11). Swagelok fitting (12, 1/16" NPT) holds the outflow capillary, sealed against the confining fluid with O-rings at (13) and (14). A PPEK frit (15) protects the outflow capillary port, and (16) is the PEEK mesh placed between the sample and titanium adapater.

The hydraulic system consists of a stainless-steel tank filled partially with water (confining fluid) and argon gas that is pressurised (schematic in Fig. 9-1). This ensures a constant confining pressure that dampens any changes in room temperature. The confining fluid is tap water mixed with distilled water (and some braided cupper wire to suppress bacterial growth) and pumped by small membrane pumps, by compressed air-driven pumps, or from a reservoir pressurised with compressed air. The system is built form industrial components (mostly Swagelok stainless steel components) and protected by safety heads.

The infiltration of the artificial porewater is driven by compressed helium from a partly filled PTFE-coated stainless steel tank (schematic in Fig. 9-1). A distribution head made in-house from Grade-2 titanium is fitted at the lower end of the supply tank to feed a desired number of PEEK capillary tubes (1/16" OD, 1.6 mm).

Two 6-port 2-position stream switching valves made of PEEK and other inert polymer materials are used as injection valve and sampling valve (Fig. 9-1). The sampling valve provides the flexibility to divert the normal flow path from a sampling syringe intermittently to an in-line pH flow-through cell. A 6-port valve also provides the option to connect separate flow lines for calibrating a pH cell such that the miniature electrode does not need to be removed from the cell.

Measurement of pressure is done by semi-conductor transmitters (Keller-Druck) and indicated also by stainless steel pressure gauges and/or digital indicators in some cases. All pressures are continuously monitored by a USB-based data acquisition system (16 differential channels, 24-bit A/D converter) connected to a dedicated small PC. Temperatures are also monitored, either using type-K bimetallic Inconel-sheathed sensors or Pt-100 / Pt-1000 resistance sensors (normally connected to a pH meter, or EC-meter).

A list of some of the more critical components and products provides information on materials, specifications and manufacturers (Tab. 9-2). The list is not complete.

The filter discs used above and below the core sample are made of a fine PEEK fabric with a measured thickness of 0.07 mm, a mesh size of 35 µm, with 22 % open area. The PEEK weaving threads appear to be flattened and sintered, and a filter volume is difficult to specify. PEEK capillary tubing (1/16" OD) is used as flow lines to and from the sample core. The fluid-wetted parts are therefore only titanium, PEEK, Teflon tape, and some other chemically inert high-performance polymers (valves). The capillary end near the sample surface is protected by a small filter (0.5 µm, PEEK) seated in a small cylindrical cavity of the titanium adapter (Figs. 9-2 and 9-3). The fluid displaced from the core at very low flow velocities is therefore largely free of particles. Colloids are not significantly mobilised from claystones of the Mesozoic clay-rich strata with porewater-like solutions, as indicated by some tests performed in previous work with/without ultra-centrifugation and comparison of silica and alumina analysis using photometric methods (true aqueous concentration) versus plasma methods (including any colloids).

Tab. 9-2: List of components used for advective displacement equipment.

Component	Specification	Product	Manufacturer/Vendor
Pressure cylinder for APW	PTFE-coated, stainless steel, 124 bar, 0.5 or 1 L	3016L-HDF8-1000-T 3016L-HDF4-500-T	Swagelok
Valves for hydraulic and gas system	Stainless steel, 1/8" and 6 mm ports, 340 bar	SS-ORS2 SS-1RS6MM	Swagelok
Pressure transmitters	Mostly 100 bar range	Mostly series 21Y	Keller-Druck
Data acquisition system	16 differential analogue inputs; 24 bit A/D conversion; USB device	USB-2416	MC Measurement Computing
Titanium custom parts	Grade 2 titanium	Adapters, distribution heads	Machined in-house
PEEK/PEAK valves	6-port, 2-position, 10 – 32 sockets, 0.4 mm bore	C2-2346	Vici/Valco
PEEK capillary	1/16" OD, 0.5 and 0.75 mm ID		Several vendors
Syringe adapters (female luer adapters)	PEEK (some PTFE), for 1/16" capillaries or 10 – 32 valve sockets	Several brands	IDEX/Upchurch Vici/Valco

A critical issue in systems with very low flow rates is the presence of significant dead volume, particularly at the outflow, that contributes to mixing, transient membrane/osmotic effects at interfaces to dense clay materials or may provide space for bacterial growth. The set-up presented here (Tab. 9-3) has much reduced dead volumes compared to earlier work, a most important aspect being the thin PEEK fabric mesh selected in lieu of a relatively bulky titanium filter disc (typically 1 – 2 mm thick). The dead volumes are listed for the inflow capillary (0.75 mm ID), the outflow capillary (0.50 mm ID), the PEEK filter insert, and an estimate for the PEEK membrane (with variants that include titanium foil spacers). The volumes of the membrane and variants are not well defined, because some of the nominally free pore space will gradually collapse under pressure. The PEEK fabric is firm enough to withstand the compression forces used in this work, at least for several months.

The PEEK mesh was a recent improvement in reducing dead volume, but it was not entirely clear how creep may affect the material over extended time periods. The following variants were tested during the first series of experiments involving samples from Bülach-1 (Fig. 9-3):

- A single layer of PEEK mesh
- A double layer of PEEK mesh
- A single layer of PEEK mesh with some spacers cut from a thin titanium foil (0.12 mm) arranged along the outer margin of the core diameter
- A single layer of PEEK mesh with a thin titanium foil mask (0.05 mm) having a star-shaped pattern cut by water jetting (50 % open area)

At later times, only a single layer of PEEK mesh was used as it proved that the mesh did not collapse during several month-long experiments.

Tab. 9-3: Dead volumes of different components of the advective displacement apparatus.

Component	**Material**	**Dimension**	**Porosity** [-]	**Volume** [ml]
Capillary, inlet	PEEK	0.75 mm ID 60 cm length		0.27
Capillary, outflow	PEEK	0.50 mm ID 60 cm length		0.18
Capillary filter	PEEK, 0.5 µm	1.14 mm DM 0.8 mm thickness	0.5	0.0002
PEEK mesh	PEEK, 35 µm mesh	80 mm DM 0.07 mm thick	~0.5	< 0.15 (*)
Ti spacers	Titanium	0.12 mm thick	0.9	< 0.54
Ti mask	Titanium	0.05 mm thick	0.5	< 0.05
Conductivity cell	Stainless steel, PTFE	1.0 mm DM 10 mm long		0.008
pH cell	POM	Complex shape		0.02 – 0.03
Inlet/outlet valve	PEEK etc.	Equivalent to capillary bore		< 0.002

(*) At loading conditions, the weave will be significantly compressed – only an estimate.

Fig. 9-3: Different types of filters used between sample and titanium adapaters.

PEEK mesh (left), double layer of PEEK mesh with titanium foil spacers (middle), titanium foil mask (right, used in combination with PEEK mesh). Also visible is a small central filter that protects the capillary port.

9.3 Sample preparation for advective displacement

Preparation includes the inspection of X-ray CT images (Fig. 9-4) for selecting samples that are not fractured, and do not contain obvious anomalous strata (pyrite-rich layers, layers with abundant macro-fossils, large nodules). The CT data set is obtained from the normal workflow directly from IRM (Forensic Medicine, University of Bern) comprising the entire core segment contained in their original packaging (inner vacuumed food plastic bag, outer vacuumed plasticised aluminium bag).

Sample cutting is planned before opening the sample bag, and all equipment prepared, including a rock saw for dry cutting, and a food-grade vacuum packaging machine for protecting the core segments immediately after cutting. Two to four cuts are required to prepare a central cylinder for the experiment, one or two adjacent short cylinders for sample pre-characterisation, and the ends on either side that are kept in storage for a limited time as reference material. The length of the central segment is 80 – 110 mm, and that of adjacent parts 20 – 30 mm, depending on the overall length of the useable core. If possible, two adjacent sections were processed for pre-characterisation, but in some cases only a part on one side of the experiment core was sufficiently large for accompanying analytical work. The cutting positions are marked on the core and all cuts are performed within a minimal amount of time, taking less than 1 minute per cut. The rock-saw used is mitre saw (Metabo KGS 305 M) custom-equipped with a diamond blade (300 mm DM) appropriate for dry cutting (Fig. 9-4). Cores up to 105 mm diameter can be cut without re-positioning, and the cutting width is 3 mm. Care has to be taken to cut exactly parallel surfaces bordering the central cylindrical segment used later for advective displacement experiments.

The samples for pre-characterisation are further processed as detailed below, usually within 0.5 – 3 hrs of cutting, with rock samples protected temporarily in vacuumed plastic bags. The sample cylinder used for the experiment is trimmed on a lathe also within 0.5 – 3 hrs, protected during short storage. A dedicated lathe is used for trimming cores from an original diameter of 95 mm (Bülach-1, Trüllikon-1) to a final diameter of 80 mm. This is done with sample holders made of POM, one held by the collet chuck, and the other one pushed against the sample end by the tailstock. Standard cutting segments are used (Eriks cutting insert, DCGT 11T304 AL KNH 9010). Rotation speed is approximately 560 rpm, and a cutting advance of about 0.05 mm/turn is selected (ca. 3.6 mins for 100 mm length). A cutting thickness of 1.5 mm per traverse is adequate, requiring a total of 5 traverses to trim 7.5 mm of radial thickness. This process is minimising exposure to air, because the end surfaces are covered by the POM sample holders, and each traverse is trimming off the exposed surface from the previous traverse. The only exposure is therefore the duration of the last traverse (ca. 3 mins) and some short handling time. The trimmed sample is protected by plastic foil and by vacuum plastic packaging until further processing as described below (usually on the same day). Care is taken to keep track of the original core orientation with respect to top and base of a borehole.

The stream of cuttings produced during turning are collected for some analytical work described in Section 9-11, to examine possible contamination effects from the drilling fluid.

Fig. 9-4: Initial steps of sample inspection, cutting and turning.

Planing of cutting locations (a); mitre saw with diamond balde (b); cutting of core segments (c); trimming of core segment to a diameter of 80 mm on althe; white pieces are made of POM and hold the sample (d).

Preparatory work for the advective displacement experiment includes the cleaning of titanium adapters, steel inserts, replacement of old capillary tubing, replacement of O-rings, cleaning/ replacement/testing of EC and pH electrodes, and cleaning/replacement of polymer-lined steel tanks used for pressurising the artificial fluid.

The procedure for performing an advective displacement experiment involves the following steps, starting form a cylindrical core sample (see above) with neatly cut ends at right angle to the core axis and parallel to one another. As a first task, the sample core has to be mounted between titanium adapters and protected by Teflon and rubber sleeves (Fig. 9-5).

1. Measuring the length of the sample cylinder at four marginal positions. Measuring the diameter of the core at two positions at the top and base. Measuring the mass of the core. All work is done while the core is still protected in plastic foil, after unpacking from a vacuumed bag used for storage between cutting and preparation.
2. Assembling the titanium end pieces with filter discs, and PEEK mesh on either side of the core sample.

3. Filling of any significant breakouts on the core surface or along the edges with compressed Teflon tape. This avoids intrusion of the rubber sleeves that might otherwise get punctured when applying confining pressure.
4. Wrapping of the core with some overlap onto the titanium adapters with wide Teflon tape (2.5 cm), with about 70 % of overlap winding up and down along the core about 4 – 5 times.
5. Covering of the Teflon and remaining exposed titanium with two layers of standard latex rubber sleeves as used in geotechnical testing. The ends are sealed with clear silicone sealant used for sanitary installations.
6. Finally, the ends of the rubber sleeves are taped with elastic electric tape to provide a firm initial seal.

Fig. 9-5: Preparation of core assembly for advective displacement.

Titanium end piece with filter at capillary port (a); PEEK mesh between titanium end piece and sample core (b, c); Core assembly wrapped with Teflon tape (d); latex rubber sleeve cut to length € and sealed with silicone sealant (f); ends secured with eletcric tape (g). The core diametre is 80 mm.

The orifices in the titanium adapters for the PEEK capillary tubes are temporarily plugged and the core assembly intermittently stored in a refrigerator or directly mounted into the apparatus.

Layers of overlapping Teflon tape chemically seal the core against the confining water including a part of the titanium couplings (Fig. 9-5). A firm hydraulic seal is provided by two layers of latex sleeves, the ends being additionally treated with silicone sealant. A few wraps of electric tape compress the latex sleeves at the ends onto the titanium couplings for a reliable initial seal. The system becomes self-sealing after applying an external hydraulic pressure.

Tab. 9-4: List of components used for the core assembly.

Component	**Specification**	**Product**	**Manufacturer/Vendor**
Filter disc at capillary port	PEEK frit, 0.5 µm, DM 1.14 mm, PCTFE rim, OD 4.88 mm	A-735X MicroFilter Frit	IDEX
PEEK mesh	PEEK woven mesh, 35 µm	12" × 12" sheets	Amazon
Rubber sleeves	Pure latex	Model 28-WF4075	Wykeham-Farrance
Silicone sealant	Clear, for wet rooms	Coltogum Sanitär	Hardware stores
Titanium foil, spacers	Grade 2	0.12 mm thickness	Unknown
Titanium foil, mask	Grade 2	0.05 mm thickness	Unknown
Titanium, round stock	Grade 2	Adapters	Machined in-house

Mounting of the core assembly into the core infiltration apparatus involves the following steps (Fig. 9-6):

1. Feeding a PEEK capillary (0.75 mm DI) through the lower steel insert and mounting of the core assembly. An additional small O-ring is placed around the capillary at a small seat at the interface between the steel insert and the titanium adapter. The capillary is extended all the way to the small filter disc located at the surface of the sample core.
2. This combined part is inserted into the top end of the pressure vessel with a long spindle extended from the base to provide a defined position. The part can then be lowered in a controlled fashion.
3. The upper insert is prepared in the same way as the lower insert and mounted on top of the partially inserted core assembly. The combined parts are then lowered all the way. The cap is mounted at the top, and a spindle inserted from the top to confine the length of the core assembly. A roller bearing is placed between the upper insert and the base of the spindle. This avoids torsion of the core assembly when screwing down the spindle and applying some moderate force.
4. The capillary tubes, inlet and outflow, are first left open, and the pressure vessel is filled with water, with air escaping through the top venting tube. Then, confining pressure is applied stepwise. Normally, the experiment is left under confining pressure overnight to allow for sample consolidation and making sure that no leaks are present, either in the confining system, or in the sealing layer between the core and the confining water.
5. The capillaries are connected to the injection valve and the sampling valve, and the injection is started. Before injection, a moderate vacuum is applied shortly to the lower end of the core, and the infiltration is directly started against vacuum. This can be done using a 4-port or 6-port two-position stream switching valve.
6. A moderate vacuum is also shortly applied to the head space of the core at the sampling valve, and switched to the neighbouring port where a syringe is attached.

The experiment is checked rather frequently during the first day for any leaks in the confining system or infiltration system. There may be a time lag of approximately 2-10 days until the first drops of displaced pore fluid arrive at the sampling syringe (depending on hydraulic conductivity and applied head gradient). First arrival is indicated by an instantaneous increase in electric conductivity. Any gas bubbles transported are also visible as short periods where the electric conductivity is very low.

9.4 Determination of hydraulic conductivity

The hydraulic conductivity [K, m/s] can be evaluated for each sampling interval according to Darcy's law, using the average volumetric flow rate [Q, m^3/s] obtained from sampling with syringes, the average hydraulic head difference for the sampling period [h, m_{H2O}] (or integrated from pressure logs), sample length [L, m] and cross sectional area [A, m^2]:

$$K = \frac{QL}{Ah}$$

Syringe friction may have to be accounted for as a backpressure (reducing the nominal head difference), but this is only significant for small syringes (1 and 2 ml) at the commonly used pressure differences > 3 MPa. Such a term is introduced in the equation below, in equivalent units of hydraulic head [h_{syr}, m_{H2O}].

Above equation considers the volumetric flow rate. We do record volumetric information from sampling syringes, but reading accuracy is limited and errors are rather large. More accurate data is recorded for sample masses at every change of syringes. Converting mass to volume requires a density correction at elevated salinities, using sample mass [M, kg], sample density [ρ, kg/m^3], and sampling duration [t, s]. A temperature correction to a reference temperature [T_{ref}] is also added, and a correction for syringe friction. A mean pore fluid density may be assumed for an entire experiment for simplicity if differences are not large.

$$K = \frac{\frac{M}{\rho t}L}{A(h-h_{syr})}\left[1 + \left(T - T_{ref}\right)0.025\right]$$

Hydraulic conductivity is temperature dependent (due to a viscosity effect) and our raw data is evaluated at our laboratory temperature of 20 – 25 °C, but the reported values are referenced to 25 °C. The temperature dependence is significant and approximately 2.5 % per Kelvin at these temperatures. Alternatively, the intrinsic permeability may be evaluated, a property that is material specific and largely independent of temperature and fluid properties (conversion requires the hydrodynamic viscosity and fluid density, both as functions of temperature).

Uncertainties on length measurements (average of four measurements for length and diameter) are about 0.5 ‰, and 1 ‰ for pressure. Uncertainties on measuring liquid masses > 1 g are negligible (< 0.1 ‰). Combined uncertainties are therefore small, less than 5 ‰ for samples > 1 ml. Larger uncertainties arise from occasional small fluid-losses during the change of syringes. For short sampling intervals with small sample masses (< 0.5 g), a potential loss of 1 – 2 drops of fluid (0.02 – 0.05 g) during syringe changes may dominate uncertainties (5 – 10 %). Also, the effects of expanding and contracting small gas bubbles in the flow path may interfere with a steady out flow rate for short time periods. Earliest samples may contain a small amount of gas (from the dead volume at outflow, or any gas-filled porosity) and this leads to commonly observed reduced conductivities for the earliest sampling intervals.

Fig. 9-6: Mounting of a core assembly (core sample, DM 80 mm, with titanium end pieces) into a pressure vessel for an advective displacement experiment (see text for details).

The method of advective displacement yields very accurate sample-specific hydraulic conductivities compared to any indirect methods (e.g. in situ testing). Very slow core consolidation may be observable if measurements are extended over weeks to months. The measurements refer to a layered medium in direction perpendicular to layering.

9.5 In-line measurement of EC and pH

Electric conductivity is measured continuously in all experiments with small-volume flow-through cells that are normally used in ion-chromatography (Metrohm; Fig. 9-7). These cells have a bore diameter of 1 mm and an internal volume of only approximately 12 µl. The electrodes are made of stainless steel, separated by PTFE parts. Signal conditioning is made by either conductivity transmitters (JUMO ecoTRANS) or conductometers (Metrohm 712). Temperature compensation (2 %/K) is performed for most channels by the transmitter or meter, either based on room temperature or on dedicated temperature sensors attached to the conductivity cell. Otherwise, the same temperature correction is applied in Excel when post-processing uncompensated raw data. The internal reference temperature chosen is 22 °C, close to the prevalent laboratory temperature.

Two electronic switching boxes are used whereby up to 4 conductivity cells can be connected sequentially to a single meter/transmitter. These boxes also provide a position signal to identify the conductivity cell that is being recorded. The conductivity is retransmitted as analogue norm signal to the data acquisition system, the same unit that also records all other sensor signals.

The nominal cell constants are rather large for these small sensors (15 – 17 cm^{-1}), and the behaviour is somewhat non-linear towards higher conductivities. The cell constant is first matched to a primary commercial standard near 12 mS/cm (0.1 M KCl). In case where several cells are handled by a single instrument, any differences among cells are included in the individual conductivity calibrations. The same is true for effects caused by different lengths of signal cables installed. Each cell is calibrated with 4 – 5 standards between 12 and 55 mS/cm (Tab. 9-5), and a calibration curve (2-parameter exponential function) fitted in Excel. This function is used to post-process the electric conductivity logs. The conductivity standards consist of a commercial standard, and four secondary standards prepared in our laboratories.

The result of this relatively time-consuming calibration procedure is that the observed electrical conductivities at early stages of an advective displacement experiment can be properly quantified to provide an absolute estimate of salinity. There may be a long-term drift towards low apparent transmissivities due to electrode corrosion. This is assessed at the end of an experiment with a calibration check. The results of the calibrations are included in the data reports of each borehole.

The overall relationship used to accommodate all the corrections discussed above, is:

$$EC_{22} = a\left(EC_{DAQ}\left[1 + \left(T - T_{ref}\right) \cdot 0.02\right]\right)^{b}$$

where *EC* is the electric conductivity, either at 22 °C, or obtained from data acquisition (EC_{DAQ}). The fitting parameters *a* and *b* are obtained from the conductivity calibration. The temperature term with (T-T_{ref}) is only necessary if the DAQ data is not temperature-compensated to 22 °C (T_{ref}). The factor 0.02 refers to the temperature dependence of conductivity that is close to 2 %/K near 20 °C for NaCl-type salt solutions.

The uncertainties cannot be exactly established, mainly due to not well-constrained uncertainties in the secondary standards. Apart from any effects of long-term drift due to electrode corrosion, the measurements should be accurate to ± 2 %. There are some larger errors in relative terms at very low conductivities (pure water, tap water), but this is not relevant.

Tab. 9-5: Electric conductivity standards used for calibration.

Standard/salt	**Concentration**	**Nominal electric conductivity** [mS/cm]	**Electric conductivity at 22 °C reference temperature** [mS/cm]
KCl, commercial	0.1 M	12.90 at 25 °C	12.15
KCl	0.2 M	22.44 at 20 °C	23.38
$NaNO_3$	42.5 g/L	38.7 at 20 °C	39.6
NaCl	30 g/kg	48.6 at 25 °C	45.4
KCl	0.5 M	58.67 at 25 °C	55.15

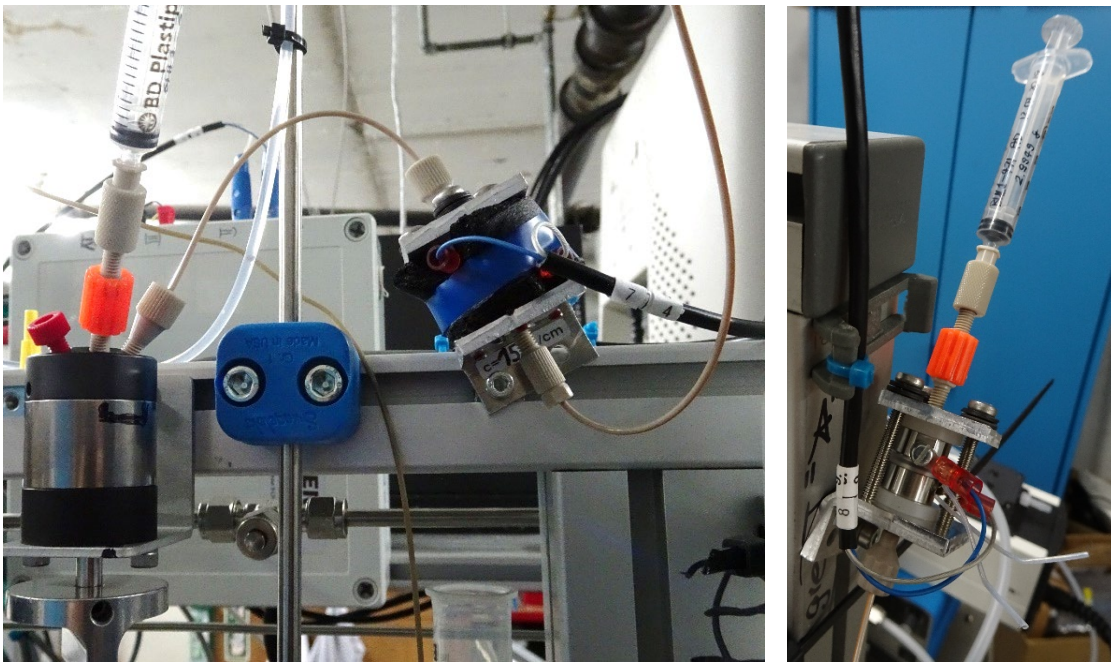

Fig. 9-7: Flow-through cell for electric conductivity.

Left: outflow from the experiment is from the top-right, through the cell (thermally insulated with neoprene) to a valve where a sampling syringe is mounted; right: conductivity cell without insulation, and sampling syringe directly attached to the cell.

The pH is measured from time to time in-line with small flow-through cells fitted with miniature pH electrodes (Orion Ross micro-pH combination electrode, Fig. 9-8). The cells are manufactured in-house from POM, with sockets (10-32 threading) for 1/16" PEEK capillary tubing for inflow and outflow. The internal volume is approximately 20 µl, depending on the immersion depth of the electrode. The cell is connected to a PEEK 6-port 2-position stream switching valve. In this way, apart from feeding a sampling stream, also a separate inlet and outlet for calibrating the electrode can be accommodated. The electrode is left installed in the cell and switching from measurement to sampling (and calibration) is done by changing the valve position. This is important because these small electrodes respond sensitively to mechanical handling. Normally, one cell is used for several nearby experiments, simply by a bridging connection from the sampling valve to the electrode valve.

When measuring pH, sampling is halted for the duration of a pH measurement, and this is normally combined with replacing a full syringe with an empty one. The required duration for pH measurement is 6 – 12 hrs, dictated by a low outflow rate of only about 0.2 ml/day. The combined dead volume of the extra flow line and pH cell is approximately 50 µl.

A difficulty is that installation of these small and fragile glass electrodes requires some expertise and very careful handling also during operation (opening of orifice, calibration). The most stable readings during calibration could be obtained in a slightly dynamic mode rather than at stagnant conditions. In a dynamic mode, the calibration solutions are slowly flowing through the pH cell, driven by an elevation gradient, with an open delivery syringe located at higher elevation, and an open waste syringe to receive the outflow at a lower elevation. In this way, an electrode is calibrated with standards at pH 4 and 7, and before and after each measurement, the pH 7 standard is measured as drift control. Normally, these calibration checks give values that are close together, and a small drift correction may be applied if significant. Any longer-term electrode drift is also corrected relative to the offset at pH 7 of the control measurements. If this offset is becoming larger, a new calibration is performed. The overall uncertainty is difficult to assess accurately, but likely not better than ± 0.05 pH units. The procedure is relatively efficient once cells are installed and calibrated. Electrode storage solution (3 M KCl) is filled into the flow-through cells when not in use.

All pH electrodes are connected to JUMO (ecoTRANS) conductivity transmitters, and temperature compensation is implemented with a dedicated Pt-100 temperature sensor located on or near the pH flow-through cells. The transmitter provides an analogue norm signal for pH to the data acquisition system for continuous recording.

The following relationship is used to obtain final pH values:

$$pH_{22} = pH_{raw,22} - (pH_{Std7} - 7.00)$$

Where pH_{Std7} is the average of the control measurements before and after with a pH 7 standard solution, and 7.00 accounts for the true value after initial calibration. Ph_{22} is the value compensated to a reference temperature of 22 °C. $"pH_{raw,22}"$ is the value provided by the pH transmitter, referenced to 22 °C. The temperature dependence of pH is small at circum-neutral pH values.

9.6 Sampling of extracted aliquots

Sampling of aliquots from the outflow is done by means of syringes. This provides a good isolation from atmosphere and adds only a small amount of back pressure due to syringe friction. Sampling may take days to weeks for an aliquot, and therefore water-tight and air-tight syringes are required. These criteria are met by standard polypropylene syringes with rubber seals. The rubber seals are, however, lubricated with a silicone lubricant, and we discovered that this does add some dissolve organic carbon to samples, including also some low molecular weight organic acids. This affects some of the earlier samples from the first Bülach borehole. The protocol was adjusted, and the syringes were cleaned with alcohol and shortly dried in a drying oven. This did not completely eliminate the TOC addition but made it rather small compared to that contained in the samples originating from the rock samples. The friction is somewhat increased by the cleaning process. Independent tests with rubber-free syringes showed that these are frequently not water-tight over extended periods of time. Gas-tight glass syringes with Teflon seals are not practical and induce rather high and greatly varying friction.

Fig. 9-8: Minitaure pH flow-through cell with micro Ross electrode.

Image in the centre shows connections to a two-position valve used for switching from sampling to pH measurement, and also calibration. Right: pH transmitter, with output signal to data acquisition.

The standard procedure is therefore to use standard syringes with rubber seals with capacities of 1, 2, 5, and 10 ml capacity. Small syringes are used at early times when more frequent sampling is required. We use mostly luer-lock type syringes with luer-lock caps, but for some sizes also syringes with normal luer orifices and caps.

The syringes are weighed including a dedicated cap, then attached to the luer adapter at the sampling valve, and date/time and masses recorded. There may be some gas sampled at early times, either from a small amount of dead volume, or any amount of gas-filled porosity, or gas produced by microbial activity. In such a case, the gas contained in a syringe is slightly under pressure due to syringe friction. This friction should be relaxed before changing a syringe to avoid spilling some drops of sample. Normally, a syringe change is not associated with any spillage, but 0.5 to 2 drops may be spilled on occasion (0.01-0.05 ml). This is only significant for small sample volumes below 1 ml.

Intermittent sample storage is a tricky issue and requires some compromise. Sampling itself may take 1 – 3 weeks and during this time syringes are subject to ambient temperature but are reasonably well protected from atmosphere. During this time, any supersaturation may lead to precipitation of solids, and any microbial activity may alter some aspects of sample composition (e.g. sulphate reduction by oxidation of organic carbon). Storage after sampling may be done in a refrigerator or at ambient conditions. Both have their merits and disadvantages. If supersaturation with respect to carbonates is an issue, cold storage will help because carbonate solubility is

increasing with decreasing temperature. If supersaturation with respect to gypsum or celestite is an issue, cold storage has adverse effects because solubility is decreasing towards colder temperatures. The best strategy is therefore to minimise storage time, and perform some essential measurements (e.g. pH, TIC) and preservation steps (acidification of an aliquot for cation analysis) as soon as possible after sampling.

It turned out that at least the samples from Bülach-1 are saturated with respect to calcite and gypsum (and dolomite and celestite) and therefore there really is no ideal storage condition. Because growth of some bacterial filaments or fungal hyphae were observed in one or two cases, a preservation method with chromate solution added to syringes prior to sampling was also tested. This requires some special pre-filtration before analysis and did not seem to make much of a difference. The procedure was abandoned for later work.

The following sampling procedure was established during the first Bülach borehole, but there may be some deviations due to availability of personnel or laboratory facilities:

- A first sample of 0.05 – 0.4 ml is discarded. This sample commonly also includes a little bit of gas displaced from the head space. The electric conductivity recorded during sampling the first drops varies a bit, from slightly smaller to a bit larger relative to a stable early elution plateau that is reached within a short time period.
- A first sample of 0.5 – 0.7 ml is taken, followed by one of ca. 1 – 1.5 ml. These two samples are immediately pre-treated and filed into the analytical procedures (see below).
- An in-line pH is measured.
- A further one or two samples of approximately 1 – 2 ml are taken.
- A second in-line pH is measured.
- Sample sizes are increased to 2 – 2.5 ml, and a 3rd pH measurement performed.
- After 5-6 samples, sample volume is increased to 5 ml, and in-line pH is measured less frequently. Larger sample, 10 – 12 ml, are used for Core samples with elevated hydraulic conductivity, and some samples may be skipped for analysis.

Some details about sample handling and pre-treatment are provided below. In case only information on the early extracts is desired (just porewater information, but not transport), the experiment may be stopped after taking 3-4 samples.

9.7 Determination of core density, water content and other bulk properties

Working with a defined sample shape (cylinder) offers the possibility to very accurately determine some bulk physical properties complementary to standard methods performed on fragmented material. The minimum amount of data required for the interpretation of an advective displacement experiment are the bulk wet density and the water content. The bulk wet density can be determined from the core mass and the core dimensions (volume), whereas the water content is initially determined from fragmented samples taken adjacent to the core sample, from above and below. In some cases, only sufficient sample material was available from one side of the core sample. Note that the initial bulk wet density may relate to a partially saturated state, whereas the derived bulk dry density (from water content and bulk wet density) is independent of the initial saturation state.

Normally, the core dimensions (volume) and mass, and the water content are determined also post-mortem. This allows to detect any water uptake during the experiment, any changes in dimension, and a more accurate determination of the water content taken along a profile of 5 sub-samples. The following formulae and relationships are used:

L_C: core length 4 measurements with calliper gauge

D_C: core diameter 4 measurements with calliper gauge, 2 at top and base

M_C: core mass (wet)

ρ_{pw}: density of porewater, estimated (or calculated) from concentrations

$V_C = \left(\frac{D_C}{2}\right)^2 \pi\, L_C$ core volume

$\rho_{b,w} = \frac{M_C}{V_C}$ bulk wet density

WC_{wet}, WC_{dry}: water loss on drying at 105 °C, relative to wet/dry mass

$M_W = M_C \cdot WC_{wet}$ water mass contained in core (excluding dissolved salts)

$\rho_{b,d} = \frac{M_C - M_W}{V_C}$ bulk dry density

M_{DS}: mass of dissolve solids

$\rho_g = \frac{M_C - M_W - M_{DS}}{V_C - (M_W + M_{DS})/\rho_{pw}} \approx \frac{M_C - M_W}{V_C - V_W}$ grain density

$\emptyset_{WC} = \frac{(M_W + M_{DS})/\rho_{pw}}{V_C} \approx \frac{V_W}{V_C}$ porosity fraction based on water content

Errors associated with above quantities are very small, < 0.5 ‰ for length measurements, and < 0.1 ‰ for mass measurements, such that the error on the bulk wet density is ~ 1 ‰, and about 1.5 ‰ for the bulk dry density. If significant breakouts are present from sample cutting, this may dominate the error (a geometric sample volume that is too large), and lead to low apparent densities. The volume or mass of breakouts can be estimated to evaluate if a correction is required. Typical sample masses of the cores processed are 900 – 1200 g, and a 1 ‰ breakout would correspond to 0.9 – 1.2 g, and this would be quite an obvious and dramatic feature. Commonly observed breakouts are at the millimetre scale, along edges, or rarely along discrete lithological layers, and do not add significantly to the measurement uncertainty (a very small systematic error).

The bulk dry density can be obtained more reliably by the above method compared to a direct measurement, because the latter bears the uncertainty of volumetric changes of the rock skeleton induced by the drying process. Intrinsically, the bulk includes the mass of the salts originally dissolved in the porewater.

Also grain density – a non-trivial measurement if a high accuracy is required – can be calculated with small errors of approximately < 2 ‰. At elevated salinities, the calculation should account for the mass of the dissolved salts (M_{DS}) and also the salt volume in solution (here expressed with a density correction applied to porewater mass) as indicated in the first expression on the right-hand-side of the equation.

The water-content porosity (porewater filled porosity fraction) is simply the ratio of the porewater volume and the core volume. A density correction is required at elevated salinities to convert the measured water loss to a porewater volume including the dissolved salts.

A main issue is whether the sample core is initially fully saturated, or partially desaturated. This is most reliably assessed by measuring core volume and mass at the end of an advective displacement experiment, in comparison to the initial state. If not done, the bulk wet density, water content relative to wet mass, and water-content porosity refer to a sample with an unknown saturation ratio.

With post-mortem measurements of core mass [$M_{C,final}$] and core dimensions, the truly saturated bulk wet densities and water-loss porosity can be established with the same relationships given above. Any difference to the initial evaluation provides information on any initially gas-filled porosity fraction. Core volume is assumed to have remained constant in the following equation:

$$\emptyset_{gas} = \frac{M_{C,final} - M_{C,init}}{V_C}$$ volume fraction occupied by gas

The total porosity is (ϕ_{WC} + ϕ_{gas}), and the gas-filled porosity proportion $\phi_{gas}/(\phi_{WC} + \phi_{gas})$. The inverse ratio represents the porosity fraction filled with pore fluid, and this is equal to the saturation ratio.

9.8 Chloride-accessible porosity (bromide-accessible porosity)

The chloride accessible porosity fraction – or anion-exclusion effect – is a key parameter in scaling chloride concentrations obtained from aqueous extracts to porewater concentrations, and thus also for the interpretation of chloride profiles at the formation scale. Bromide data may be treated in analogy, although less work has been performed on this component and its exclusion effects in dense clay media.

Pore space in claystones may be subdivided into two domains in a simplistic model. One domain is associated with "clay porosity" and negatively charged clay surfaces (Donnan porosity, "micro-porosity"), and the other one contains charge-neutral pore fluid not affected by electrostatic effects (free porosity, "macro-porosity"). Anions are suppressed from the Donnan porosity by electrostatic forces and accumulated in the free porosity. In reality, there is no clear division but gradual transitions depending on the details of the pore network and distribution of minerals with surface charge. A further simplifying assumption associates the mobile portion of the pore fluid that is moved by a hydraulic gradient with the free porosity, and the shear-surface towards the stagnant portions would coincide with interfaces to the Donnan porosity. Given these simplifying assumptions, it is straightforward to deduce an anion-accessible porosity fraction [ϕ_i] for a chemically conservative species. It is simply the ratio of the concentration measured in the aqueous extracts scaled to the entire porewater content, and the concentration measured in the early aliquots displaced from a core sample:

$$C_i^{AqEx\_PW} = C_{AqEx}^i \frac{1}{WC} \frac{L}{S}$$ concentration scaled to WC

$$\emptyset_i = \frac{C_i^{AqEx\_PW}}{C_i^{AD}}$$ anion-accessible porosity fraction

In the equations above, [$C_i^{AqEx\_PW}$, mg/kg] is the concentration scaled to porewater by means of the gravimetric water content [*WC*, g/g, relative to wet mass] and the liquid/solid ratio [*L/S*, g/g, wet solid] used in the aqueous extract. At the commonly used L/S of 1, the scaling factor is 20 (1/WC) at a water content of 5 wt.%, for example. The quantity [C_i^{AD}, mg/kg] is the concentration of the anion measured in the early aliquots from an advective displacement experiment.

In practice, this may work well for conservative anions that do not significantly form aqueous complexes such as chloride and bromide, and perhaps also for iodide, although low concentrations and analytical difficulties may be a limiting factor. Sulphate and bicarbonate are not conservative anions and are also complexed to a significant degree, and such a simple model is not appropriate. There is little insight if this may also be applicable to low molecular weight organic acids, but previous experience indicates that other processes may be dominant in the mobilisation of these components during advective displacement and aqueous extraction.

In reality, the distribution of porosity types is a continuum and its description also would require aspects of pore geometry and connectivity (presence of dead-end pores, for example). Other methods that are used to derive the anion-exclusion effects (squeezing, through-diffusion experiments) may not probe a sample in the same way as advective displacement does, and the obtained value for an anion-exclusion effect may be method-specific to a certain degree. There is relatively little known about this effect for divalent anions: sulphate is commonly a reactive component, and to a significant degree complexed to form neutral and monovalent species.

9.9 Preparation of the artificial porewater

An artificial porewater (APW) is required to be injected and to displace the in situ pore fluid. This APW is site-specific and is based on available knowledge regarding salinity and other compositional aspects. A composition is estimated in the absence of information. The same APW may be used for an entire borehole (e.g. from Brown Dogger to Liassic), or different compositions may be used if warranted by data. The same composition as used for advective displacement experiments for the Schlattingen borehole was used for the boreholes Bülach-1 and Trüllikon-1.

The approach to design an APW is similar to that used for defining the reference porewater for the Opalinus Clay (Mäder 2009). The procedure is also described in a report describing three advective displacement experiments with samples from the Schlattingen borehole (Mäder & Waber 2017b).

Common features include that saturation with respect to calcite and dolomite is imposed in the modelling calculation, and a partial pressure of CO_2 of $10^{-2.2}$ bar is prescribed. The partial pressure of CO_2 is imposed with an $Ar - CO_2$ gas mixture that is also used in the advective displacement experiments for the initial condition. The details are included in the data reports of the individual boreholes.

9.10 Sample preparation for accompanying analyses

Differences regarding the procedures used for sample treatment for AD experiments and the standard procedures used for PW samples are briefly highlighted. The strategy used for PW samples aims at averaging subsamples (fragmented samples) across an entire representative core section. Accompanying analysis of AD samples can only average properties from short core sections adjacent to the section used for the AD experiment. The obtained data reflects therefore a larger degree of sample heterogeneity because of sampling parallel to lithological layering, with only limited averaging across layering.

The standard pre-characterisation includes measurement of water content, aqueous extracts, Ni-en extracts, and mineralogy. The starting material are two short cylindrical sections of 20 – 40 mm length cut from above and below the sections used for advective displacement (Section 9-3). The procedure includes the following steps, minimising exposure to air:

- Removing outer margins by hammering, and also sections of the cut surfaces.
- Fragmentation of the material by hammering and subsampling aliquots (optionally in duplicate) for water content (40 – 100 g) and aqueous extracts (30 g), and a single sample for Ni-en extracts (30 g). This is done for two segments, one from above and one from below the core section used for the AD experiment). In case of limited material, aqueous extracts and Ni-en extracts may be done with 15 g.
- Samples for water content are immediately weighed, and those for the extracts are immediately added to the previously prepared solutions. Test solutions were prepared under anoxic conditions, and samples for extractions transferred back into an anaerobic chamber. The head spaces of the containers were quickly flushed with argon to avoid any oxygen.
- Some surplus material is vacuum-packed as backup material.

Deviations from the above procedure includes a reduction of sample mass for the aqueous and Ni-en extracts to 15 mg in case not sufficient sample materials is available (from cores that are shorter than the minimum required lengths). In some cases, only material from one side of the Ad sample is available or selected, dictated either by a limited core length, or by the presence of some significant heterogeneity (pyrite-rich layer, large nodules).

After this, the samples are passed on to the analytical teams for further processing and analysis in the same way as done for PW samples.

A slightly different procedure is followed for any post-mortem analysis of the core sample used for advective displacement. The sample is extracted from the advective displacement apparatus leaving the core assembly intact, still wrapped in Teflon and latex rubber. The following procedure is followed for measurement of water content, and any aqueous extracts or en-extracts desired:

- The rubber and Teflon wraps are removed, and so are the PEEK filters at top and base.
- Any excess fluid at surfaces (mostly where the filters were located) is blotted off by a tissue.
- The core sample is wrapped in a layer of plastic foil. The length and diameter are measured and the sample is weighed.
- The plastic wrap is removed and weighed, and the core sample is vacuum-packed in a plastic bag for short interim storage.
- The core sample is cut in half along the core axis by dry cutting. One half is vacuum-packed as backup sample, while the other one is temporarily sealed until further processing.
- Further processing includes splitting the half-core parallel to bedding in 5 approximately equal-length segments with a chisel.
- The five segments are fragmented by hammering, and aliquots subsampled for measurements of water content, and any aliquots desired for aqueous extracts and/or Ni-en extracts.

Of importance for all advective displacement experiments is to obtain an accurate water content – here as an average of 5 layers. This also provides information on lithological heterogeneities (porosity in this case). A comparison to water content measurements from pre-characterisation will also reveal the presence of partially saturated conditions of the sample after delivery, either due to the presence of a gas phase at in situ conditions, or any desaturation during sample unloading (degassing, relaxation), handling and storage.

9.11 Analytical methods

Our standard analytical methods are used for analysing aqueous extracts and Ni-en extracts (Chapter 6). Likewise, the mineralogical analyses are also performed according to protocols (Sections 4.1 and 4.3), and so are BET measurements (if performed; Section 5.3) and C-N-S measurements (Section 4.2).

The aim for the displaced porewater aliquots to collect at least three small samples that are sufficient for a full characterisation of what is closest to the in situ porewater, in combination with at least two in-line pH measurements. Some experiments are monitored for an extended time to monitor chemical trends, break-through and break-out of tracers, e.g. information that allows to derive transport properties. Sampling size can be increased for later times, and this makes the analysis somewhat easier and allows measuring some additional parameters. All samples are collected in small syringes (1, 2, 5, 10 ml) attached to the out-flow capillary of an AD experiment. Samples may be stored for a few days to able to pool samples from experiments running in parallel.

The analytical procedures for the displaced porewater aliquots depend on the quantity of sample available and the objective. Only a subset of parameters may be measured for the earliest and smallest aliquots. This may vary in some details from AD experiment to AD experiment. The analysis includes a combination of the following:

- Splitting of a sample into fractions for anion analysis (pre-diluted), cation analysis (pre-diluted), and an undiluted fraction for stable isotope analysis. Commonly, a pH measurement is done as well on a small aliquot.
- Further dilutions are prepared as required at the time of performing the measurements.
- Some samples are dedicated to just a few parameters, such as stable isotope analysis and pH measurement. This allows to process smaller samples that have been collected over a shorter time.
- For some samples, special attention is directed towards analysing the organic carbon types and inorganic carbon. These samples are processed and analysed within 1 – 2 days of withdrawing a sample.

The exact treatment of samples and methods applied is described in the data report. The analytical protocols are usually those specified in this report for the specific analytical instruments (Chapter 13).

An exception are the samples collected for evaluating possible contamination effects by the drilling fluid. These samples were collected when trimming cores on a lathe from 95 mm DM to 80 mm DM as used for the AD experiments (Section 9-3). The fine-grained material was split – an aliquot sent to Hydroisotop GmbH (measurement of Na-fluoresceine) and another on dried and prepared for aqueous extracts. Because these samples are already partially dried during the turning process, the preparation (drying etc.) was done under aerobic conditions. These samples are therefore not comparable to those from using the anaerobic protocol (Section 6.1), but simply serve to detect potential contaminants contained in the drilling fluid.

10 High-Pressure Squeezing

M. Mazurek

Squeezing tests are performed at the Central Research Institute of Electric Power Industry (CRIEPI), Abiko, Japan. One of the reasons for choosing this laboratory is the ability of CRIEPI's rig to work at pressures of up to 512 MPa. The rig is illustrated in Fig. 10-1a and a scheme of the device is shown in Fig. 10-1b. The sample chamber is cylindrical (diameter 5 cm, height 10 cm), and fiber glass filters (Whatman GF/B 1.0 μm, 47 mm diameter) are attached on the upper and lower sample surfaces, where porewater is collected in syringes. Pressure is exerted by a piston located above the sample chamber.

Rock samples are cleaned, evacuated and heat sealed in an Al-coated plastic tube immediately after core recovery at the drill site. They are stored in a refrigerator at 4 °C prior to shipping and also at CRIEPI before the experiments are started. Samples are dry cut to polygonal prisms to the size and shape needed for the squeezing apparatus, weighed and then inserted into the sample chamber (Fig. 10-2). This procedure requires about 15 – 20 mins. Depending on the lithology and the expected water content of the sample, the first pressure step is chosen at 100 – 200 MPa, followed by squeezing at 300, 400 and 500 MPa. Holding times at any pressure step are 2 – 4 days, so the total extraction time varies between 10 and 20 days. Strain of the sample during squeezing is monitored by recording the piston movement over time. Squeezed waters are collected separately at each pressure step. They are stored cool, in 2 or 4 mL glass vessels and are then sent to RWI, Uni Bern, for chemical and isotopic analysis.

After disassembly, the squeezed cores are heat-sealed in plastic foil immediately and stored cool. After shipping to the University of Bern, a suite of post-mortem analyses are performed, including the determination of the water content by drying at 105 °C, followed by aqueous extraction tests. The obtained data allow the derivation of the total water and Cl^- budgets in the samples (total Cl^- = squeezed + leached Cl^-, total water content = squeezed water + water content of the squeezed sample) and so the original Cl^- concentration in units of $mg/L_{porewater}$. Comparing the latter with the Cl^- concentration in the squeezed water, which is considered to represent the free porewater, leads to the estimation of the Cl^--accessible porosity fraction.

High-pressure squeezing, in particular at higher pressure steps, leads to experimental artefacts. The concentrations of monovalent ions (mainly Cl^-, Na^+, K^+) decrease with increasing pressure, which is attributed to effects of ion filtration during flow through the nanometric pore network. Concentrations of bivalent cations are only weakly affected by filtration (see also Bresler 1973, Kharaka & Berry 1973), and the concentrations of Ca^{2+}, Mg^{2+} and Sr^{2+} tend to increase with squeezing pressure. This is considered to be the consequence of the increased solubility of carbonate minerals at higher pressures. Mazurek et al. (2015) concluded that the first aliquot of the squeezed water is the best approximation of the porewater because it originates from the rim portions of the core, where fluid pressure (governing mineral solubility) is relatively limited and the travel distance through the pore network is minimal (which limits the effects of filtration). This conclusion was further confirmed by Rufer & Mazurek (2018) who equilibrated rock samples with an artificial porewater (APW) and then subjected the samples to squeezing. The major-element composition of the squeezed water was found to be very close to that of the APW.

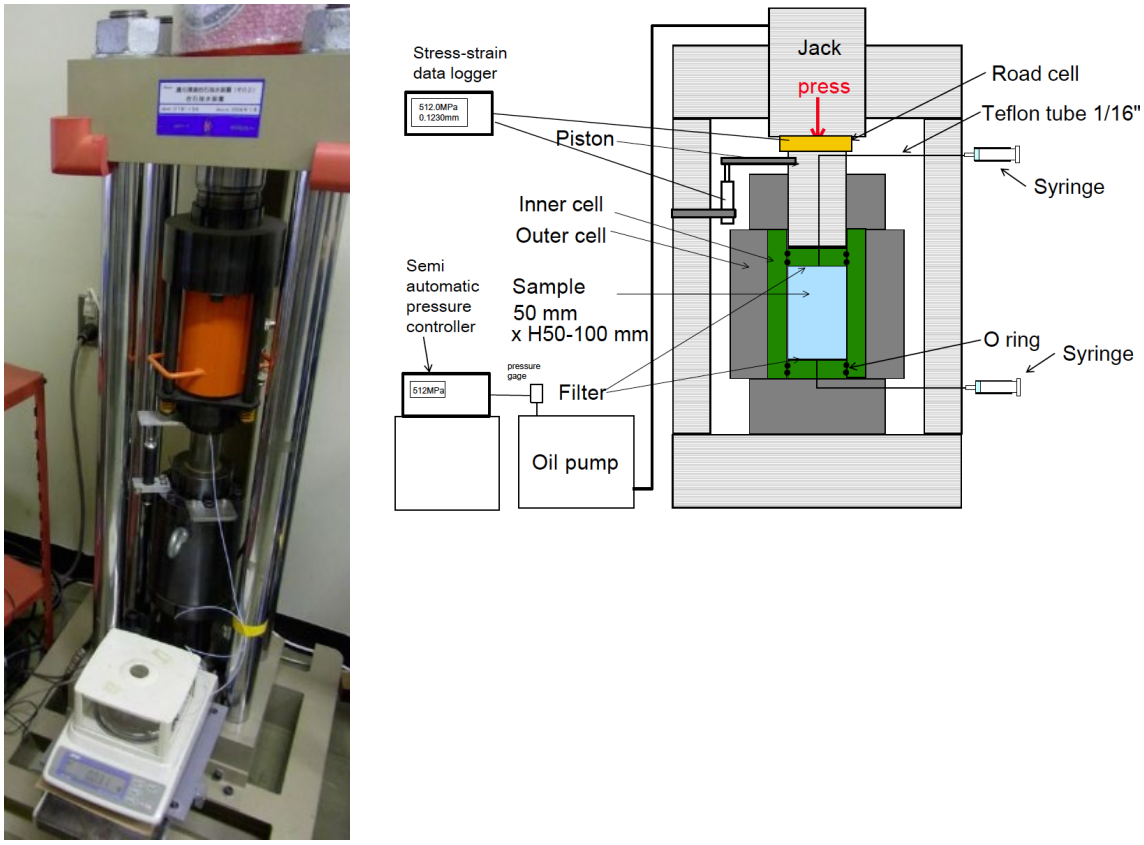

Fig. 10-1: Rock squeezing apparatus at CRIEPI, (a) photo and (b) scheme.

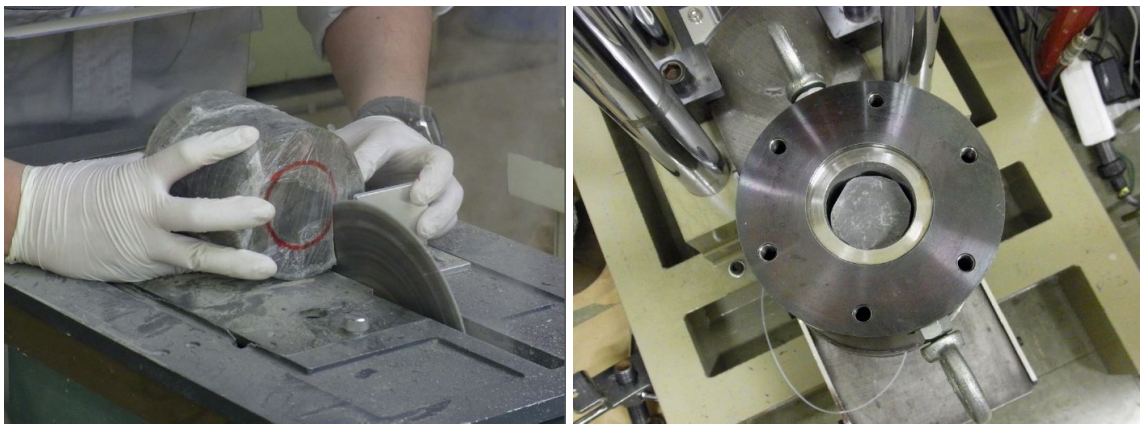

Fig. 10-2: (a) Dry cutting of sample and (b) placement in sample chamber of the squeezing apparatus.

11 Chemical Out-Diffusion Technique

H.N. Waber, T. Gimmi

Out-diffusion experiments are based on the premise that porewater contained in a rock sample equilibrates over time with an experiment solution, in which the rock sample is immersed in a closed container. Method development of out-diffusion experiments goes back to crystalline rocks, which have a favourable mineralogical composition in terms of slow mineral reaction rates. For crystalline rocks, out-diffusion experiments could be successfully applied to derived porewater concentrations of chemically conservative compounds (Cl^-, Br^-), pore diffusion coefficients of these compounds, and more recently also assessing mineral reactions by monitoring the complete chemical changes in the experiment solution as a function of time (e.g. Waber & Smellie 2008, Waber et al. 2012, Eichinger & Waber 2013, Eichinger et al. 2018). The effects of rock sample perturbation by the drilling process and drilling fluid contamination have been investigated in detail for isotropic and anisotropic crystalline rock types (Waber et al. 2011, Meier et al. 2015).

In sedimentary rocks, reaction rates of major minerals such as carbonates, sulphates and sulphides are fast and dissolution reactions will take place in a no longer negligible degree. In clay-rich rocks the exchange between experiment solution and porewater in the rock sample will cause swelling of clay minerals and change the ion-accessible porosity due to the commonly large differences in composition and ionic strength of the two solutions. Therefore, the out-diffusion technique is still limited to non-swelling rocks. First attempts of out-diffusion experiments were conducted with Canadian carbonate rocks containing brine-type porewater compositions (Waber et al. 2007, Koroleva et al. 2008, Hobbs et al. 2011) that were followed by application to limestone samples of the Effingen Member in northern Switzerland (Waber & Gimmi 2008, Mazurek et al. 2012). There, it was found that the derived Cl^- concentration as well as the Cl^- pore diffusion coefficients agree reasonably well with those determined by other techniques.

In the Nagra Site Investigation Programme, the out-diffusion technique is applied to carbonate/sand-rich lithologies and lithologies of low water content (< 2 wt.%) of Jurassic and Triassic age where the squeezing and advective displacement techniques are no longer applicable.

As for other porewater experiments, originally saturated rock material is a pre-condition for the success of such experiments. During the experiment, mineral dissolution must be kept at a minimum. This can be achieved by preparing an appropriate composition of the test solution so that dissolution is suppressed by mineral saturation, and by monitoring inevitable carbonate mineral dissolution using carbon isotopes. However, so far it is not feasible to carry out the out-diffusion experiments in an O_2-free environment (glovebox), so this is a source of susceptibility to sulphide oxidation and associated mineral reactions.

Advantages of the chemical out-diffusion approach include:

- The technique is non-destructive compared to aqueous extraction and squeezing approaches.
- The ratio of rock volume not affected by drilling and sample preparation is large compared to through-diffusion experiments this minimising the effect of such perturbations on the derived results.
- The technique may deliver porewater concentrations of chemically conservative compound as well as their pore diffusion coefficient.

Disadvantages of the chemical out-diffusion approach include:

- The inevitable mineral reactions during the experiment and associated possible (minor) changes in porosity/permeability.
- The lack of completely controlled conditions with respect to gas exchange.
- The long experiment duration until the attainment of steady-state conditions.

11.1 Sample preparation

Unlike with clay rocks, cutting of limestones and dolostones require little water to be efficient. In analogy to crystalline rocks of similar low permeability, however, the application of minimised water during cutting is expected to not affect more than the outermost rim of the cut surface in the range of the average grain size (i.e. < 1 mm to few mm depending of rock type).

The laboratory preparation of the drillcore received from the drill site occurs in two steps. Firstly, top and bottom of the core are cut off within a few minutes to obtain a full diameter section of 12 – 15 cm in length as received from the drill site. This section is quickly cleaned dry, vacuum-packed and stored for further conditioning. The central uncontaminated and saturated material of the top and bottom part of the drillcore is used for water-content measurements (*cf.* Section 5.1) and optional aqueous extractions (*cf.* Section 6.1).

Subsequently, the vacuum-packed full diameter section is overcored using a 52 mm diamond drill what results in a perfectly shaped cylinder of 50 mm in diameter and 12 – 15 cm. Again, little water is applied to speed up the coring process. Depending on the friability of the rock this process lasts between about 5 and 8 mins. After rapid cleaning dry, the mass of the core is recorded using an analytical balance. The obtained cylinder is then placed into a pre-prepared vapour-tight PVC container and the mass is recorded again. Finally, the container is filled with experiment solution as schematically shown in Fig. 11-1 with the mass of added experiment solution and the total mass of PVC container, rock cylinder and experiment solution being recorded. The solid:liquid (S:L) ratio in the experiment vessel is optimised in order to allow removal of small solution aliquots (*time-series samples*) for chemical analyses including pH until equilibrium conditions between the porewater and the experiment solutions are attained.

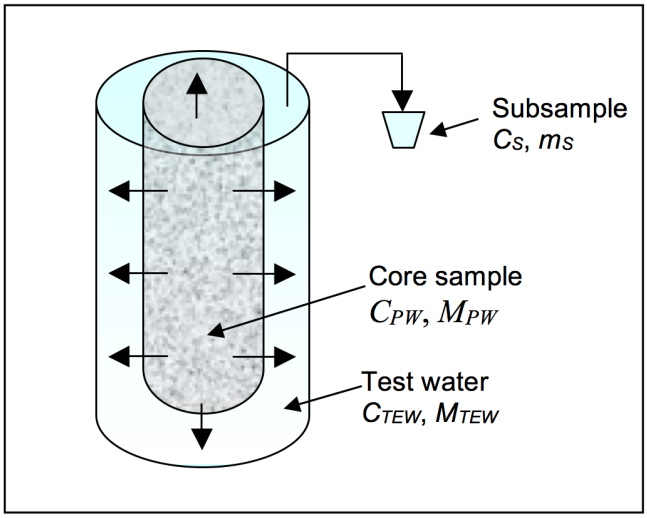

Fig. 11-1: Schematic illustration of the set-up used for out-diffusion experiments.

11.2 Experimental procedure

In contrast to earlier out-diffusion experiments and in order to get clearly defined boundary conditions for diffusion calculations, the experiment solution is chosen to be degassed ultrapure water. Bacterial activity is minimised by adding a small amount of $HgCl_2$ (< 1 µg/L) to the experiment solution. To accelerate out-diffusion, the vapour-tight PVC containers are placed into a rotating water bath with a constant temperature of 45 °C. For practical reasons, the experiments are carried out under atmospheric conditions, so some degree of oxidation will occur.

Termination of the experiment occurs when the chemically conservative compounds Cl^- and Br^- reach constant concentrations for a long enough time span. The PVC containers are then removed from the water bath and the experiment solution is quickly cooled down to ambient conditions by placing the container into a water bath at 20 °C. Subsequently, the mass of the still closed and filled container is recorded. The experiment solution is the removed and immediately analysed for alkalinity by titration and pH (*cf.* Chapter 13). An aliquot of the experiment solution is acidified for cation analyses whereas the other part is left unchanged for anion analyses using ion-chromatographic and spectrometric analytical techniques (*cf.* Chapter 13).

The rock cylinder, which is still wet at its surface is then removed from the container and placed on an analytical balance. The mass of the rock cylinder is recorded during evaporation of the surface water until the appearance of the surface is the same as that of the entire drillcore received from the drill site. This latter mass is taken as the mass of wet (saturated) rock. In combination with the mass of dry rock after complete drying at 105 °C it serves for the derivation of the gravimetric wet water content, w_w, of the rock cylinder as described in Section 5.1. The water-loss porosity, ϕ_{WL} , is then derived using either the grain density, ρ_g, or the bulk wet density, ρ_{bw}, of the rock. The grain density is derived two-fold, once using He-pycnometric techniques and once using the volume of the out-diffusion cylinder (*cf.* Section 5.2). Grain density by He-pycnometry is determined on sample aliquots prepared from the top and bottom sections of the entire drill core. The well-defined sample shape (cylinder) allows determining very accurately some bulk physical properties such as the bulk wet density, ρ_{bw}, and after drying the bulk dry density, ρ_{bd}, of the rock complementary to standard methods performed on fragmented material. This allows detecting any water uptake during the experiment, any changes in dimension, and a more accurate determination of the water content and water-loss porosity, respectively.

Using geochemical modelling approaches the amount of calcite and dolomite dissolved in this ultrapure water until equilibrium with both mineral phases is reached can be well quantified. Analysis of the isotope composition of total dissolved carbon, $\delta^{13}C_{DIC}$, in the final solution will put an additional strong constraint on these model calculations to correct for mineral dissolution during the experiment by applying isotope mass-balance considerations. It should be noted that the amount of calcite and dolomite dissolution is almost negligible (approx. 2.9 mmol/L of calcite and 0.14 mmol/L of dolomite at 20 °C) compared to the total inventory of these minerals in the rock cylinder (total mass ~ 600 – 800 g). As this dissolution will essentially take place at the rock cylinder surface the largest proportion of the rock volume will not be affected. Thus, the diffusion properties will basically remain unchanged, except for the outermost rim that is anyway inevitably affected b the overcoring process. As a consequence, the time-series samples collected within about the first 48 hrs are expected to display a different behaviour compared to the later ones collected over about 4 – 12 months depending on the diffusivity of the rock.

11.2.1 Monitoring of diffusive equilibration

Steady state with respect to out-diffusion of Cl^- and Br^- from the porewater of the rock sample to the experimental solution is attained when the time-series concentrations of chemical conservative compounds (Cl^-, Br^-) reach a plateau, *i.e.* when they remain constant over time. According

to previous experience with rock types of similar diffusivity, steady state is expected to be reached after about 50 – 100 days. To ensure complete equilibration, the experiments are run over at least 4 months with some rock types requiring much longer duration.

The attainment of equilibrium conditions in the out-diffusion experiments is monitored by taking small time-series samples of the experiment solution of 0.5 mL at regular intervals. Initially, such time-series samples are collected at intervals of several hours to a few days and later at intervals of a few weeks. These time-series samples are immediately analysed for pH and later for complete major cation and anion compositions using ion-chromatographic techniques as described in Chapter 13.

11.2.2 Composition of equilibrated experimental solution

After termination of the experiment, the experiment solution is the removed from the experiment vessel and filtrated using 0.2 µm PES filters. The immediately analysed pH and total alkalinity combined with chemical analyses of dissolved compounds (*cf.* Chapter 13) are used for geochemical model calculations to derive mineral saturation states and modelled estimates of the mineral reactions that took place during the experiment.

For the chemically conservative compounds Cl^- and Br^-, the concentrations in the equilibrated experiment solution directly serve as boundary conditions in the derivation of their pore diffusion coefficients. For reactive compounds, the concentrations in the equilibrated experiment solution first have to be corrected for the amounts introduced to actual porewater concentration by mineral and exchange reactions and pore diffusion coefficients can be attempted to be derived by reactive-transport model simulations.

11.3 Deriviation of porewater concentrations

The concentration of the chemically conservative compounds Cl^- and Br^- measured in the final experiment solution after termination of the experiment is converted to porewater concentration by mass balance according to:

$$C_{PW} = \frac{\left(M_{PW}\,\alpha + M_{ExSi} - \sum^{n} M_S\right) C_{ExS\infty} - \left(M_{ExSi}\,C_{ExSi}\right) + \sum^{n} M_S\,C_S}{M_{PW}\,\alpha} \qquad (11\text{-}1)$$

where C = concentration per mass of porewater, M = mass, α = anion-accessible porosity fraction, n = number of subsamples, PW = porewater, ExS = experiment solution, S = small-sized subsample taken for Cl^- time series, i = at the beginning of the experiment, and ∞ = at the end of the experiment.

For reactive compounds, this mass-balance approach is no longer valid and reactive-transport model simulations have to be applied to derive estimates of the in situ water composition.

11.4 Estimation of diffusion coefficients

Diffusion parameters can be calculated from the time-series data. It is noted that these out-diffusion experiments have been carried out on preserved saturated core samples with a total mass of > 600 g whereas conventional diffusion experiments are usually carried out on smaller (often below 100 g) samples that have often been re-saturated. A pore diffusion coefficient for Cl^- (and possibly Br^-) can be estimated by visually fitting the observed concentrations in the test solution

with concentrations calculated for radial diffusion out of a cylinder. This approach is well constrained because of the well-defined shape of the overcored rock cylinder used in the experiment. In view of the large cylindrical outer surface of the core compared to the top and bottom surfaces, transport through the latter was neglected and diffusion across the axial surface only was considered in modelling. This allows a 1-D radial transport equation for diffusion to be used:

$$\theta \frac{\partial C}{\partial t} = \frac{1}{r} \frac{\partial}{\partial r} \left(r D_e \frac{\partial C}{\partial r} \right) \tag{11-2}$$

where θ is volumetric water content accessible for Cl^- (*i.e.* the water-loss porosity if no anion exclusion occurs); C is Cl^- concentration in porewater; D_p is pore diffusion coefficient; $D_e = \theta \bullet D_p$ is effective diffusion coefficient; r is space coordinate ($0 < r \leq a$); a is radius of the core; and t is time.

The containers are gently rotated throughout the experiment to ensure complete mixing of the experimental solution. Thus, mixing of the test solution surrounding the core is much faster than the expected diffusion within the s of the rock. It is thus justified to assume that the solutes diffusing out of the core quickly mix in the surrounding test solution. In this case, the boundary condition at r = a (*i.e.* at the core/test solution interface) becomes:

$$V_w \frac{\partial C_w}{\partial t} = -A D_e \left. \frac{\partial C}{\partial r} \right|_{r=a} \tag{11-3}$$

where V_w is the volume of the experimental solution surrounding the core; $C_w = C_{(r=a,t)}$ is the Cl^- concentration in the experimental solution; $A = 2\pi aL$ is cylindrical outer surface of the core; and L is length of the core. At $r = 0$, a zero gradient boundary condition applies. Initially, the concentration in the surrounding solution is zero, whereas for the porewater a homogeneous value of $C_{(r<a,\ t=0)} = C_{ExS,t=0}$ is assumed. This is reasonable considering the generally good match between data and simulations.

An analytical solution for the above equations for diffusion out of a cylinder into a well-mixed reservoir is (Crank 1975):

$$C(r,t) = C_{eq} - \left(C_{ExS,t=0} - C_{eq} \right) \sum_{n=1}^{\infty} \frac{4(\beta+1)\exp\left(-D_p q_n^2 t / a^2\right)}{\left(4 + 4\beta + \beta^2 q_n^2\right)} \frac{J_0(q_n r / a)}{J_0(q_n)} \tag{11-4}$$

Here, $\beta = V_w/(\pi a^2 L\theta)$ is ratio of the reservoir volume to the volume of porewater within the cylinder; $C_{eq} = C_{ExS,t=0}/(\beta+1)$ is the final equilibrium concentration; and q_n are the positive, non-zero roots of

$$\beta q_n J_0(q_n) + 2 J_i(q_n) = 0 \tag{11-5}$$

which are obtained for each value of β numerically with a Newton-Raphson algorithm. $J_0(x)$ and $J_i(x)$ are Bessel functions of the first kind of order zero and one respectively. In applying the above solution, the small effect on the transient phase of removing 0.5 mL aliquots from the reservoir solution for analyses is neglected. However, this effect is accounted for when calculating the initial concentration $C_{ExS,t=0}$ from the final equilibrium concentration C_{eq} and the corresponding mass balance.

There is some unquantifiable uncertainty related to physical and chemical adjustments of the rock samples to the new conditions, i.e. to ambient pressure and to contact with deionised water. This results in a more or less significant alteration of the original porosities and transport properties compared to those for in situ conditions. Nevertheless, the estimated pore diffusion coefficients for Cl^- are at least valid within a factor of about 2 to 4 as shown by comparison with independently derived pore diffusion coefficients (e.g. Mazurek et al. 2012, Van Loon 2012). An advantage of the out-diffusion experiments is the large mass of rock involved compared to conventional through-diffusion experiments. To some degree these balances induced chemical perturbations such as mineral dissolution, which are shown below to be of minor importance. It also minimises the relative effects of cutting or sawing the rock but might not reduce effects of stress release.

The original D_p values is obtained for the experimental temperature of 45 °C. These values are corrected for temperature and reported as D_p values at 25 °C. The correction is performed according to the Arrhenius equation:

$$D_p(T) = D_p(T_{ref}) \exp\left[-\frac{E_a}{R}\left(\frac{1}{T} - \frac{1}{T_{ref}}\right)\right] \quad (11\text{-}6)$$

where E_a is the activation energy of the diffusion process and R is the gas constant (8.314 J/mol/K). A value of E_a = 19 kJ/mol was used for the correction, which is similar to values reported for diffusion of HTO in bulk water (Mills 1973) and of HTO in compacted clays (Van Loon et al. 2005, González Sánchez et al. 2008). This leads to a correction factor for the data at 45 °C of 0.62.

The effective diffusion coefficient, D_e, for Cl^- is obtained by multiplying D_p by the relevant porosity for Cl^- diffusion, *i.e.* the anion-accessible porosity, which is related to the water-loss porosity by a reduction factor and as derived by advective displacement and through-diffusion experiments.

12 X-Ray Computed Tomography of Core Samples

U. Mäder

Medical X-ray computed tomography was used to scan a subset of core samples while still vacuum-packed in plastic and plasticised aluminium bags. Cores processed included all AD cores and some DI cores, as well as PW cores of the clay-rich sequence (separate project, managed by Lukas Keller of ZHW). The resultant 3D images used for our studies served to (1) select appropriate samples or sample sections for all AD experiments (Section 9.3), and (2) to select appropriate DI samples (for diffusion experiments) at different stages of sample preparation.

The scans were performed at the Institute of Forensic Medicine (IRM) of the University of Bern by Nicole Schwendener (IRM) and Lukas Keller (ZHW) using a Siemens Somatom Definition AS 64 (Siemens, Forchheim, Germany) medical scanner. The scanner was operated with the same settings for all campaigns at 140 keV using propriety image reconstruction software. Reconstruction was done to a voxel size of 0.25 × 0.25 × 0.4 mm, producing X-Y greyscale images stacked in Z-direction in Dicom format.

A medical scanner performs continuous imaging of a rotating array of X-ray sources and detectors arranged on opposite sides of the rotor (doughnut), while the sample is moved in Z-direction through the centre of rotation. The detectors record X-ray attenuation, and this is related to material density and atomic number and arrangement. It is also affected by sharp discontinuities and material contrasts (air/solid). The greyscale is intrinsically calibrated to air and water and given in Hounsfield units (HU), with air at -1024 HU, water at 0 HU, and a maximum of +3071 HU. Geo-materials typically cover a range of 1700 – 2500 HU, with pyrite exceeding this range. The reconstruction of the primary data to X-Y sections stacked in Z-direction is done by propriety software, with selection of parameters, contained in kernels optimised for specific medical applications. While the spatial resolution is limited, the contrast is very good, and imaging is fast and relatively inexpensive. A quantitative image analysis by segmentation would require some post-processing of the reconstructed images to reduce artefacts such as those arising from beam hardening (polychromatic X-ray sources).

We used the data stacks with open-access viewers (e.g. Mango) to inspect core quality (fractures, joints, veins), mineralogical layering (pyrite-rich layers and nests, hard grounds), and the presence of any vugs or large fossil fragments. This was done by adjusting contrast and brightness in a non-quantitative manner and inspecting mostly in section views parallel to the core axis. This provides a very rapid basis for selecting appropriate cores for a given analytical method or experiment.

13 Chemical Analyses of Experiment Solutions

H.N. Waber, P. Bähler, C. Pichler

The preparation of experiment solutions and type and sequence of chemical analyses performed in the chemistry labs of RWI, University of Bern, depend on solution type and volume of solutions obtained from the different experiments. Solution volumes received in the labs vary between about 0.1 mL and 30 mL. This requires careful prioritisation of the analyses to be conducted and correct sample stabilisation and storage immediately after receipt of the samples in the lab. The very small sample volumes inhibit that all parameters can be analysed on all samples. However, great efforts have been undertaken in the past two years allowing analyses of the complete major and trace element compositions, pH, total dissolved inorganic and organic carbon and stable water isotopes ($\delta^{18}O$, $\delta^{2}H$) on samples as small as about 0.6 mL.

After collection, all experiment solutions are prone to changes in their composition. The most prominent changes are induced by exchange with atmospheric CO_2 and O_2. In- or out-gassing of CO_2 will provoke calcite precipitation and modification of pH, alkalinity and the concentrations of total inorganic carbon (TIC) and Ca^{2+}. Exchange with atmospheric O_2 will initiate oxidation of reduced compounds such as dissolved Fe^{2+} and organic carbon compounds. Although great care is taken none of the experiments can be conducted under completely sterile conditions. Therefore, bacterial decomposition of mainly organic compounds and its consequences on the solution's carbonate system must be considered as well.

To circumvent most of the issues, the solution samples are processed as quick as possible in the laboratory and analysed for the most crucial parameters like pH and TIC/TOC within minutes to a few hours after sample collection and arrival in the laboratory, respectively. Similarly, sample stabilisation (e.g. acidification) and conditioning (dilution) is conducted within one hour after sample collection. Whereas this is possible for all experiments conducted in the RWI-laboratories, this is not possible for solutions obtained from high-pressure squeezing as these experiments are conducted in Japan (*cf.* Chapter 10). For these squeezing-solutions substantial changes in their chemical composition have to be taken into account due to the long storage time and large temperature and pressure fluctuations (e.g. transport by airfreight) until arrival in the laboratory. These solutions are, therefore, most prone to mineral precipitation, evaporation and contamination until they can be analysed in the laboratory.

All experiment solutions are also prone to contamination by experimental equipment (e.g. filters, tubing), sample containers (e.g. syringes, bottles) and during sample collection and storage (e.g. evaporation). Contamination sources are regularly checked by analysing blank samples of the various sample containers (syringes, bottles, tubing), filters used in the experiments (e.g. high-pressure squeezing, advective displacement) and solutions for chemical and isotope compositions. For aqueous and CEC extraction experiments and out-diffusion experiments blank samples are run with each sample batch, in addition, following exactly the same protocol as the samples themselves to monitor potential contamination. These numerous blank tests and their analytical data are internally recorded an available upon request.

Aqueous and CEC extract solutions deliver the largest solution volumes. For clay-rich rock types and conducted at S:L ratios of 1 and with a mass of rock of 30 g about 15 g to 25 g of the initially applied 30 g of solution can be recovered from the suspensions by phase separation via centrifugation and filtration after the extraction experiments. For clay poor rocks the solution recovery is commonly higher between about 25 g and 28 g. The same accounts for S:L ratios smaller than 1 for all rock types as such S:L ratios are produced by lowering the rock mass, but not the mass of experiment solution. It should be noted that all solutions are initially prepared by gravimetric means. For CEC extract solutions the same accounts for the first dilution step of the experiment

solutions (commonly 1:10) due to their high ionic strength. Subsequent larger dilutions are then prepared by volumetric means. Aqueous extract solutions are of low ionic strength and thus a density of 1 and these solutions are volumetrically diluted from the beginning.

Out-diffusion experiments deliver the largest volume of experiment solution after termination of the experiment. The mass of these final solutions varies between about 80 g and 100 g, is of low ionic strength and the solutions are diluted volumetrically. In contrast, the time-series samples are only of 0.5 mL in volume. The variable but low ionic strength of these solutions allows volumetric dilution from the beginning.

Advective displacement and high-pressure squeezing experiments deliver the smallest volumes of experiment solutions being as low as 0.1 mL. As the composition of these samples is supposed to be similar to that of the porewater in the rock, these solutions are commonly of high ionic strength with a density lager than 1. Consequently, and also due to the higher precision such samples are diluted gravimetrically until a dilution of about 1:100 followed by volumetric dilution to higher dilutions. In addition, these solutions are inspected by optical and UV-methods prior to stabilisation and conditioning in order to record potential mineral precipitation (e.g. calcite is common in squeezed solutions), bacterial activity (observed in some solutions of advective displacement, high-pressure squeezing and out-diffusion experiments), and the presence of larger amounts of hydrocarbons, which are unfavourable for the analytical instruments.

As the RWI laboratories are research laboratories we do strictly not follow DIN- or other norms, which are often not suited for the types of analyses to be conducted on porewater experimental solutions. The RWI laboratories have developed their own analytical procedures that are documented in internal manuals, which are available upon request. The RWI-laboratories also follow a strict protocol for quality assurance (Section 13.6).

It has to be noted that the procedures of solution sample preparation, stabilisation and analyses requires well-ahead planning of all experimentalists, a great concerted logistic effort between experimentalists and lab staff and great flexibility of the lab staff to comply with all requirements necessary for highest quality standards.

The generic procedure for solution preparation of the various porewater experiment solutions is documented in the RWI-Lab Method: *Präp_Lösungen_v1_05022019.docx.*

13.1 pH and alkalinity

For aqueous and CEC extract solutions pH measurements are conducted on about 1 – 2 mL of solution using Metrohm flat-membrane Pt glass electrode 6.0256.100 immediately after phase separation.

On aqueous extract solutions and the final solution of the out-diffusion experiments total alkalinity is titrated on volumes of about 2 mL using a Metrohm OMNIS Titrator supplied with the OMNIS titration-software and following the procedure described in the internal protocol (Alk_Titr_v2_20082019.docx). Total alkalinity is also determined on late samples of advective displacement experiments where larger solution volumes are available.

For small-sized volumes of advective displacement, high-pressure squeezing, and out-diffusion time-series solutions pH measurements are conducted on about 50 µL using a Ross glass combination micro pH-electrode 8220BNWP with an Orion Versastar pH-meter all by Thermo-Scientific.

The complete procedure for pH and alkalinity determinations is documented in the RWI-Lab Method: *Alk_Titr_v2_20082019.docx*.

13.2 Major anions and cations

Ion-chromatographic (IC) techniques are applied for cation and anion analyses of solutions from aqueous extraction, advective displacement, high-pressure squeezing, and out-diffusion experiments. Optical emission inductively coupled plasma spectrometric (ICP-OES) techniques are applied for trace element analyses of all experiment solutions and for cation analyses of CEC extract solutions with the anions of these solutions being analysed by IC techniques.

13.2.1 Ion-chromatography (IC)

IC analyses of major cations (Na, K, NH_4, Ca, Mg, Sr) and anions (F, Cl, Br, NO_3, SO_4) are conducted using a Metrohm 850 Professional IC and the MagIC Net 3.3 (2019) software. The system is equipped with a Metrohm 58 Professional Sample Processor, two Metrohm Dosino 800 systems for automated eluent preparation, pick-up mode and logical sample dilution, column temperature control, electric conductivity detectors, and – for anions – upstream MSM und MCS suppression.

Major cation analyses are performed using the Metrohm Metrosep C4-150/4.0 separation column (Nr. 6.1050.420) with a Metrosep C4 Guard/4.0 pre-column (Nr. 6.1050.500) and an upstream Metrosep RP 2 Guard/3.5 column (Nr. 6.1011.030) for the protection of the main columns. The eluent solution for cation analyses is composed of 1.7 mM HNO_3^- and 0.7 mM dipicolinic acid solution.

Major anion analyses are performed using a Metrosep ASupp7-250/4.0 column (Nr. 6.1006.630) with a Metrosep ASupp 4/5 Guard/4.0 pre-column (Nr. 6.1006.500) and an upstream Metrosep RP 2 Guard/3.5 column (Nr. 6.1011.030) for the protection of the main columns. The eluent solution for anion analyses is composed of 3.6 mM Na_2CO_3 solution.

Dissolved iodide is analysed using a Metrosep ASupp5-150/4.0 column (Nr. 6.1006.520) with a Metrosep ASupp 4/5 Guard/4.0 column (Nr. 6.1006.500) and an upstream Metrosep RP 2 Guard/3.5 column (Nr. 6.1011.030) for the protection of the main columns. The eluent for such analyses is 3.2 mM Na_2CO_3 and 4.5 mM $NaHCO_3$ solution.

Analyses of the low molecular weight organic (LWMO) compounds acetate, formate, lactate and propionate are conducted the same set-up as for major anions with a 3.0 mM Na_2CO_3 eluent solution.

The eluent solution for anion analyses is composed of 3.6 mM Na_2CO_3, and that for the analyses of iodine of 3.2 mM Na_2CO_3 and 4.5 mM $NaHCO_3$. For the preparation of the eluent solution ultrapure reagents from commercial producers are used. As calibration and check standards serve certified commercial standard solution available from Fluka, Merck and Sigma-Aldrich chemical companies.

Major anion analyses on CEC extract solutions are conducted similar to those for other experiment solution except for the pre-treatment of the solutions. Prior to analyses the large inventory of Ni^{2+} and ethylenediamine in the extract solution is removed by chromatographic techniques using a Metrohm IC-H (Nr. 6.1012.110) that has been activated with ultrapure water and cleaned with 0.1 mmol/L HCl.

For cations, anions and iodide 2 calibration ranges composed of 6 certified standard solutions per element are produced for each sample batch. For LMWO 1 calibration range composed of 6 certified standard solutions is produced per compound (requirements: $r^2 \geq 0.9995$, RSD ≤ 2 %). This allows accurate determination of low and elevated ion concentrations in the same run. The calibration ranges and resulting quantification limits (QL) in undiluted solutions are:

- Cations: 0.1 – 1 mg/L and 1 – 10 mg/L; QL = 0.1 mg/L
- Anions: 0.016 – 0.4 mg/L and 0.4 – 10 mg/L; QL = 0.016 mg/L
- Iodide: 0.04 – 0.4 mg/L and 0.4 – 4 mg/L; QL = 0.04 mg/L
- LMWO:0.2 – 5 mg/L; QL = 0.2 mg/L

Method validation, derivation of quantification limits and extended analytical uncertainties are derived according to the guidelines by SECO (2010).

The extended analytical uncertainties are:

- Na^+: ± 6 %, K^+: ± 9 %, NH_4^+: ± 4 %, Mg^{2+}: ± 4 %, Ca^{2+}: ± 8 %, Sr^{2+}: ± 10 %
- F^-: ± 5 %, Cl^-: ± 5 %, Br^-: ± 4 %, I^-: ± 5 %, NO_3^-: ± 6 %, SO_4^{--}: ± 6 %, PO_4^{---}: ± 6 %
- Formate, Acetate, Lactate, Propionate: ± 10 %

The complete procedures for IC analyses conducted on the various porewater experiment solutions are documented in the RWI-Lab Methods: *IC-Kat_v3_25022019.docx, IC-An-v3_22022019.docx, IC-Iodid_v2_03082016.docx, IC-Org_v1_17042014.docx.*

13.2.2 Inductively coupled plasma spectrometry (ICP-OES)

ICP-OES techniques are applied for the analyses of cations (Na, K, Ca, Mg, Sr and optional Ba, Fe) including the index cation (Ni) in CEC extract solutions.

The system used is an axial ICP-OES Varian 720 ES equipped with an autosampler Varian SPS-3 and supported by the ICP Expert II Ver. 1.1.2 software and Varian Spectroscopy Database Administrator Ver. 1.6.0.20.

Solution samples are diluted with 1% HNO_3 by a factor of 10 before injection. For the evaluation of matrix effects, the concentrations of the internal yttrium standard (VWR Nr. 1.19809.0100) must be reproduced during the entire measuring cycles by ≤ 10 % otherwise the sample has to be re-analysed at higher dilution. For quantification the best suited adsorption line is selected with the aid of the instruments software and based on visual inspection.

For CEC extract solutions with their strongly elevated solution matrix, the recovery of each element is routinely checked by spiking aliquots of the solution with known concentrations of Na, K, Ca, Mg, Sr and Ni.

The calibration range for each element is from 0.005 mg/L to 5 mg/L including 8 certified standard solutions. The calibration must comply with the requirements of $r^2 \geq 0.9995$ and RSD ≤ 2 % in order to be accepted. Certified multi-element and single element standard solution from Merck and Sigma-Aldrich chemical companies are used.

The quantification limits (QL) in undiluted solutions are:

- Na: 0.01 mg/L, K: 0.05 mg/L, Mg: 0.005 mg/L, Ca: 0.1 mg/L, Sr: 0.005 mg/L, Ba: 0.005 mg/L, Fe: 0.01 mg/L
- Ni: 0.01 mg/L

The extended analytical uncertainties are:

- Na^{+}: ± 7 %, K^{+}: ± 5 %, Mg^{2+}: ± 9 %, Ca^{2+}: ± 7 %, Sr^{2+}: ± 4 %, Ba^{2+}: ± 5 %, Fe_{tot}: ± 5 %
- Ni^{2+}: ± 6 %

The analytical precision of the Ni^{2+}analyses is ≤ 2 %.

The complete procedures for ICP-OES analyses conducted on the various porewater experiment solutions are documented in the RWI-Lab Method: *ICP_v2_11022019.*

13.3 Trace elements

Trace element concentrations of Sr, Ba, Fe, Al, and Si in solutions from aqueous extraction, advective displacement, high-pressure squeezing, and out-diffusion experiments are conducted by ICP-OES techniques as described in Section 13.2.2.

The quantification limits (QL) in undiluted solutions are:

- Sr: 0.005 mg/L, Ba: 0.005, Fe: 0.01 mg/L, Al: 0.05 mg/L, Si: 0.05 mg/L

The extended analytical uncertainties are:

- Sr^{2+}: ± 4 %, Ba^{2+}: ± 5 %, Fe_{tot}: ± 5 %, Al^{3+}_{t}: ± 9 %, Si: ± 7 %

The complete procedures for ICP-OES analyses conducted on the various porewater experiment solutions are documented in the RWI-Lab Method: *ICP_v2_11022019.*

13.4 Inorganic and organic carbon

Total dissolved inorganic carbon (TIC) and dissolved organic carbon (TOC) is determined infrared spectrometric techniques using an Analytic Jena Multi N/C 2100S equipped with an infrared NDIR-detector and an APG autosampler and supported by the Software multiWin (aj).

TIC is determined directly by oxidation of the dissolved inorganic to CO_2 using 10 % phosphoric acid, which is diluted from 85 % phosphoric acid (p.a., Merck), injecting the released CO_2 with synthetic air and analysing with the NDIR infrared detector.

TOC can be determined in two different ways depending on sample volume and required quantification level. The simple way is the derivation of TOC concentration by difference of the total carbon (TC) and the TIC concentration in a solution.

TC is analysed by thermocatalytic oxidation of the solution at 750 °C and oxidation of all carbon using a platinum catalyser and oxygen. The released CO_2 is then analysed with the NDIR infrared detector.

Alternatively, non-purgeable organic carbon, NPOC, is determined by expulsion of organic carbon from the solution using 2 mol/l HCl, which is diluted from 37 % HCl (p.a., Merck), injection of the released carbon with synthetic air into the oven at 750 °C where it is thermocatalytically oxidised to CO_2 using a platinum catalyser and oxygen and finally analysed with the NDIR infrared detector.

For direct determination of TIC and the TOC by difference of TC – TIC 2 calibration ranges composed of 6 standard solutions are produced for each sample batch. These standard solutions are internally produced just before the conduction of TIC/TOC analyses. The standard solutions are prepared from p.a. grade, dried Na_2CO_3, $NaHCO_3$, and $C_8H_5KO_4$. The calibration curves must comply with the requirements of $r^2 \geq 0.999$, RSD ≤ 3 %).

For the TIC/TOC and the NPOC techniques the calibration ranges and resulting quantification limits (QL) in undiluted solutions are:

- TC: 1 – 10 mg/L and 10 – 100 mg/L; QL = 1 mg/L
- TIC: 0.5 – 5 mg/L and 5 – 50 mg/L; QL = 0.5 mg/L
- NPOC: 1 – 7.5 mg/L and 7.5 – 50 mg/L; QL = 1 mg/L

The extended analytical uncertainties are:

- TIC: ± 5 %
- TOC: ± 7 % for the TC-TIC difference technique and ± 6 % for the NPOC technique

The complete procedures for TIC/TOC analyses conducted on the various porewater experiment solutions are documented in the RWI-Lab Methods: *TC-TIC_Diff_v2_20082019.docx* and *TOC-v3_20082019.docx.*

13.5 Stable water isotopes

The stable oxygen and hydrogen isotope ratios of water ($\delta^{18}O$ and $\delta^{2}H$) are analysed using a Picarro L2120-i cavity ring down spectrometer (CRDS) with vaporization module V1102-i as described in Chapter 7.1.

For the small volumetric samples from advective displacement and high-pressure squeezing experiments special micro-sample inlets with a volume of 100 µL are used. To eliminate any evaporation after receipt of the solutions in the laboratory, preparation of such samples is coordinated with the preparation and stabilisation of the samples for chemical analyses and subsequent analyses for the stable water isotopes.

The complete procedures for the analyses of $\delta^{18}O$ and $\delta^{2}H$ on the various porewater experiment solutions are documented in the RWI-Lab Methods: *Pic_Manual_v3_05072019.docx.*

13.6 Quality assurance

The quality assurance of all solution analytical results produced at the chemistry labs of RWI, University of Bern follow the guidelines provided by SECO (2010).

For all analytical instruments so-called "control-cards" are produced on regular intervals on which all measurements of certified and check standard solution solutions are recorded and statistically evaluated. These control-cards serve as important basis to monitor potential machine drifts e.g. due to temperature and pressure fluctuation and machine wear.

All calibration curves have to comply with the requirements given above for the individual techniques and in every analytical run independent (certified) external and internal standards are analysed as well and have to comply within the extended analytical uncertainty of the specific element or isotope.

On a regular basis, inter-laboratory comparisons with commercial and university laboratories are conducted. Participation on official inter-laboratory comparisons organised by world-wide organisations (e.g. IAEA, WHO) are, however very costly and time consuming and has not yet been done.

The workflow in the labs is well-organised using pre-prepared order sheets, lab journals, log-books, calculation sheets and results sheets that allow tracking of each single analytical data to its solution and customer, i.e. the members of the RWI and associates.

Back-ups on the servers of the Institute of Geological Sciences are performed on a daily basis for all instrument raw data and all processed data.

Finally, a "6-eyes principle" is applied to all produced data before their distribution to the customer.

14 References

Baeyens, B. & Bradbury, M.H. (1994): Physico-chemical characterisation and calculated in situ porewater chemistries for a low permeability Palfris Marl sample from Wellenberg. Nagra Technical Report NTB 94-22.

Benvenuti, C. & Chiggiato, P. (1996): Pumping characteristics of the St707 nonevaporable getter (Zr70V24.6-Fe5.4wt%). Journal of Vacuum Science & Technology A – Vacuum Surfaces and Films 14, 3278-3282.

Bigler, T. (2003): Heliummessung im Porenwasser gering durchlässiger Gesteinsschichten. Diploma Thesis, Institute of Physics, University of Bern.

Bigler, T., Ihly, B., Lehmann, B.E. & Waber, H.N. (2005): Helium production and transport in the low-permeability Callovo-Oxfordian Shale at the Site Meuse/Haute Marne, France. Nagra Arbeitsbericht NAB 05-07.

Blanc, P., Legendre, O. & Gaucher, E.C. (2007): Estimate of clay minerals amounts from XRD pattern modeling: The Arquant model. Physics and Chemistry of the Earth 32, 135-144.

Bradbury, M.H., Baeyens, B., Pearson, F.J. & Berner, U. (1997): Derivation of in situ Opalinus Clay porewater compositions from experimental and geochemical modeling studies. Nagra Technical Report NTB 97-07.

Bresler, E. (1973): Anion exclusion and coupling effects in nonsteady transport through unsaturated soils: I. Theory. Soil Science of America Proceedings 37, 663-669.

Brunauer, S, Emmett, P.H. & Teller, E. (1938): Adsorption of gases in multimolecular layers. J. Amer. Chem. Soc. 60, 309-319.

Burke, E.A.J. (2001): Raman microspectrometry of fluid inclusions. Lithos 55, 139-158.

Crank, J. (1975): The mathematics of diffusion, 2nd edition. Oxford, University Press.

Diamond, L.W. (2003a): Systematics of H_2O inclusions. *In:* Samson, I.M., Anderson, A.J. & Marshall, D.D. (eds.): Short Course 32. Fluid Inclusions: Analysis and Interpretation. Mineralogical Association of Canada, 55-79.

Diamond, L.W. (2003b): Introduction to gas-bearing aqueous fluid inclusions. *In:* Samson, I.M., Anderson, A.J. & Marshall, D.D. (eds.): Short Course 32. Fluid Inclusions: Analysis and Interpretation. Mineralogical Association of Canada, 101-158.

Diamond, L.W., Aschwanden, L. & Caldas, R. (2015): Fluid inclusion study of drill core and outcrop samples from the Bruce Nuclear Site, Southern Ontario. NWMO-TR-2015-24. Nuclear Waste Management Organization NWMO, Toronto, Canada.

Dumon, M. & Van Ranst, E. (2016): PyXRD v0.6.7 (2016): A free and open-source program to quantify disordered phyllosilicates using multi-specimen X-ray diffraction profile fitting. Geosci. Model Dev. 9, 41-57. www.geosci-model-dev.net/9/41/2016/doi:10.5194/gmd-9-41-2016

Eichinger, F. & Waber, H.N. (2013): Matrix porewater in crystalline rocks: Extraction and analysis. NWMO Technical Report TR 2013-23. Nuclear Waste Management Organization, Toronto, Canada, 94 pp, available at www.nwmo.ca.

Eichinger, F., Rufer, D. & Waber, H.N. (2018): Matrix porewater and gases in porewater in Olkiluoto bedrock from drilling OL-KR56. Posiva Working Report 2018-07. Posiva Oy, Olkiluoto, Finland, 128 p.

Friedman, I., O'Neil, J. & Cebula, G. (1982): Two new carbonate stable-isotope standards. Geostandards Newsletter 6, 11-12.

Füchtbauer, H. (1988): Sedimente und Sedimentgesteine. Schweizerbart'sche Verlagsbuchhandlung, Stuttgart, 1141 p.

Gimmi, T. & Waber, H.N. (2014): DR experiment: Diffusion and retention analysis of bromide, iodide and organic carbon in BDR-1 overcore samples. Unpubl. Mont Terri Technical Note. Mont Terri Project, Switzerland.

Gimmi, T., Leupin, O.X., Eikenberg, J., Glaus, M., Van Loon, L.R., Waber, H.N., Wersin, P., Wang, H.A.O., Grolimund, D., Borcaa, C.N., Dewonck, S. & Wittebroodt, C. (2014): Anisotropic diffusion at the field scale – I: A four-year multi-tracer diffusion and retention experiment at the Mont Terri URL (Switzerland). Geochim Cosmochim Acta 125, 373-393. http://dx.doi.org/10.1016/j.gca.2013.10.014

Goldstein, R.H. & Reynolds, T.J. (1994): Systematics of fluid inclusions in diagenetic minerals. SEPM Society for Sedimentary Geology, Tulsa, 199 p.

González Sánchez, F., Van Loon, L., Gimmi, T., Jakob, A. & Glaus, M. (2008): Self diffusion of water and its dependence on temperature and ionic strength in highly compacted montmorillonite, illite and kaolinite. Applied Geochemistry 23, 3840-3851.

Hadi, J., Wersin, P., Mazurek, M., Waber. H.N., Marques Fernandes, M., Baeyens, B., Honty, M., De Craen, M., Frederickx, L., Dohrmann, R. & Fernández, A.M. (2019): Intercomparison of CEC methods within the GD project. Mont Terri Project Technical Report 2017-06. Mont Terri Project, Switzerland, 162 pp.

Hall, D.L., Sterner, S.M. & Bodnar, R.J. (1988): Freezing point depression of NaCl-KCl-H_2O solutions. Econ. Geol. 83, 197-202.

Hobbs, M.Y., de Haller, A., Koroleva, M., Mazurek, M., Spangenberg, J., Mäder, U. & Meier, D. (2011): Borehole DGR-3 and DGR-4 porewater investigations. OPG Supporting Technical Reports OPG-RWI-TR 08-40. Ontario Power Generation, Toronto, Canada.

Horita, J., Wesolowski, D.J. & Cole, D.R. (1993): The activity-composition relationship of oxygen and hydrogen isotopes in aqueous salt solutions: I. Vapor-liquid water equilibration of single salt solutions from 50 to 100°C. Geochim. Cosmochim. Acta 57, 2797-2817.

IAEA (2016): Reference Sheet for IAEA-603. 2016-08-28, 7pp. International Atomic Energy Agency IAEA, Vienna. Available for download at https://nucleus.iaea.org/rpst/ReferenceProducts/ReferenceMaterials/Stable_Isotopes/13C18and7Li/IAEA-603.htm

Kharaka, Y.F. & Berry, F.A.F. (1973): Simultaneous flow of water and solutes through geological membranes. 1 – Experimental investigations. Geochim. Cosmochim. Acta 37, 2577-2603.

Kim, S.T., Coplen, T.B. & Horita, J. (2015): Normalization of stable isotope data for carbonate minerals: Implementation of IUPAC guidelines. Geochim. Cosmochim. Acta 158, 276-289.

Koroleva, M., De Haller, A., Mäder, U.K., Waber, H.N. & Mazurek, M. (2008): Borehole DGR2: Pore-water investigations. RWI Technical Report TR 08-02. Institute of Geological Sciences, University of Bern, Switzerland.

de Laeter, J. R., Böhlke, J.K., de Bièvre, P., Hidaka, H., Peiser, H.S., Rosman, K.J.R. & Taylor, P.D.P. (2003): Atomic weights of the elements (Review 2000 – IUPAC Technical Report). Pure and Appl. Chem. 75/6, 683-800.

Lee, J.Y., Marti, K., Severinghaus, J.P., Kawamura, K., Yoo, H.S., Lee, J.B. & Kim, J.S. (2006): A redetermination of the isotopic abundances of atmospheric Ar. Geochim. Cosmochim. Acta 70, 4507-4512.

Leya, I. & Wieler, R. (1999): Nucleogenic production of Ne isotopes in Earth's crust and upper mantle induced by alpha particles from the decay of U and Th. J. Geophys. Res. Solid Earth 104/B7, 15439-15450.

Locock, A.J., Chesterman, D., Caird, D. & Duke, M.J.M. (2012): Miniaturization of mechanical milling for powder X-ray diffraction. Powder Diffr. 27/3, 189-193.

Madsen, I.C., Scarlett, N.V.Y. & Kern, A. (2011): Description and survey of methodologies for the determination of amorphous content via X-ray powder diffraction. Z. Kristallogr. 226, 944-955.

Mäder, U. (2004): Porewater chemistry (PC) experiment: A new method of porewater extraction from Opalinus clay with results for a sample from borehole BPC-A1. Unpubl. Mont Terri Technical Note. Mont Terri Project, Switzerland.

Mäder, U. (2006): Porewater chemistry, porosity and hydraulic conductivity of Callovo-Oxfordian claystone at the EST-322 deep drilling site sampled by the method of advective displacement (laboratoire de recherche souterrain de Meuse / Haute-Marne). Nagra Arbeitsbericht NAB 05-04.

Mäder, U.K. (2009): Reference porewater for the Opalinus Clay and 'Brown Dogger' for the provisional safety-analysis in the framework of the sectorial plan – interim results (SGTZE). Nagra Arbeitsbericht NAB 09-14.

Mäder, U. (2018): Advective displacement method for the characterization of pore water chemistry and transport properties in claystone. Geofluids 2018, Article ID 8198762, 11 p. https://doi.org/10.1155/2018/8198762.

Mäder, U. & Waber, H.N. (2017a): Characterization of pore water, ion transport and water-rock interaction in claystone by advective displacement experiments. Water-Rock Interaction International Symposium WRI-15. Proc. Earth & Planet. Sci 17, 917-920.

Mäder, U. & Waber, H.N. (2017b): Results of advective displacement / multi-component transport experiments from claystone samples of the Schlattingen borehole. Nagra Arbeitsbericht NAB 17-16.

Mäder, U., Waber, H.N. & Gautschi, A. (2004): New method for porewater extraction from claystone and determination of transport properties with results for Opalinus clay (Switzerland). *In:* Wanty, R.B. & Seal, R.R. (eds.): Proceedings WRI-10 (11th International Symposium on Water-Rock Interaction). Balkema, New York, USA, 445-448.

Mäder, U., Gimmi, Th. & Hobbs, M.Y. (2008): Porewater Chemistry (PC) Experiment: Ion-specific transport properties derived from a core infiltration experiment from borehole BPC-A1. Unpubl. Mont Terri Technical Note. Mont Terri Project, Switzerland.

Mazurek, M., Waber, H.N., Mäder, U.K., Gimmi, T., de Haller, A. & Koroleva, M. (2012): Geochemical synthesis for the Effingen Member in boreholes at Oftringen, Gösgen and Küttigen. Nagra Technical Report NTB 12-07.

Mazurek, M., Oyama, T., Wersin, P. & Alt-Epping, P. (2015): Pore-water squeezing from indurated shales. Chemical Geology 400, 106-121.

Mazurek, M., Wersin, P. & Hadi, J. (2017): Opalinus Clay in the shallow decompaction zone: Geochemical investigations on drill core samples from borehole Lausen KB. Nagra Arbeitsbericht NAB 16-58.

McNaught, A.D. & Wilkinson, A. (1997): IUPAC – Compendium of Chemical Terminology, 2nd Edition. Blackwell Scientific Publications, Oxford, UK. ISBN 0865426848.

Meier, D.B., Waber, H.N., Gimmi, T., Eichinger, F. & Diamond, L.W. (2015): Reconstruction of in-situ porosity and porewater compositions of low-permeability crystalline rocks: Magnitude of artefacts induced by drilling and sample recovery. J. Cont. Hydrol. 183, 55-71.

Mertens, G., Reynolds, R.C.R. & Rieko, A.R. (2016): NEWMOD-2 – A Computer Program for Qualitative and Quantitative 1-D X-ray Diffraction Pattern Modeling. DOI: 10.3997/2214-4609.201600406. Conference: Fifth EAGE Shale Workshop.

Mills, R. (1973): Self-diffusion in normal and heavy water in the range 1 – 45°. J. Phys. Chem. 77, 685-688.

Nagra (2002): Projekt Opalinuston: Synthese der geowissenschaftlichen Untersuchungsergebnisse – Entsorgunsnachweis für abgebrannte Brennelemente, verglaste hochaktive sowie langlebige mittelaktive Abfälle. Nagra Technical Report NTB 02-03.

Oakes, C.S., Bodnar, R.J. & Simonson, J.M. (1990): The system $NaCl\text{-}CaCl_2\text{-}H_2O$. I. The ice liquidus at 1 atm total pressure. Geochim. Cosmochim. Acta 54, 603-610.

Osenbrück, K., Lippmann, J. & Sonntag, C. (1998): Dating very old pore waters in impermeable rocks by noble gas isotopes. Geochim. Cosmochim. Acta 62, 3041-3045.

O'Connor, B.H. & Chang, W.J. (1986): The amorphous character and particle size distributions of powders produced with the Micronizing Mill for quantitative x-ray powder diffractometry. X-Ray Spectrometry 15/4, 267-270.

Pawley, G.S. (1981): Unit-cell refinement from powder diffraction scans. J. Appl. Cryst. 14, 357-361.

Pearson, F.J., Arcos, D., Bath, A., Boisson, J.Y., Fernandez, A.M., Gaebler, H.E., Gaucher, E.C., Gautschi, A., Griffault, L., Hernan, P. & Waber, H.N. (eds.) (2003): Mont Terri Project – Geochemistry of water in the Opalinus Clay Formation at the Mont Terri Rock Laboratory. Federal Office of Water and Geology (FOWG), Geology Series No. 5, Bern, Switzerland.

Poole, J.C., McNeill, G.W., Langman, S.R. & Dennis, F. (1997): Analysis of noble gases in water using a quadrupole mass spectrometer in static mode. Applied Geochemistry 12, 707-714.

Prinn, R.G. (2004): Ozone, hydroxyl radical, and oxidative capacity. *In:* Holland, H.D. & Turekian, K.K. (eds.): Treatise on Geochemistry, 1-19.

Reynolds, R.C. (1985): A Computer Program for the Calculation of One- dimensional Diffraction Pattern of Mixed-layer Clays. R.C. Reynolds, 8 Brook RD., Hanover, NH 03755, USA.

Rietveld, H.M. (1969): A profile refinement method for nuclear and magentic structures. J. Appl. Cryst. 2, 65-71.

Roedder, E. (1984): Fluid inclusions. *In:* Ribbe, P.E. (ed.): Reviews in Mineralogy 12, 644. Mineralogical Society of America.

Rogge, T. (1997): Eine molekular-diffusive Methode zur Bestimmung des Porenwassergehaltes und der Zusammensetzung von stabilen Isotopen im Porenwasser von Gestein. Unpubl. Diploma thesis, University of Heidelberg, Germany.

Rufer, D. (2019): Field Manual: Drill core sampling for analytical purposes. Nagra Arbeitsbericht NAB 19-13.

Rufer, D. & Mazurek, M. (2018): Pore-water extraction and characterization: benchmarking of the squeezing and adapted isotope diffusive exchange methods. NWMO Technical Report, Nuclear Waste Management Organization, Toronto, Canada.

Rufer, D., Waber, H.N. & Gimmi, T. (2018): Identifying temporally and spatially changing boundary conditions at an aquifer – aquitard interface using helium in porewater. Applied Geochemistry 96, 62-77.

Rübel, A. (2000): Stofftransport in undurchlässigen Gesteinsschichten – Isotopenuntersuchungen im Grund- und Porenwasser. PhD Thesis Universität Heidelberg. Der Andere Verlag, Osnabrück, Deutschland.

Rübel, A. & Bath, A. (2003): Pore water extraction by vaccum distillation and diffusive equilibration for oxygen and hydrogen stable isotope analyses. Annex 4 *in:* Pearson et al.: Mont Terri Project – Geochemistry of Water in the Opalinus Clay Formation at the Mont Terri Rock Laboratory. Federal Office of Water and Geology (FOWG), Geology Series No. 5, Bern, Switzerland, 238-244.

Rübel, A.P., Sonntag, C., Lippmann, J., Pearson, F.J. & Gautschi, A. (2002): Solute transport in formations of very low permeability: Profiles of stable isotope and dissolved noble gas contents of pore water in the Opalinus Clay, Mont Terri, Switzerland. Geochim. Cosmochim. Acta 66, 1311-1321.

Samson, I.M., Anderson, A.J. & Marshall, D.D. (2003): Fluid Inclusions: Analysis and Interpretation. Short Course 32. Mineralogical Association of Canada, 1-374.

SECO (2010): Leitfaden zur Validierung chemisch-physikalischer Prüfverfahren und zur Abschätzung der Messunsicherheit. SECO, Staatssekretariat für Wirtschaft, Schweizerische Akkreditierungsstelle SAS, Dokument Nr. 324.dw, Ausgabe November 2010, Rev. 01. Eidgenössisches Volkswirtschaftsdepartement EVD, Bern.

Sültenfuss, J., Roether, W. & Rhein, M. (2009): The Bremen mass spectrometric facility for the measurement of helium isotopes, neon, and tritium in water. Isotope in Environmental and Health Studies 45, 83-95.

Tolstikhin, I., Kamensky, I., Tarakanov, S., Kramers, J., Pekala, M., Skiba, V., Gannibal, M. & Novikov, D. (2010): Noble gas isotope sites and mobility in mafic rocks and olivine. Geochim. Cosmochim. Acta 74, 1436-1447.

van Geldern, R. & Barth, J.A.C. (2012): Optimization of instrument setup and post-run corrections for oxygen and hydrogen stable isotope measurements of water by isotope ratio infrared spectroscopy (IRIS). Limnol. Oceanogr. Methods 10, 2012, 1024-1036

Van Loon, L.R. (2012): Effective diffusion coefficients and porosity values for argillaceous rocks: Measured and estimated values for provisional safety analyses for SGT-E2. NagraTechnical Report NTB 12-03.

Van Loon, L.R., Muller, W. & Iijima, K. (2005): Activation energies of the self diffusion of HTO, ^{22}Na and ^{36}Cl in a highly compacted argillaceous rock (Opalinus Clay). Applied Geochemistry 20, 961-972.

Waber, H.N. (2012): Laboratoire de Recherche Souterrain Meuse / Haute-Marne – Geochemical Data of Borehole EST433. Nagra Arbeitsbericht NAB 09-16.

Waber, H.N. (2018): Deep drilling campaign for SGT-E3: Laboratory Workflow RWI, University of Bern (Version 1.0, 10.12.2018). Unpubl Nagra Internal Report.

Waber, H.N. & Gimmi, T. (2008): Out-diffusion experiments. Chapter 11 *in:* Waber (ed.) (2008): Borehole Oftringen: Mineralogy, Porosimetry, Geochemistry, Pore Water Chemistry. Nagra Arbeitsbericht NAB 08-18.

Waber, H.N. & Rufer, D. (2017): Porewater geochemistry, method comparison and Opalinus Clay – Passwang Formation interface study at the Mont Terri URL. NWMO Tech. Rep. TR-2017-10. Nuclear Waste Management Organization, Toronto, Canada. Also published as Mont Terri Technical Report TR 2017-02.

Waber, H.N. & Smellie, J.A.T. (2008): Characterisation of pore water in crystalline rocks. Applied Geochemistry 23, 1834-1861.

Waber, H.N., Gaucher, E.C., Fernández, A.M. & Bath, A. (2003a): Aqueous leachates and cation exchange properties of Mont Terri claystones. *In:* Pearson, F.J. et al.: Mont Terri Project – Geochemistry of water in the Opalinus Clay Formation at the Mont Terri Rock Laboratory. Federal Office of Water and Geology (FOWG), Geology Series No. 5, Wabern, Switzerland (available at www.mont-terri.ch), 200-237.

Waber, H.N., Pearson, F.J., Hobbs, M.Y. & Oyama, T. (2003b): Sondierbohrung Benken: Characterisation of porewater from argillaceous rocks. Unpubl. Nagra Internal Report.

Waber, H.N., Mäder, U.K., Koroleva, M. & De Haller, A. (2007): Testing methods for the characterisation of saline pore water in an Ordovician Limestone (Cobourg Formation, St. Mary's Quarry, Ontario) – Feasibility Study. RWI Technical Report TR 07-01. Institute of Geological Sciences, University of Bern.

Waber, H.N., Gimmi, T. & Smellie, J.A.T. (2011): Effects of drilling and stress release on hydraulic properties and porewater chemistry of crystalline rocks. J. Hydrol. 405, 316-332.

Waber, H.N., Gimmi, T. & Smellie, J.A.T. (2012): Reconstruction of palaeoinfiltration during the Holocene using porewater data (Laxemar, Sweden). Geochim. Cosmochim. Acta 94, 109-127.

Weiss, R.F. (1970): The solubility of nitrogen, oxygen and argon in water and seawater. Deep-Sea Research 17, 15.

Weiss, R.F. (1971): Solubility of helium and neon in water and seawater. J. Chem. Eng. Data 16, 235-241.

Wersin, P., Mazurek, M., Waber, H.N., Mäder, U.K., Gimmi, T., Rufer, D. & de Haller, A. (2013): Rock and porewater characterisation on drillcores from the Schlattingen borehole. Nagra Arbeitsbericht NAB 12-54.

Wersin, P., Mazurek, M., Mäder, U.K., Gimmi, T., Rufer, D. & Lerouge, C. (2016): Constraining porewater chemistry in a 250 m thick argillaceous rock sequence. Chem. Geol. 434, 43-61.

Zeelmaekers, E., Honty, M., Derkowski, A., DeCraen, M., Vandenberghe, N. & VanGeet, M. (2010): A new and improved methodology for qualitative and quantitative mineralogical analysis of Boom Clay. Clay in Natural & Engineered Barriers for Radioactive Waste Confinement. 4th International Meeting – Nantes, France.

Appendix A: Summary of first order error estimates for various measurements

T. Gimmi

Abstract

This memo provides general formulas for the calculation of the error (or uncertainty) of the output value of a function that depends on several correlated or uncorrelated input variables. First-order error propagation is considered. Specific formulas for first-order propagated errors of various petrophysical and geochemical functions for uncorrelated input variables are given.

Notation	
C_{aqex}	Concentration of aqueous extract, per mass of water
$C_{Ni\,ex}$	Concentration of Ni in Ni-en extract solution, per mass of water
$C_{Ni\,st}$	Concentration of Ni in added stock solution, per mass of water
C_{pw}	Pore water concentration of solutes in accessible pores, per mass of water, or isotope pore water concentration
f_a	Fraction of anion accessible pore volume per total porosity
$f(x_1, x_2, .., x_n)$	Function of variables x_i (e.g., f calculated from measurements x_i)
g	Vector with derivatives of function f (eq. 1)
m_{pw}	Mass of pore water of sample
m_r	Mass of dry rock sample
$m_{rw} = m_r + m_{pw}$	Mass of wet rock sample
m_{salt}	Mass of dissolved salts in pore solution
m_{twf}	Mass of final test water (diffusive exchange)
m_{twi}	Mass of initial test water (diffusive exchange)
$m_{w,add}$	Mass of water added for aqueous extract
m_{wst}	Mass of added stock solution (Ni-en extract)
Δm_k	Mass of the displaced kerosene
Δm_p	Mass of the displaced paraffin
Ni_c	Nickel consumption, equivalents per mass of dry rock (Ni-en extract)
r_{saw}	Ratio of mass of dry solid to mass of added water (e.g. aqueous extract)
$s = m_{salt}/(m_{pw} + m_{salt})$	Salinity fraction of pore solution
$S_w = m_{pw}/m_{pwis}$	Water saturation of sample relative to in-situ condition (with m_{pwis} the mass of pore water under in situ conditions)
SL	Ratio of mass of dry solid to mass of pore water and added water (e.g. Ni-en extract)
V	Variance-covariance matrix of variables x_i (eq. 1), or bulk volume (total volume) of sample
V_s	Volume of solid
V_{solu}	Volume of pore water solution
V_w	Volume of water
$w = m_{pw}/m_r$	Gravimetric water content per dry weight
$w_w = m_{pw}/m_{rw}$	Gravimetric wet water content
x_i	Variable of function f

ϕ	Porosity (volume of pores per total sample volume)
ϕ_{WL}	Water-loss porosity (porosity determined from w or w_w)
ϕ_{pycn}	Pycnometer porosity (porosity determined from bulk and grain density)
ρ_{bd}	Bulk dry density (mass of dry rock per total sample volume)
ρ_{bw}	Bulk wet density (mass of wet rock per total sample volume)
ρ_g	Grain density of rock
ρ_k	Density of kerosene
ρ_p	Density of paraffin
ρ_w	Density of water
ρ_{solu}	Density of pore water solution
σ_f^2	Variance (square of the standard error) of function f
$\sigma_{x_i}^2$	Variance (square of the standard error) of variable x_i
$\sigma_{x_i x_j}$	Covariance of variables x_i and x_j

A.1 General formulas

First order error approximation of variance of function f with correlated variables x_i

$$\sigma_f^2 = g^T V\, g = \sum_{i=1}^{n} \left(\frac{\partial f}{\partial x_i}\sigma_{x_i}\right)^2 + \sum_{i=1}^{n}\sum_{j=1, j\neq i}^{n} \left(\frac{\partial f}{\partial x_i}\right)\left(\frac{\partial f}{\partial x_j}\right)\sigma_{x_i x_j} \tag{1}$$

First order error approximation of variance of function f with uncorrelated variables x_i

$$\sigma_f^2 = \sum_{i=1}^{n} \left(\frac{\partial f}{\partial x_i}\sigma_{x_i}\right)^2 \tag{2}$$

Notes:

(1) In this memo, the term 'error' is used synonymously to 'uncertainty' (sometimes, the former is more restrictively defined, e.g. as difference between the true value and the measured value).

(2) Eq. (1) can be used for correlated variables, provided the covariances $\sigma_{x_i x_j}$ are known.

(3) If all variables are (assumed to be) uncorrelated, eq. (2) is appropriate. If some variables are correlated, applying eq. (2) can lead to considerable over- or underestimation of the error of f.

(4) For strongly non-linear functions *f*, errors calculated with eq. (1) or (2) maybe over- or under-estimated.

(5) The quantities of interest considered in the following section can usually be calculated in different ways from different input variables; errors have then to be calculated accordingly.

(6) As a consequence of note (3), one should generally try to express the function f with basic variables that were directly measured and are most likely uncorrelated.

(7) Below, in some cases the mass of pore water or the mass of displaced measuring fluid (e.g. kerosene) is used. These quantities are in fact obtained as a difference of two mass measurements. To account for this, the corresponding measurement error should be increased as compared to the error of the direct mass measurement. Alternatively, formulas involving explicitly the differences can be used, as partly also shown below.

(8) σ_{x_i} may represent a standard deviation, but more generally any error associated to a variable x_i.

(9) If the function f is a sum or a difference of two variables u and v, i.e., if $f = u + v$ or $f = u - v$, squared errors of the function f according to eq. (2) are the sum of the squared errors of each variable, i.e.,

$$\sigma_f^2 = \sigma_u^2 + \sigma_v^2,$$

and squared relative errors of f are weighted sums of the squared relative errors of the variables u and v, i.e.,

$$\left(\frac{\sigma_f}{f}\right)^2 = \left(\frac{u}{f}\right)^2 \left(\frac{\sigma_u}{u}\right)^2 + \left(\frac{v}{f}\right)^2 \left(\frac{\sigma_v}{v}\right)^2$$

(10) If the function f is a product or a ratio of two variables u and v, i.e., if $f = uv$ or $f = u/v$, squared relative errors of the function f according to eq. (2) are given as the sum of the squared relative errors of the variables u and v, i.e.,

$$\left(\frac{\sigma_f}{f}\right)^2 = \left(\frac{\sigma_u}{u}\right)^2 + \left(\frac{\sigma_v}{v}\right)^2$$

(11) For gravimetric water contents or also bulk wet densities, propagated errors are often relatively small, as mass measurements have comparably low errors. Errors of such quantities can also be estimated from measurements on several subsamples. These errors (standard deviations) are typically larger than the propagated errors as they include also small-scale heterogeneities, which can affect the quantities of interest. In such cases, most often the larger error values are reported. In any case, the type of error (calculated according to first order propagation or standard deviation) should always be indicated.

A.2 Specific formulas

A.2.1 Gravimetric water content w per dry weight of sample

$$w = \frac{m_{pw}}{m_r} \tag{3}$$

$$\sigma_w^2 = \left(\frac{m_{pw}}{m_r^2}\sigma_{m_r}\right)^2 + \left(\frac{1}{m_r}\sigma_{m_{pw}}\right)^2 = \left(\frac{w}{m_r}\sigma_{m_r}\right)^2 + \left(\frac{w}{m_{pw}}\sigma_{m_{pw}}\right)^2 \tag{4}$$

$$\left(\frac{\sigma_w}{w}\right)^2 = \left(\frac{\sigma_{m_r}}{m_r}\right)^2 + \left(\frac{\sigma_{m_{pw}}}{m_{pw}}\right)^2 \tag{5}$$

where $\sigma_{m_{pw}}$ should account for the error of the difference calculation, e.g.,

$\sigma^2_{m_{pw}} = \sigma^2_{m_{rw}} + \sigma^2_{m_r} \approx 2\sigma^2_{m_r}$ or $\sigma_{m_{pw}} \approx \sqrt{2}\sigma_{m_r}$ (ignoring correlations).

Using the formula with the primarily measured quantities (to account partially for correlations), we have:

$$w = \frac{m_{rw} - m_r}{m_r} \tag{6}$$

$$\sigma_w^2 = \left(\frac{\sigma_{m_{rw}}}{m_r}\right)^2 + \left(\frac{\sigma_{m_r} m_{rw}}{m_r^2}\right)^2 = \left(\frac{m_{rw}}{m_r}\right)^2 \left[\left(\frac{\sigma_{m_{rw}}}{m_{rw}}\right)^2 + \left(\frac{\sigma_{m_r}}{m_r}\right)^2\right] \tag{7}$$

$$\left(\frac{\sigma_w}{w}\right)^2 = \left(\frac{\sigma_{m_{rw}}}{\left(m_{rw} - m_r\right)}\right)^2 + \left(\frac{\sigma_{m_r}}{m_r}\frac{m_{rw}}{\left(m_{rw} - m_r\right)}\right)^2 = \left(\frac{m_{rw}}{m_{rw} - m_r}\right)^2 \left[\left(\frac{\sigma_{m_{rw}}}{m_{rw}}\right)^2 + \left(\frac{\sigma_{m_r}}{m_r}\right)^2\right] \tag{8}$$

Alternatively, we can also write:

$$w = \frac{m_{pw}}{m_{rw} - m_{pw}} \tag{9}$$

$$\sigma_w^2 = \left(\frac{m_{rw}\sigma_{m_{pw}}}{(m_{rw} - m_{pw})^2}\right)^2 + \left(\frac{m_{pw}\sigma_{m_{rw}}}{(m_{rw} - m_{pw})^2}\right)^2 \tag{10}$$

$$\left(\frac{\sigma_w}{w}\right)^2 = \left(\frac{m_{rw}}{(m_{rw} - m_{pw})}\frac{\sigma_{m_{pw}}}{m_{pw}}\right)^2 + \left(\frac{\sigma_{m_{rw}}}{(m_{rw} - m_{pw})}\right)^2 = \left(\frac{m_{rw}}{m_{rw} - m_{pw}}\right)^2 \left[\left(\frac{\sigma_{m_{pw}}}{m_{pw}}\right)^2 + \left(\frac{\sigma_{m_{rw}}}{m_{rw}}\right)\right] \tag{11}$$

Note that slightly different error values are obtained depending on the used formula and the used value for the errors of the variables, e.g., for $\sigma_{m_{pw}}$ in eq. (5), as shown in Section 3.

If w is calculated from the water content w_w per wet weight (see next section), we have

$$w = \frac{w_w}{1 - w_w} \tag{12}$$

$$\sigma_w^2 = \left(\frac{\sigma_{w_w}}{(1 - w_w)^2}\right)^2 \tag{13}$$

$$\left(\frac{\sigma_w}{w}\right)^2 = \left(\frac{1}{(1 - w_w)}\frac{\sigma_{w_w}}{w_w}\right)^2 \tag{14}$$

Note for high salinity samples: The dry sample mass includes also the mass of precipitated salts, whereas the mass of pore water obtained as difference of wet and dry sample mass does not include the mass of salts dissolved in the pore water. Alternative definitions for samples with high salinity pore water exist.

A.2.2 Gravimetric water content w_w per wet weight of sample

$$w_w = \frac{m_{pw}}{m_{rw}} \tag{15}$$

$$\sigma_{w_w}^2 = \left(\frac{m_{pw}}{m_{rw}^2}\sigma_{m_{rw}}\right)^2 + \left(\frac{\sigma_{m_{pw}}}{m_{pw}}\right)^2 = \left(\frac{w_w}{m_{rw}}\sigma_{m_{rw}}\right)^2 + \left(\frac{w_w}{m_{pw}}\sigma_{m_{pw}}\right)^2 \tag{16}$$

$$\left(\frac{\sigma_{w_w}}{w_w}\right)^2 = \left(\frac{\sigma_{m_{rw}}}{m_{rw}}\right)^2 + \left(\frac{\sigma_{m_{pw}}}{m_{pw}}\right)^2 \tag{17}$$

See comment above regarding $\sigma_{m_{pw}}$. Alternatively, we have

$$w_w = \frac{m_{pw}}{m_r + m_{pw}} \tag{18}$$

$$\sigma_{w_w}^2 = \left(\frac{m_r}{(m_r + m_{pw})^2}\right)^2 \sigma_{m_{pw}}^2 + \left(\frac{m_{pw}}{(m_r + m_{pw})^2}\right)^2 \sigma_{m_r}^2 \tag{19}$$

$$\left(\frac{\sigma_{w_w}}{w_w}\right)^2 = \left(\frac{\sigma_{m_r}}{m_r}\frac{m_r}{\left(m_r + m_{pw}\right)}\right)^2 + \left(\frac{\sigma_{m_{pw}}}{m_{pw}}\frac{m_r}{\left(m_r + m_{pw}\right)}\right)^2 = \left(\frac{m_r}{m_r + m_{pw}}\right)^2 \left[\left(\frac{\sigma_{m_r}}{m_r}\right)^2 + \left(\frac{\sigma_{m_{pw}}}{m_{pw}}\right)\right] \tag{20}$$

Or, we can write

$$w_w = \frac{m_{rw} - m_r}{m_{rw}} \tag{21}$$

$$\sigma_{w_w}^2 = \left(\frac{\sigma_{m_r}}{m_{rw}}\right)^2 + \left(\frac{m_r\,\sigma_{m_{rw}}}{m_{rw}^2}\right)^2 \tag{22}$$

$$\left(\frac{\sigma_{w_w}}{w_w}\right)^2 = \left(\frac{\sigma_{m_r}}{m_r}\frac{m_r}{\left(m_{rw} - m_r\right)}\right)^2 + \left(\frac{\sigma_{m_{rw}}}{m_{rw}}\frac{m_r}{\left(m_{rw} - m_r\right)}\right)^2 = \left(\frac{m_r}{m_{rw} - m_r}\right)^2 \left[\left(\frac{\sigma_{m_r}}{m_r}\right)^2 + \left(\frac{\sigma_{m_{rw}}}{m_{rw}}\right)^2\right] \tag{23}$$

If w_w is calculated from the water content w per dry weight, we have

$$w_w = \frac{w}{1+w} \tag{24}$$

$$\sigma_{w_w}^2 = \left(\frac{\sigma_w}{(1+w)^2}\right)^2 \tag{25}$$

$$\left(\frac{\sigma_{w_w}}{w_w}\right)^2 = \left(\frac{1}{(1+w)}\,\frac{\sigma_w}{w}\right)^2 \tag{26}$$

Note for high salinity samples: The wet sample mass includes the mass of dissolved salts in the pore water, whereas the mass of pore water obtained as difference of wet and dry sample mass does not. Alternative definitions for samples with high salinity pore water exist.

A.2.3 Grain (or solid) density ρ_g from kerosene (or any other fluid) pycnometry

$$\rho_g = \frac{m_r \rho_k}{\Delta m_k} \tag{27}$$

$$\sigma_{\rho_g}^2 = \left(\frac{\rho_k}{\Delta m_k}\sigma_{m_r}\right)^2 + \left(\frac{m_r}{\Delta m_k}\sigma_{\rho_k}\right)^2 + \left(\frac{m_r \rho_k}{\Delta m_k^2}\sigma_{\Delta m_k}\right)^2 \tag{28}$$

$$\left(\frac{\sigma_{\rho_g}}{\rho_g}\right)^2 = \left(\frac{\sigma_{m_r}}{m_r}\right)^2 + \left(\frac{\sigma_{\rho_k}}{\rho_k}\right)^2 + \left(\frac{\sigma_{\Delta m_k}}{\Delta m_k}\right)^2 \approx \left(\frac{\sigma_{\rho_k}}{\rho_k}\right)^2 \tag{29}$$

Note: Relative error of kerosene density is typically the largest contribution.

Note for high salinity samples: The mass and volume of the dry sample include generally also the mass and volume of precipitated salts, respectively. As long as the density of the salts is similar to the grain density of the sample, the bias is small.

A.2.4 Grain (or solid) density ρ_g from He pycnometry

$$\rho_g = \frac{m_r}{V_s} \tag{30}$$

$$\sigma_{\rho_g}^2 = \left(\frac{1}{V_s}\sigma_{m_r}\right)^2 + \left(\frac{m_r}{V_s^2}\sigma_{V_s}\right)^2 \tag{31}$$

$$\left(\frac{\sigma_{\rho_g}}{\rho_g}\right)^2 = \left(\frac{\sigma_{m_r}}{m_r}\right)^2 + \left(\frac{\sigma_{V_s}}{V_s}\right)^2 \tag{32}$$

Note: Volume of solid is obtained from He pressure difference. The relative error of volume of solid is typically the largest contribution, and the error of the grain density is typically obtained as a standard deviation from repeated volume measurements.

Note for high salinity samples: *cf.* Section A.2.3.

A.2.5 Bulk wet density ρ_{bw} from paraffin pycnometry

$$\rho_{bw} = \frac{m_{rw}\rho_p}{\Delta m_p} \left(= \frac{(m_r + m_{pw})\rho_p}{\Delta m_p} \right) \tag{33}$$

$$\sigma^2_{\rho_{bw}} = \left(\frac{\rho_p}{\Delta m_p} \sigma_{m_{rw}} \right)^2 + \left(\frac{m_{rw}}{\Delta m_p} \sigma_{\rho_p} \right)^2 + \left(\frac{m_{rw}\rho_p}{\Delta m_p^2} \sigma_{\Delta m_p} \right)^2 \tag{34}$$

$$\left(\frac{\sigma_{\rho_{bw}}}{\rho_{bw}} \right)^2 = \left(\frac{\sigma_{m_{rw}}}{m_{rw}} \right)^2 + \left(\frac{\sigma_{\rho_p}}{\rho_p} \right) + \left(\frac{\sigma_{\Delta m_p}}{\Delta m_p} \right)^2 \approx \left(\frac{\sigma_{\rho_p}}{\rho_p} \right)^2 \tag{35}$$

Note for high salinity samples: The wet sample mass includes the mass of dissolved salts in the pore water.

A.2.6 Bulk dry density ρ_{bd} from gravimetric dry water content and bulk wet density

$$\rho_{bd} = \frac{\rho_{bw}}{1+w} \tag{36}$$

$$\sigma^2_{\rho_{bd}} = \left(\frac{\sigma_{\rho_{bw}}}{1+w} \right)^2 + \left(\frac{\rho_{bw}\sigma_w}{(1+w)^2} \right)^2 \tag{37}$$

$$\left(\frac{\sigma_{\rho_{bd}}}{\rho_{bd}} \right)^2 = \left(\frac{\sigma_{\rho_{bw}}}{\rho_{bw}} \right)^2 + \left(\frac{w}{1+w} \frac{\sigma_w}{w} \right)^2 \tag{38}$$

Note for high salinity samples: *cf.* notes in Section A.2.1 and A.2.5.

A.2.7 Bulk dry density ρ_{bd} from gravimetric wet water content and bulk wet density

$$\rho_{bd} = \rho_{bw}\left(1 - w_w\right) \qquad \text{(assuming that } m_{rw} - m_{pw} = m_s\text{)} \tag{39}$$

$$\sigma^2_{\rho_{bd}} = \left((1-w_w)\,\sigma_{\rho_{bw}} \right)^2 + \left(\rho_{bw}\sigma_{w_w} \right)^2 \tag{40}$$

$$\left(\frac{\sigma_{\rho_{bd}}}{\rho_{bd}} \right)^2 = \left(\frac{\sigma_{\rho_{bw}}}{\rho_{bw}} \right)^2 + \left(\frac{w_w}{1-w_w} \frac{\sigma_{w_w}}{w_w} \right)^2 \tag{41}$$

Note for high salinity samples: See notes in Section A.2.2 and A.2.5.

A.2.8 Water-loss porosity ϕ_{WL} from gravimetric wet water content and bulk wet density

$$\phi_{WL} = \frac{w_w \rho_{bw}}{\rho_w} \tag{42}$$

Note: Total volume is defined through (measured) bulk wet density in this formula.

Note for high salinity samples: The pore water density is mostly set to 1 g cm^{-3}. This is about appropriate for samples with relatively low salinity (below that of seawater). It is also justified when considering that the gravimetric water content relates to the mass of the evaporated water and not to the mass of solution, such that $w_w\, \rho_{bw} = m_{pw}/V$ and $\phi_{WL} = V_w/V$. For high salinity samples, it may be necessary to convert V_w to the volume of the pore water solution V_{solu} in order that ϕ_{WL} exactly corresponds to the porosity, according to

$$\frac{V_{solu}}{V_w} = \frac{\rho_w}{\rho_{solu}} \frac{1}{(1-s)}$$

with ρ_{solu} the density of the pore water solution and s the salinity fraction of the solution.

$$\left(\sigma_{\phi_{WL}}\right)^2 = \left(\frac{\rho_{bw}}{\rho_w}\sigma_{w_w}\right)^2 + \left(\frac{w_w}{\rho_w}\sigma_{\rho_{bw}}\right)^2 + \left(\frac{w_w \rho_{bw}}{\rho_w^2}\sigma_{\rho_w}\right)^2 \tag{43}$$

$$\left(\frac{\sigma_{\phi_{WL}}}{\theta_{WL}}\right)^2 = \left(\frac{\sigma_{w_w}}{w_w}\right)^2 + \left(\frac{\sigma_{\rho_{bw}}}{\rho_{bw}}\right)^2 + \left(\frac{\sigma_{\rho_w}}{\rho_w}\right)^2 \tag{44}$$

A.2.9 Water-loss porosity ϕ_{WL} from gravimetric dry water content and bulk dry density

$$\phi_{WL} = \frac{w \rho_{bd}}{\rho_w} \tag{45}$$

Note: Total volume is defined through (measured or calculated) bulk dry density in this formula.

Note for high salinity samples: *cf.* Section A.2.8.

$$\left(\sigma_{\phi_{WL}}\right)^2 = \left(\frac{\rho_{bd}}{\rho_w}\sigma_w\right)^2 + \left(\frac{w}{\rho_w}\sigma_{\rho_{bd}}\right)^2 + \left(\frac{w \rho_{bd}}{\rho_w^2}\sigma_{\rho_w}\right)^2 \tag{46}$$

$$\left(\frac{\sigma_{\phi_{WL}}}{\theta_{WL}}\right)^2 = \left(\frac{\sigma_w}{w}\right)^2 + \left(\frac{\sigma_{\rho_{bd}}}{\rho_{bd}}\right)^2 + \left(\frac{\sigma_{\rho_w}}{\rho_w}\right)^2 \tag{47}$$

A.2.10 Water-loss porosity ϕ_{WL} from gravimetric wet water content and grain density

$$\phi_{WL} = \frac{w_w \rho_g}{w_w \rho_g + (1 - w_w)\rho_w} \tag{48}$$

Note: Total volume is assumed to equal the sum of water volume and solid volume in this formula. Introduces error for unsaturated sample (where volumetric water content is not equal to porosity, anyway).

Note for high salinity samples: *cf.* Section A.2.8.

$$\left(\sigma_{\phi_{WL}}\right)^2 = \left(\frac{w_w(1-w_w)\rho_w}{\left(w_w\rho_g + (1-w_w)\rho_w\right)^2}\sigma_{\rho_g}\right)^2 + \left(\frac{w_w(1-w_w)\rho_g}{\left(w_w\rho_g + (1-w_w)\rho_w\right)^2}\sigma_{\rho_w}\right)^2 + \left(\frac{\rho_g\rho_w}{\left(w_w\rho_g + (1-w_w)\rho_w\right)^2}\sigma_{w_w}\right)^2 \tag{49}$$

$$\left(\frac{\sigma_{\phi_{WL}}}{\phi_{WL}}\right)^2 = \left(\frac{(1-w_w)\rho_w}{\left(w_w\rho_g + (1-w_w)\rho_w\right)}\frac{\sigma_{\rho_g}}{\rho_g}\right)^2 + \left(\frac{(1-w_w)\rho_w}{\left(w_w\rho_g + (1-w_w)\rho_w\right)}\frac{\sigma_{\rho_w}}{\rho_w}\right)^2 + \left(\frac{\rho_w}{\left(w_w\rho_g + (1-w_w)\rho_w\right)}\frac{\sigma_{w_w}}{w_w}\right)^2 \tag{50}$$

A.2.11 Pycnometer porosity ϕ_{pycn} from grain density and bulk dry density

$$\phi_{pycn} = 1 - \frac{\rho_{bd}}{\rho_g} \tag{51}$$

$$\left(\sigma_{\phi_{pycn}}\right)^2 = \left(\frac{\sigma_{\rho_{bd}}}{\rho_g}\right)^2 + \left(\frac{\rho_{bd}}{\rho_g^2}\sigma_{\rho_g}\right)^2 \tag{52}$$

$$\left(\frac{\sigma_{\phi_{pycn}}}{\phi_{pycn}}\right)^2 = \left(\frac{\rho_{bd}}{\rho_g - \rho_{bd}}\frac{\sigma_{\rho_{bd}}}{\rho_{bd}}\right)^2 + \left(\frac{\rho_{bd}}{\rho_g - \rho_{bd}}\frac{\sigma_{\rho_g}}{\rho_g}\right)^2 \tag{53}$$

Note: A porosity calculated from densities is denoted as pycnometer porosity, following the definitions given in Nagra (2002, NTB 02-03, p. 237 and 239). Sometimes, it is also called physical porosity, but this is not recommended here.

Note for high salinity samples: *cf.* Section A.2.3 and A.2.6 or A.2.7.

A.2.12 Pycnometer porosity ϕ_{pycn} from grain density, bulk wet density and wet water content

$$\phi_{pycn} = 1 - (1 - w_w)\frac{\rho_{bw}}{\rho_g} \tag{54}$$

$$\left(\sigma_{\phi_{pycn}}\right)^2 = \left(\frac{(1-w_w)}{\rho_g}\sigma_{\rho_{bw}}\right)^2 + \left(\frac{\rho_{bw}}{\rho_g}\sigma_{w_w}\right)^2 + \left(\frac{\rho_{bw}(1-w_w)}{\rho_g^2}\sigma_{\rho_g}\right)^2 \tag{55}$$

$$\left(\frac{\sigma_{\phi_{pycn}}}{\phi_{pycn}}\right)^2 = \left(\frac{(1-w_w)\rho_{bw}}{[\rho_g-(1-w_w)\rho_{bw}]}\frac{\sigma_{\rho_{bw}}}{\rho_{bw}}\right)^2 + \left(\frac{\rho_{bw}w_w}{[\rho_g-(1-w_w)\rho_{bw}]}\frac{\sigma_{w_w}}{w_w}\right)^2 + \left(\frac{(1-w_w)\rho_{bw}}{[\rho_g-(1-w_w)\rho_{bw}]}\frac{\sigma_{\rho_g}}{\rho_g}\right)^2 \tag{56}$$

Note for high salinity samples: Cf. 2.3 and 2.8.

A.2.13 Pore water solute concentration C_{pw} based on mass of added water and water content

If the aqueous extracts are prepared from dry sample material, we have

$$C_{pw} = C_{aqex}\frac{m_{w,add}}{m_{pw}}\frac{S_w}{f_a} = C_{aqex}\frac{1}{r_{saw}w}\frac{S_w}{f_a} \tag{57}$$

$$\sigma^2_{C_{pw}} = \left(\frac{C_{pw}}{C_{aqex}}\sigma_{C_{aqex}}\right)^2 + \left(\frac{C_{pw}}{m_{w,add}}\sigma_{m_{w.add}}\right)^2 + \left(\frac{C_{pw}}{S_w}\sigma_{S_w}\right)^2 + \left(\frac{C_{pw}}{m_{pw}}\sigma_{m_{pw}}\right)^2 + \left(\frac{C_{pw}}{f_a}\sigma_{f_a}\right)^2 \tag{58}$$

$$\left(\frac{\sigma_{C_{pw}}}{C_{pw}}\right)^2 = \left(\frac{\sigma_{C_{aqex}}}{C_{aqex}}\right)^2 + \left(\frac{\sigma_{m_{w,add}}}{m_{w,add}}\right)^2 + \left(\frac{\sigma_{S_w}}{S_w}\right)^2 + \left(\frac{\sigma_{m_{pw}}}{m_{pw}}\right)^2 + \left(\frac{\sigma_{f_a}}{f_a}\right)^2 \tag{59}$$

or

$$\sigma^2_{C_{pw}} = \left(\frac{C_{pw}}{C_{aqex}}\sigma_{C_{aqex}}\right)^2 + \left(\frac{C_{pw}}{r_{saw}}\sigma_{r_{saw}}\right)^2 + \left(\frac{C_{pw}}{S_w}\sigma_{S_w}\right)^2 + \left(\frac{C_{pw}}{w}\sigma_w\right)^2 + \left(\frac{C_{pw}}{f_a}\sigma_{f_a}\right)^2 \tag{60}$$

$$\left(\frac{\sigma_{C_{pw}}}{C_{pw}}\right)^2 = \left(\frac{\sigma_{C_{aqex}}}{C_{aqex}}\right)^2 + \left(\frac{\sigma_{r_{saw}}}{r_{saw}}\right)^2 + \left(\frac{\sigma_{S_w}}{S_w}\right)^2 + \left(\frac{\sigma_w}{w}\right)^2 + \left(\frac{\sigma_{f_a}}{f_a}\right)^2 \tag{61}$$

If the aqueous extracts are prepared from wet sample material, we have

$$C_{pw} = C_{aqex}\left(1+\frac{m_{w,add}}{m_{pw}}\right)\frac{S_w}{f_a} = C_{aqex}\left(1+\frac{1}{r_{saw}w}\right)\frac{S_w}{f_a} \tag{62}$$

$$\sigma^2_{C_{pw}} = \left(\frac{C_{pw}}{C_{aqex}}\sigma_{C_{aqex}}\right)^2 + \left(\frac{C_{pw}\,\sigma_{m_{w,add}}}{\left[m_{pw}+m_{w,add}\right]}\right)^2 + \left(\frac{C_{pw}}{S_w}\sigma_{S_w}\right)^2 + \left(\frac{C_{pw}\,m_{w,add}\,\sigma_{m_{pw}}}{\left[m_{pw}+m_{w,add}\right]m_{pw}}\right)^2 + \left(\frac{C_{pw}}{f_a}\sigma_{f_a}\right)^2 \quad (63)$$

$$\left(\frac{\sigma_{C_{pw}}}{C_{pw}}\right)^2 = \left(\frac{\sigma_{C_{aqex}}}{C_{aqex}}\right)^2 + \left(\frac{m_{w,add}}{\left[m_{pw}+m_{w,add}\right]}\frac{\sigma_{m_{w,add}}}{m_{w,add}}\right)^2 + \left(\frac{\sigma_{S_w}}{S_w}\right)^2 + \left(\frac{m_{w,add}}{\left[m_{pw}+m_{w,add}\right]}\frac{\sigma_{m_{pw}}}{m_{pw}}\right)^2 + \left(\frac{\sigma_{f_a}}{f_a}\right)^2 \quad (64)$$

or

$$\sigma^2_{C_{pw}} = \left(\frac{C_{pw}}{C_{aqex}}\sigma_{C_{aqex}}\right)^2 + \left(\frac{C_{pw}}{\left[r_{saw}w+1\right]}\frac{\sigma_{r_{saw}}}{r_{saw}}\right)^2 + \left(\frac{C_{pw}}{S_w}\sigma_{S_w}\right)^2 + \left(\frac{C_{pw}}{\left[r_{saw}w+1\right]}\frac{\sigma_w}{w}\right)^2 + \left(\frac{C_{pw}}{f_a}\sigma_{f_a}\right)^2 \quad (65)$$

$$\left(\frac{\sigma_{C_{pw}}}{C_{pw}}\right)^2 = \left(\frac{\sigma_{C_{aqex}}}{C_{aqex}}\right)^2 + \left(\frac{1}{\left[r_{saw}w+1\right]}\frac{\sigma_{r_{saw}}}{r_{saw}}\right)^2 + \left(\frac{\sigma_{S_w}}{S_w}\right)^2 + \left(\frac{1}{\left[r_{saw}w+1\right]}\frac{\sigma_w}{w}\right)^2 + \left(\frac{\sigma_{f_a}}{f_a}\right)^2 \quad (66)$$

In both formulas above it is assumed that no anion exclusion occurs in the slurry of the extract. Relations for cases with some anion exclusion in the slurry can be found elsewhere (Gimmi & Waber 2014, Gimmi et al. 2014).

Note for high salinity samples: C_{pw} as given above is a mass-based concentration (per mass of pore water not including the solutes). For dilute samples, the volumetric concentration (per volume of water V_w) can be calculated by multiplying it by ρ_w. For saline solutions, the concentration per volume of solution is obtained by multiplying it by $(1-s)\rho_{solu}$ (*cf.* note for high salinity samples in Section A.2.8).

A.2.14 Concentrations of stable water isotopes in pore water from diffusive exchange experiments

The pore water isotope concentration can be calculated from the initial and final concentrations in the test water, the mass of test water, and either the mass of pore water in the sample (middle part) or the mass of the wet rock and the gravimetric wet water content of the sample (right part):

$$C_{pw} = C_{twf} + \frac{m_{tw}}{m_{pw}}\left(C_{twf} - C_{twi}\right) = C_{twf} + \frac{m_{tw}}{w_w\, m_{rw}}\left(C_{twf} - C_{twi}\right) \quad (67)$$

This leads to the following propagated errors:

$$\sigma^2_{C_{pw}} = \left(\left[1+\frac{m_{tw}}{m_{pw}}\right]\sigma_{C_{twf}}\right)^2 + \left(\frac{m_{tw}}{m_{pw}}\sigma_{C_{twi}}\right)^2 + \left(\frac{\left[C_{twf}-C_{twi}\right]}{m_{pw}}\sigma_{m_{tw}}\right)^2 + \left(\frac{\left[C_{twf}-C_{twi}\right]m_{tw}}{m^2_{pw}}\sigma_{m_{pw}}\right)^2 \quad (68)$$

or

$$\sigma_{C_{pw}}^2 = \left(\left[1 + \frac{m_{tw}}{w_w\, m_{rw}}\right]\sigma_{C_{twf}}\right)^2 + \left(\frac{m_{tw}}{w_w\, m_{rw}}\sigma_{C_{twi}}\right)^2 + \left(\frac{\left[C_{twf} - C_{twi}\right]}{w_w\, m_{rw}}\sigma_{m_{tw}}\right)^2 + \left(\frac{\left[C_{twf} - C_{twi}\right] m_{tw}}{w_w^2\, m_{rw}}\sigma_{w_w}\right)^2 + \left(\frac{\left[C_{twf} - C_{twi}\right] m_{tw}}{w_w\, m_{rw}^2}\sigma_{m_{rw}}\right)^2 \tag{69}$$

$$\left(\frac{\sigma_{C_{pw}}}{C_{pw}}\right)^2 = \left(\frac{\left[m_{pw} + m_{tw}\right] C_{twf}}{\left\{\left[m_{pw} + m_{tw}\right]C_{twf} - m_{tw}C_{twi}\right\}}\frac{\sigma_{C_{twf}}}{C_{twf}}\right)^2 + \left(\frac{m_{tw}C_{twi}}{\left\{\left[m_{pw} + m_{tw}\right]C_{twf} - m_{tw}C_{twi}\right\}}\frac{\sigma_{C_{twi}}}{C_{twi}}\right)^2 + \left(\frac{\left[C_{twf} - C_{twi}\right] m_{tw}}{\left\{\left[m_{pw} + m_{tw}\right]C_{twf} - m_{tw}C_{twi}\right\}}\frac{\sigma_{m_{tw}}}{m_{tw}}\right)^2 + \left(\frac{\left[C_{twf} - C_{twi}\right] m_{tw}}{\left\{\left[m_{pw} + m_{tw}\right]C_{twf} - m_{tw}C_{twi}\right\}}\frac{\sigma_{m_{pw}}}{m_{pw}}\right)^2 \tag{70}$$

or

$$\left(\frac{\sigma_{C_{pw}}}{C_{pw}}\right)^2 = \left(\frac{\left[w_w m_{rw} + m_{tw}\right] C_{twf}}{\left\{\left[w_w m_{rw} + m_{tw}\right]C_{twf} - m_{tw}C_{twi}\right\}}\frac{\sigma_{C_{twf}}}{C_{twf}}\right)^2 + \left(\frac{m_{tw}C_{twi}}{\left\{\left[w_w m_{rw} + m_{tw}\right]C_{twf} - m_{tw}C_{twi}\right\}}\frac{\sigma_{C_{twi}}}{C_{twi}}\right)^2 + \left(\frac{\left[C_{twf} - C_{twi}\right] m_{tw}}{\left\{\left[w_w m_{rw} + m_{tw}\right]C_{twf} - m_{tw}C_{twi}\right\}}\frac{\sigma_{m_{tw}}}{m_{tw}}\right)^2 + \left(\frac{\left[C_{twf} - C_{twi}\right] m_{tw}}{\left\{\left[w_w m_{rw} + m_{tw}\right]C_{twf} - m_{tw}C_{twi}\right\}}\frac{\sigma_{w_w}}{w_w}\right)^2 + \left(\frac{\left[C_{twf} - C_{twi}\right] m_{tw}}{\left\{\left[w_w m_{rw} + m_{tw}\right]C_{twf} - m_{tw}C_{twi}\right\}}\frac{\sigma_{m_{rw}}}{m_{rw}}\right)^2 \tag{71}$$

Note: For isotope concentrations in δ notation, relative errors are not meaningful.

The mass of pore water m_{pw} of the used sample or its wet water content w_w is typically determined along with C_{pw}. Then, this value and its uncertainty (e.g. from relation (16), (19) or (22)) can be directly used in equations (67) to (71).

In general, two isotope exchange experiments with different initial concentrations of the test water are performed on two subsamples. Assuming that these subsamples have identical water content, w_w can be eliminated, i.e., it does no longer appear in the equation to calculate the isotope concentration. Using index 1 and 2 for the two experiments, we then have

$$C_{pw} = \frac{m_{tw2}m_{rw1}C_{twf1}\left(C_{twf2}-C_{twi2}\right)-m_{tw1}m_{rw2}C_{twf2}\left(C_{twf1}-C_{twi1}\right)}{m_{tw2}m_{rw1}\left(C_{twf2}-C_{twi2}\right)-m_{tw1}m_{rw2}\left(C_{twf1}-C_{twi1}\right)} \tag{72}$$

Setting $a = m_{tw2}m_{rw1}\left(C_{twf2}-C_{twi2}\right)$, $b = m_{tw1}m_{rw2}\left(C_{twf1}-C_{twi1}\right)$, and $d = ab\left(C_{twf1}-C_{twf2}\right)/(a-b)^2$ we can write

$$C_{pw} = \frac{a\,C_{twf1} - b\,C_{twf2}}{a-b}$$

$$\begin{aligned}\sigma^2_{C_{pw}} = {} & \left(g_1\,\sigma_{m_{tw1}}\right)^2 + \left(g_2\,\sigma_{m_{tw2}}\right)^2 + \left(g_3\,\sigma_{m_{rw1}}\right)^2 + \left(g_4\,\sigma_{m_{rw2}}\right)^2 \\ & + \left(g_5\,\sigma_{C_{twi1}}\right)^2 + \left(g_6\,\sigma_{C_{twi2}}\right)^2 + \left(g_7\,\sigma_{C_{twf1}}\right)^2 \\ & + \left(g_8\,\sigma_{C_{twf2}}\right)^2\end{aligned} \tag{73}$$

with

$$g_1 = \frac{d}{m_{tw1}} \qquad g_2 = \frac{-d}{m_{tw2}}$$

$$g_3 = \frac{-d}{m_{rw1}} \qquad g_4 = \frac{d}{m_{rw2}}$$

$$g_5 = \frac{-d}{\left(C_{twf1}-C_{twi1}\right)} \qquad g_6 = \frac{d}{\left(C_{twf2}-C_{twi2}\right)}$$

$$g_7 = \frac{a}{a-b} + \frac{d}{\left(C_{twf1}-C_{twi1}\right)} \qquad g_8 = -\frac{b}{a-b} - \frac{d}{\left(C_{twf2}-C_{twi2}\right)}$$

After having obtained isotope pore water concentrations according to eq. (72), it is possible to reckon back the corresponding water content from the $\delta^{18}O$ or the $\delta^{2}H$ data as

$$w_w = \frac{m_{tw}}{m_{rw}}\frac{\left(C_{twf} - C_{twi}\right)}{\left(C_{pw} - C_{twf}\right)} \tag{74}$$

$$\begin{aligned}\sigma^2_{w_w} = {} & \left(\frac{w_w}{m_{tw}}\sigma_{m_{tw}}\right)^2 + \left(\frac{w_w}{m_{rw}}\sigma_{m_{rw}}\right)^2 \\ & + \left(\left[\frac{w_w}{C_{twf}-C_{twi}} + \frac{w_w}{C_{pw}-C_{twf}}\right]\sigma_{C_{twf}}\right)^2 \\ & + \left(\frac{w_w}{C_{twf}-C_{twi}}\,\sigma_{C_{twi}}\right)^2 + \left(\frac{w_w}{C_{pw}-C_{twf}}\,\sigma_{C_{pw}}\right)^2\end{aligned} \tag{75}$$

Note: If the water contents of the two subsamples differ significantly, the application of eq. (72) may lead to biased concentrations, with the bias not appearing in the propagated uncertainties. In fact, if the wet water contents for experiment 1 and 2 differ, with a ratio $q = w_{w1}/w_{w2}$, the isotope pore water concentration has to be calculated as

$$C_{pw} = \frac{a\ q\ C_{twf1} - b\ C_{twf2}}{a\ q - b} \tag{76}$$

$$\begin{aligned}\sigma^2_{C_{pw}} = &\left(g_1\ \sigma_{m_{tw1}}\right)^2 + \left(g_2\ \sigma_{m_{tw2}}\right)^2 + \left(g_3\ \sigma_{m_{rw1}}\right)^2 + \left(g_4\ \sigma_{m_{rw2}}\right)^2 \\ &+ \left(g_5\ \sigma_{C_{twi1}}\right)^2 + \left(g_6\ \sigma_{C_{twi2}}\right)^2 + \left(g_7\ \sigma_{C_{twf1}}\right)^2 \\ &+ \left(g_8\ \sigma_{C_{twf2}}\right)^2 + \left(g_9\ \sigma_q\right)^2\end{aligned} \tag{77}$$

with b, d, and g_1 through g_8 as defined on the previous page, except that a has to be replaced by $a' = a\ q = q\ m_{tw2}m_{rw1}\left(C_{twf2} - C_{twi2}\right)$ in these expressions, and

$$g_9 = \frac{a\ C_{twf1}}{aq - b} + \frac{a^2\ q\ C_{twf1}}{(aq - b)^2} = \frac{a\ C_{twf1}}{aq - b} + \frac{aq\ d\ C_{twf1}}{b\left(C_{twf1} - C_{twf2}\right)}$$

A propagated error for q has to be used in this case, e.g., $\sigma_q = \sqrt{2}\ \sigma_{w_w}$.

Instead of using w_w of the actual subsample directly in equation (67), a value determined independently on another subsample may be used. Any error related to a possible variation of the water content of different subsamples (heterogeneity, artefacts) is then of course not considered in the propagated errors of equations (68) to (71).

If, for any reason, w_w is calculated from the pycnometer porosity $\phi_{pycn} = 1 - \rho_{bd}/\rho_g = 1 - (1 - w_w)\ \rho_{bw}/\rho_g$ (where, for the last term, it is assumed that $m_{rw} - m_{pw} = m_s$) as

$$w_w = \left[1 - \left(1 - \phi_{pycn}\right)\frac{\rho_g}{\rho_{bw}}\right] \tag{78}$$

the uncertainty σ_{w_w} has to be calculated as

$$\begin{aligned}\sigma^2_{w_w} = &\left(\frac{\rho_g}{\rho_{bw}}\ \sigma_{\phi_{pycn}}\right)^2 + \left(\frac{\left[1 - \phi_{pycn}\right]}{\rho_{bw}}\ \sigma_{\rho_g}\right)^2 \\ &+ \left(\left[1 - \phi_{pycn}\right]\frac{\rho_g}{\rho^2_{bw}}\ \sigma_{\rho_{bw}}\right)^2\end{aligned} \tag{79}$$

Assuming that the sample was saturated such that the pycnometer porosity equals the volumetric water content, we could also use one of the following formulas (the first is written in terms of ϕ_{pycn}, ρ_{bw} and ρ_w, the second in terms of the primarily measured variables ρ_{bw}, ρ_g and ρ_w)

$$w_w = \phi_{pycn}\frac{\rho_w}{\rho_{bw}} = \frac{\left(\frac{1}{\rho_{bw}} - \frac{1}{\rho_g}\right)}{\left(\frac{1}{\rho_w} - \frac{1}{\rho_g}\right)} \tag{80}$$

leading to

$$\sigma_{w_w}^2 = \left(\frac{\rho_w}{\rho_{bw}}\ \sigma_{\phi_{pycn}}\right)^2 + \left(\frac{\phi_{pycn}}{\rho_{bw}}\ \sigma_{\rho_w}\right)^2 + \left(\phi_{pycn}\frac{\rho_w}{\rho_{bw}^2}\ \sigma_{\rho_{bw}}\right)^2 \tag{81}$$

or

$$\begin{aligned}\sigma_{w_w}^2 &= \left(\frac{\left(\frac{1}{\rho_{bw}} - \frac{1}{\rho_g}\right)}{\left(\frac{1}{\rho_w} - \frac{1}{\rho_g}\right)^2}\frac{1}{\rho_w^2}\ \sigma_{\rho_w}\right)^2 + \left(\frac{\left(\frac{1}{\rho_w} - \frac{2}{\rho_g} + \frac{1}{\rho_{bw}}\right)}{\left(\frac{1}{\rho_w} - \frac{1}{\rho_g}\right)^2}\frac{1}{\rho_g^2}\ \sigma_{\rho_g}\right)^2 + \left(\frac{1}{\left(\frac{1}{\rho_w} - \frac{1}{\rho_g}\right)}\frac{1}{\rho_{bw}^2}\ \sigma_{\rho_{bw}}\right)^2 \\ &= \left(\frac{w_w}{\left(\frac{1}{\rho_w} - \frac{1}{\rho_g}\right)}\frac{1}{\rho_w^2}\ \sigma_{\rho_w}\right)^2 + \left(\frac{w_w + 1}{\left(\frac{1}{\rho_w} - \frac{1}{\rho_g}\right)}\frac{1}{\rho_g^2}\ \sigma_{\rho_g}\right)^2 + \left(\frac{w_w}{\left(\frac{1}{\rho_{bw}} - \frac{1}{\rho_g}\right)}\frac{1}{\rho_{bw}^2}\ \sigma_{\rho_{bw}}\right)^2\end{aligned} \tag{82}$$

Instead of using the wet bulk density, the formulas can also be expressed with the dry bulk density (again, the first formula includes ϕ_{pycn}, the second only densities):

$$w_w = \left(1 + \frac{\rho_{bd}}{\rho_w \phi_{pycn}}\right)^{-1} = \left(1 + \frac{1}{\rho_w\left(\frac{1}{\rho_{bd}} - \frac{1}{\rho_g}\right)}\right)^{-1} \tag{83}$$

$$\begin{aligned}\sigma_{w_w}^2 = w_w^4 \Bigg[&\left(\frac{1}{\phi_{pycn}\,\rho_w}\ \sigma_{\rho_{bd}}\right)^2 + \left(\frac{\rho_{bd}}{\phi_{pycn}^2\,\rho_w}\ \sigma_{\phi_{pycn}}\right)^2 \\ &+ \left(\frac{\rho_{bd}}{\phi_{pycn}\,\rho_w^2}\ \sigma_{\rho_w}\right)^2\Bigg]\end{aligned} \tag{84}$$

or

$$\begin{aligned}\sigma_{w_w}^2 = \frac{w_w^4}{\left[\rho_w\left(\frac{1}{\rho_{bd}} - \frac{1}{\rho_g}\right)\right]^4}\Bigg[&\left(\frac{1}{\rho_{bd}^2}\ \sigma_{\rho_{bd}}\right)^2 + \left(\frac{1}{\rho_g^2}\ \sigma_{\rho_g}\right)^2 \\ &+ \left(\left\{\frac{1}{\rho_{bd}} - \frac{1}{\rho_g}\right\}^{-1}\ \sigma_{\rho_w}\right)^2\Bigg]\end{aligned} \tag{85}$$

A.2.15 Ni consumption based on Ni-en extracts

$$Ni_c = C_{Ni\,st}\frac{m_{wst}}{m_s} - C_{Ni\,ex}\frac{m_{pw} + m_{wst}}{m_s} \tag{86}$$

$$\sigma_{Ni_c}^2 = \left(\frac{m_{wst}}{m_s}\sigma_{C_{Ni\,st}}\right)^2 + \left(\frac{m_{pw}+m_{wst}}{m_s}\sigma_{C_{Ni\,ex}}\right)^2 + \left(\frac{C_{Ni\,st}-C_{Ni\,ex}}{m_s}\sigma_{m_{wst}}\right)^2 + \left(\frac{C_{Ni\,ex}}{m_s}\sigma_{m_{pw}}\right)^2 + \left(\frac{C_{Ni\,st}m_{wst}-C_{Ni\,ex}\left[m_{pw}+m_{wst}\right]}{m_s^2}\sigma_{m_s}\right)^2 \quad (87)$$

Writing $r_{saw} = m_s/\,m_{wst}$ for the ratio of mass of solid to mass of added stock solution, or $SL = m_s/\left(m_{pw}+m_{wst}\right)$ for the ratio of mass of solid to the masses of pore water and added stock solution, we can also write

$$Ni_c = \frac{(C_{Ni\,st}-C_{Ni\,ex})}{r_{saw}} - w\,C_{Ni\,ex} \approx \frac{(C_{Ni\,st}-C_{Ni\,ex})}{r_{saw}} \quad (88)$$

or

$$Ni_c = \left(C_{Ni\,st}\left[\frac{m_{wst}}{m_{pw}+m_{wst}}\right] - C_{Ni\,ex}\right)\frac{1}{SL} \approx \frac{(C_{Ni\,st}-C_{Ni\,ex})}{SL} \quad (89)$$

If the amount of stock solution m_{wst} is much larger than the amount of pore water m_{pw}, $wC_{Ni\,ex}$ is small compared to $(C_{Ni\,st}-C_{Ni\,ex})/r_{saw}$, or the term in square brackets in eq. (89) is ~1, which leads to the given approximations. Under such conditions, we have

$$\sigma_{Ni_c}^2 \approx \left(\frac{1}{r_{saw}}\sigma_{C_{Ni\,st}}\right)^2 + \left(\frac{1}{r_{saw}}\sigma_{C_{Ni\,ex}}\right)^2 + \left(\frac{C_{Ni\,ex}-C_{Ni\,st}}{r_{saw}^2}\sigma_{r_{saw}}\right)^2 \quad (90)$$

or

$$\sigma_{Ni_c}^2 \approx \left(\frac{1}{SL}\sigma_{C_{Ni\,st}}\right)^2 + \left(\frac{1}{SL}\sigma_{C_{Ni\,ex}}\right)^2 + \left(\frac{C_{Ni\,ex}-C_{Ni\,st}}{SL^2}\sigma_{SL}\right)^2 \quad (91)$$

In order to obtain Ni or other cation concentrations of the extract per mass of dry rock, concentrations per mass of water have to be multiplied by $(m_{pw}+m_{wst})/m_s$, i.e., they have to be divided by SL (*cf.* second term on the right side of eq. (86)). Furthermore, if the concentrations are originally expressed as mass of cation per mass of water or rock, concentrations expressed in, e.g., mmol charge (i.e., meq) are obtained by multiplication with v/AW, with v the valence and AW the atomic weight (for Ni, v = 2 eq mol^{-1} and AW = 58.6934 g mol^{-1}).

The above relations were derived assuming that the extracts were prepared from wet (saturated) samples. If dry samples are extracted instead, the mass of pore water m_{pw} or equally the water content w has to be set to zero in eqs. (86), (87) and (88). Then, the Ni consumption and its propagated error are given exactly by the approximations in eqs. (88) and (90).

A.3 Typical errors and some examples

Some typical errors or uncertainties of input variables:

σ_{m_r}, $\sigma_{m_{rw}}$ 0.002 g

$\sigma_{m_{pw}}$ 0.003 g (or more, if uncertainty regarding completeness of drying is considered)

$\sigma_{\Delta m_k}$, $\sigma_{\Delta m_p}$ 0.005 g

σ_{ρ_p}/ρ_p 0.012

The gravimetric water content w can be calculated from different input variables according to equations (3), (6) or (9). The resulting relative errors σ_w/w (given in %) are not necessarily equal, as shown in the table below. Note that very small sample weights were chosen, just for demonstration purpose (~ 30 – 300 g is a more typical sample weight). The propagated errors σ_w/w are different, depending on the equations and input errors used. In the table below, the error $\sigma_{m_{pw}}$ is set equal to $\sigma_{m_{rw}}$ and σ_{m_r} (first line), to $\sqrt{2}$ times (second line), or to 2 times (third line) $\sigma_{m_{rw}}$ and σ_{m_r}. Using the factor $\sqrt{2}$ leads to very similar errors for all formulas, as expected based on the error propagation.

Input variables						Calculated variables			
							via m_{pw}, m_r	via m_{rw}, m_r	via m_{pw}, m_{rw}
m_{rw}	$\sigma_{m_{rw}}$	m_r	σ_{m_r}	m_{pw}	$\sigma_{m_{pw}}$	w	σ_w/w	σ_w/w	σ_w/w
g	g	g	g	g	g	–	%	%	%
3.3	0.002	3	0.002	0.3	0.002	0.1	0.670	0.991	0.736
3.3	0.002	3	0.002	0.3	0.00283	0.1	0.945	0.991	1.039
3.3	0.002	3	0.002	0.3	0.004	0.1	1.335	0.991	1.468

Correlations between variables are ignored in the specific formulas presented above. Let us now consider the function $f = u/v$ with correlated variables u and v. We then have

$$\left(\frac{\sigma_f}{f}\right)^2 = \left(\frac{\sigma_u}{u}\right)^2 + \left(\frac{\sigma_v}{v}\right)^2 - 2\frac{\sigma_{uv}}{uv} = \left(\frac{\sigma_u}{u}\right)^2 + \left(\frac{\sigma_v}{v}\right)^2 - 2\,\mathrm{Cor}(u,v)\frac{\sigma_u\sigma_v}{uv}$$

where the covariance $\mathrm{Cov}(u,v) = \sigma_{uv}$ and the correlation $\mathrm{Cor}(u,v) = \sigma_{uv}/(\sigma_u\sigma_v)$. For fully correlated or fully anti-correlated variables ($\mathrm{Cor}(u,v) = \pm 1$) we thus have

$$\left(\frac{\sigma_f}{f}\right)^2 = \left(\frac{\sigma_u}{u}\right)^2 + \left(\frac{\sigma_v}{v}\right)^2 \mp 2\frac{\sigma_u\sigma_v}{uv}$$

For uncorrelated parameters ($\sigma_{uv} = 0$ or $\mathrm{Cor}(u,v) = 0$), the last term would drop. This shows that neglecting parameter correlations can lead to over- or underestimation of σ_f.